To the Graduate Council:

I am submitting herewith a thesis written by James S. Morris entitled "Vapor–Liquid Equilibrium of the Methane–Carbon Dioxide–Hydrogen Sulfide System Near the Critical Region." I have examined the final copy of this thesis for form and content and recommend that it be accepted in partial fulfillment of the requirements for the degree of Master of Science, with a major in Chemical Engineering.

Charles H. Byers, Major Professor

We have read this thesis
and recommend its acceptance:

H. W. Haw

Accepted for the Council:

Vice Provost
and Dean of The Graduate School

STATEMENT OF PERMISSION TO USE

In presenting this thesis in partial fulfillment of the requirments for a Master of Science degree at The University of Tennessee, Knoxville, I agree that the Library shall make it available to borrowers under rules of the Library. Brief quotations from this thesis are allowable without special permission, provided that accurate acknowledgment of the source is made.

Permission for extensive quotation from or reproduction of this thesis may be granted by my major professor, or in his absence, by the Head of Interlibrary Services when, in the opinion of either, the proposed use of the material is for scholarly purposes. Any copying or use of the material in this thesis for financial gain shall not be allowed without my written permission.

Signature James D. Morris

Date 5/9/88

VAPOR–LIQUID EQUILIBRIUM OF THE METHANE–CARBON DIOXIDE–HYDROGEN SULFIDE SYSTEM NEAR THE CRITICAL REGION

A Thesis
Presented for the
Master of Science
Degree
The University of Tennessee, Knoxville

James S. Morris
June 1988

ACKNOWLEDGEMENTS

I would like to thank my major advisor and group leader Dr. Charles H. Byers for his encouragement and helpful suggestions. I also am heavily indebted to Mr. Ron R. Brunson and Mr. Warren G. Sisson for their assistance. Without their help this thesis could not be written. Finally, I would like to give special thanks to my wife, Pamela Morris, and son, Matthew Morris, for their patience and encouragement.

ABSTRACT

The Oak Ridge National Laboratory (ORNL) has proposed a process for purifying substitute natural gas streams by absorption–fractionation in liquid CO_2. In order to further the development of this process, additional vapor-liquid equilibrium data was needed to supplement the literature data. The primary objective of the study presented here was to design, construct, and test an apparatus at the Oak Ridge National Laboratory to measure vapor-liquid equilibrium properties of binary and multicomponent systems which are of interest to this process.

The CH_4–CO_2–H_2S system and the associated binary systems have been studied in this work between 270.0 K and 288.2 K in order to test the accuracy of the experimental apparatus, supplement the literature data, and test the ability of the Peng–Robinson (PR) and Redlich–Kwong–Soave (RKS) equations of state to predict the equilibrium properties of these systems. Binary interaction parameters have been determined for each of the binary systems and used to calculate the equilibrium phase properties of the binary and ternary systems. A comparison of these calculation with the experimental results is presented. Experimental CO_2 vapor pressure measurements deviate less than 0.5 percent from the literature. Also, calculated phase equilibrium measurements of the the CH_4–CO_2 system using both the PR and RKS equations disagree with the experimental results by less than 3.5 percent and measured liquid phase compositions differ from the calculated by less than 15 percent. Similar results, less than 2 percent deviation on pressure and less than 13 percent for liquid phase

composition, were obtained when comparing literature data for the CO_2–H_2S system to the calculations of the PR and RKS equations.

Questionable phase compositions were obtained when measuring systems containing H_2S, especially when the H_2S composition was greater than 90 percent. Large deviations resulted when the calculated equilibrium properties of both equations were compared to the experimental results for the CH_4–H_2S system. The calculated pressures, for this system, were up to 12 percent below the experimental values and the experimental liquid phase compositions differed from the calculated values by greater than 50 percent at pressures up to 700 psia. This difference was smaller, less than 15 percent for liquid phase compositions, at pressures of 900 to 1000 psia. The PR equation has been found to provide more accurate pressure results (12 percent deviation versus 29 percent) for the ternary mixture than the RKS equation in the temperature and pressure range of this study.

TABLE OF CONTENTS

SECTION	PAGE
1. INTRODUCTION	1
2. THEORETICAL BACKGROUND	8
2.1 Equations of State	8
2.2 Thermodynamic Consistency	19
3. EXPERIMENTAL	23
3.1 Apparatus	23
3.2 Generalized Procedure	30
3.3 Materials	33
4. RESULTS AND DISCUSSION	35
4.1 Carbon Dioxide Vapor Pressure	35
4.2 Carbon Dioxide–Methane	39
4.3 Methane–Hydrogen Sulfide	51
4.4 Carbon Dioxide–Hydrogen Sulfide	63
4.5 Error Analysis	66
4.6 Carbon Dioxide–Methane–Hydrogen Sulfide	69
5. CONCLUSIONS AND RECOMMENDATIONS	73
5.1 Conclusions	73
5.2 Recommendations for Future Work	74
LIST OF REFERENCES	77
APPENDICES	82
APPENDIX I: OPERATING INSTRUCTIONS FOR THE ORNL VAPOR–LIQUID EQUILIBRIUM APPARATUS	83
APPENDIX II: EXAMPLE OF AN ASPEN DRS INPUT FILE AND REPORT	88

APPENDIX III: EXAMPLE OF AN ASPEN FLASH2 INPUT FILE AND REPORT 100
APPENDIX IV: EXAMPLE OF AN ASPEN TGS INPUT FILE AND REPORT 109
APPENDIX V: ASPEN SIMILATION OF PROPOSED METHANE PURIFICATION PROCESS 116
VITA 148

LIST OF TABLES

TABLE		PAGE
1	Coal gasification reactor effluent composition.	6
2	Carbon dioxide vapor pressure results.	38
3	Experimental phase equilibrium measurements for carbon dioxide–methane.	40
4	RKS calculations versus experimental results for the CH_4–CO_2 system.	45
5	PR calculations versus experimental results for the CH_4–CO_2 system.	46
6	Thermodynamic consistency test for CH_4–CO_2 using results from the PR equation.	52
7	Experimental phase equilibrium measurements for methane–hydrogen sulfide.	53
8	RKS calculations versus experimental results for the CH_4–H_2S system.	57
9	PR calculations versus experimental results for the CH_4–H_2S system.	58
10	RKS and PR calculations versus literature data for the CH_4–H_2S system at 277.6 K.	62
11	RKS and PR calculations versus literature data for the CO_2–H_2S system at 283.2 K.	65
12	Binary interaction parameters for CH_4, CO_2, and H_2S binary systems.	70
13	Phase equilibrium properties for CH_4–CO_2–H_2S at 270.0 K.	71

LIST OF FIGURES

FIGURE		PAGE
1	ORNL methane purification process.	4
2	Van der Waals' excluded volume.	10
3	Photograph of VLE apparatus.	25
4	Schematic of the experimental apparatus.	26
5	Photograph of EC and magnetic pump.	29
6	Carbon dioxide vapor pressure data.	37
7	Pressure versus composition for carbon dioxide–methane at 270.0 K.	41
8	Pressure versus composition for carbon dioxide–methane at 288.2 K.	42
9	Thermodynamic consistency test–Area I.	48
10	Thermodynamic consistency test–Area II.	49
11	Thermodynamic consistency test–Area III × RT.	50
12	Pressure versus composition for methane–hydrogen sulfide at 270.0 K.	55
13	Pressure versus composition for methane–hydrogen sulfide at 288.2 K.	56
14	Methane–hydrogen sulfide vapor phase measurements versus the literature.	59
15	Methane–hydrogen sulfide liquid phase measurements versus the literature.	60
16	Pressure versus composition for carbon dioxide–hydrogen sulfide at 283.2 K.	64

NOMENCLATURE

a	constant usually associated with attractive forces of molecules
b	constant usually associated with repulsive forces of molecules, called the excluded volume
B	second virial coefficient
C	third virial coefficient
D	fourth virial coefficient
f	fugacity
k	binary interaction parameter
K	K factor, defined as y_i/x_i
l	molecular diameter
M	denotes any partial molar property
n	total number of moles
P	absolute pressure
P_c	critical pressure
P_i^s	saturation pressure of pure substance i
R	universal gas constant
T	absolute temperature
T_c	critical temperature
T_r	reduce temperature, defined as T/T_c
v	molar volume
v_c	critical volume
v^L	molar volume of liquid phase
V	total volume
x	mole fraction of liquid phase
y	mole fraction of gas phase
Z	compressibility factor

Greek Letters

δ	constant in generalized cubic equation of state
Γ	attractive potential
ϵ	constant in generalized cubic equation of state
ς	constant in generalized cubic equation of state
η	constant in generalized cubic equation of state
σ	intermolecular separation
φ	fugacity coefficient
φ_i^s	fugacity coefficient of pure substance i at saturation
ω	accentric factor

Subscripts

c	property at the critical point
i	property of pure component i
ii	property of binary interaction of similar components i and i
ij	property of binary interaction of dissimilar components i and j
jj	property of binary interaction of similar components j and j
mix	mixture property
r	reduced variable

1. INTRODUCTION

Coal gasification processes have been in existence for many years. The development of improved industrial processes, however, was very limited because of unfavorable economics until the oil embargo of the 1970s. Although much of the industrial interest in these processes has once again subsided, the precarious dependence upon foreign oil continues to fuel some interest in this field.

The quality of the product gas from the reactors is one of the main points of interest in the study of gasification processes. The chemistry of the coal feedstock, the type of reactor, the operating conditions in the reactor, and the processes used to purify this stream all contribute to the quality and, in the past, unfavorable economics to operate these processes. The primary impurities in raw synthetic natural gas are H_2, CO, CO_2, H_2O, and sometimes N_2. The first three impurities result from competing reactions inside the reactor vessel. The basic reactions in gasification reactors are as follows:

$$C + O_2 \rightarrow CO_2 \tag{1}$$

$$C + CO_2 \rightleftharpoons 2CO \tag{2}$$

$$CO + H_2O \rightleftharpoons CO_2 + H_2 \tag{3}$$

$$C + 2H_2 \rightleftharpoons CH_4 \tag{4}$$

$$C + H_2O \rightleftharpoons CO + H_2 \tag{5}$$

The H_2O results mainly from unreacted steam and the N_2 results from the use of air instead of oxygen as the fuel.

The kinetics and thermodynamics of these competing reactions are affected greatly by the type of reactor chosen; for example, in fixed bed gasifiers the

temperature of the product gas can range from as low as 250°F in the Woodall Duckham two-stage process (Grant 1976) to as high as 2000°F. On the other hand, the pressure can range from atmospheric to several hundred psig, depending on the particular design. This is part of the reason for more recent interest in fluidized bed reactors. The operating condition of these reactors may be more easily controlled and the temperature more uniformly distributed than other reactor types.

Further contaminating the methane product are the sulfur and nitrogen compounds present in the product. Sulfur, which is present in all coals in various levels, is found in the product gases mainly as H_2S along with a small percentage of COS and trace quantities of CS_2, mercaptans, thiophene, and SO_2 . The formation of NH_3, which is the primary nitrogen compound in the product stream, is expected with the presence of H_2 and N_2 in the reactor. Impurities such as tars, phenols, and halogens can be controlled to a large degree by adjusting the operating parameters for some types of reactors. Unfortunately, the formation of the by-products of sulfur and ammonia is not controllable. Thus, a gas treatment process is needed if these compounds are to be removed from the product stream (Elliot 1981).

New gasification processes are under development which can operate at relatively lower temperatures and do not require purified gases with narrow limits in composition. These processes, however, need new separation techniques to recycle unreacted CO and H_2 and to purify the methane product. Conventional technology for this separation is cryogenic distillation or shift and methanization of the hydrogen-carbon monoxide-methane mixture. Because of the low temperatures and low pressures (below pipeline pressures) required for cryo-

genic distillation, an undesirably high energy cost is required for refrigeration and production recompression. A more desirable separation would operate at higher temperatures and at pressures closer to that needed for the gasifier.

A new process for separating CH_4 from CO and H_2, which satisfies these criteria, has been proposed at the Oak Ridge National Laboratory (ORNL). In this process, the CO_2 present in the gasifier product is used as the solvent in an absorption-fractionation process. This process operates at the high pressures necessary for pipeline gas and at temperatures which are within the range of conventional refrigeration equipment. This process is similar to the Krypton Absorption in Liquid CO_2 (KALC) (Gilliam 1979) process developed at ORNL for the removal of radioactive contaminants from nuclear reactor fuel reprocessing waste gas. A computer program and a physical properties data base have been prepared to simulate the proposed methane purification process. The proposed process is based upon the preferential absorption of methane and heavier products in liquid CO_2 at pipeline pressure.

A schematic of the process is shown in Figure 1. The synthesis gas (stream 1) which has been treated for ammonia and water removal enters the bottom of the absorber, and recycled liquid CO_2 (stream 8) is fed to the top of the absorber. The absorber is operated so that essentially all of the CH_4 exits the absorber in the liquid bottoms (stream 3); most of the CO and H_2 remain in the gas phase. The heavier components in the synthesis gas (H_2S, higher hydrocarbons, etc.) are also completely absorbed into the liquid CO_2. The bottom product from the absorber (stream 3) proceeds to the fractionator, which is operated so that almost all of the H_2 and CO in the fractionator feed are stripped into the overhead (stream 4), while the bulk of the CH_4 remains in the liquid phase.

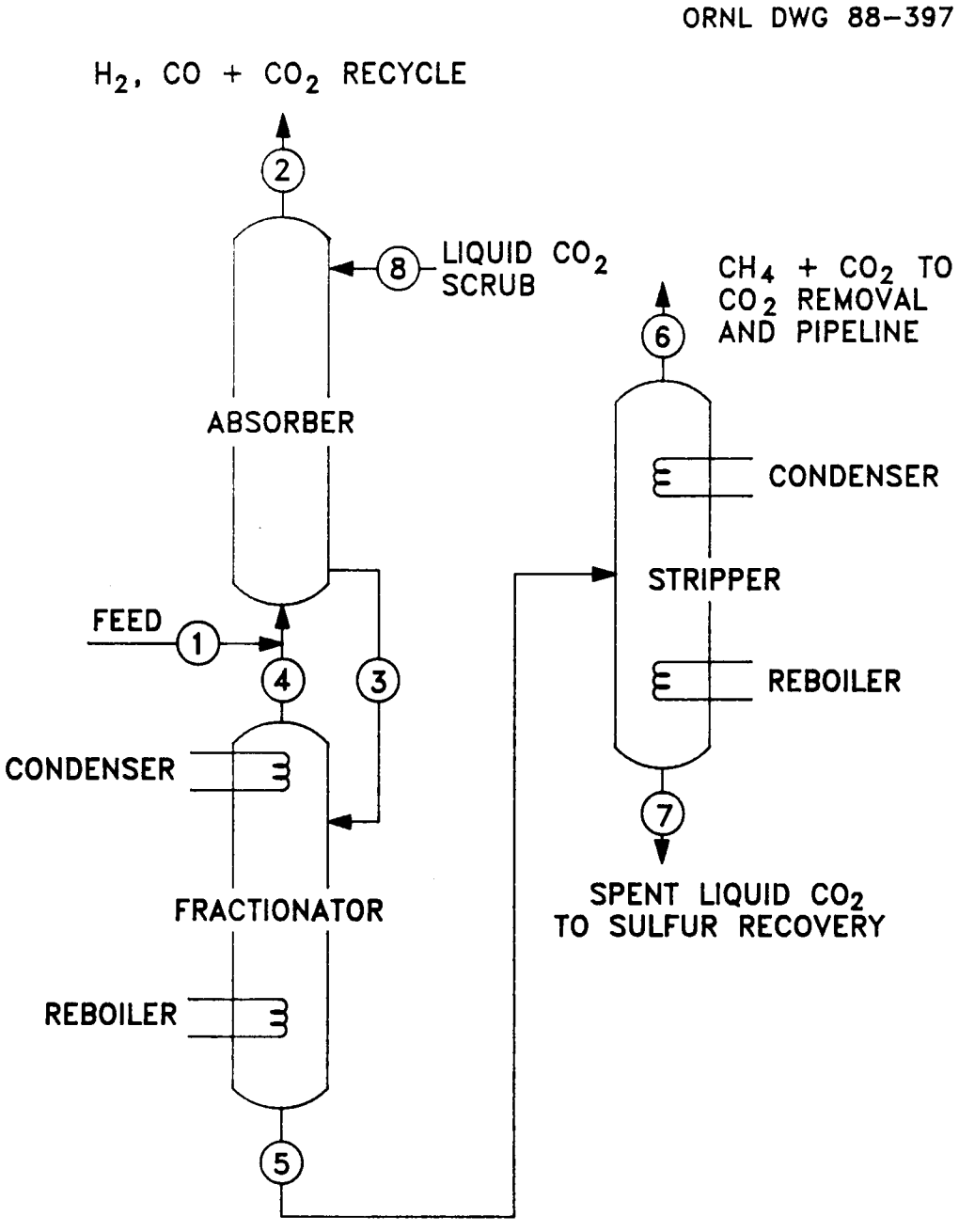


Figure 1. ORNL methane purification process.

Since the fractionator overhead also contains CH_4, it is recycled to the absorber. The fractionator bottoms (stream 5), which contains CH_4 and the heavier components, go on to the stripper. The stripper is operated at temperature and pressure conditions such that the CH_4 is concentrated in the overhead product (stream 6), while the heavier contaminants (e.g., H_2S) remain in the liquid phase (stream 7). Thus the synthesis gas (stream 1) is split into three streams: a gas stream containing the product CH_4 (stream 6), a gas stream containing the H_2 and CO (stream 2), and a liquid stream containing the heavier components (stream 7). The methane product stream will probably contain a significant amount (approximately 40 percent) of CO_2; therefore further processing is necessary. Several commercially available processes may be efficiently and cheaply applied for CO_2 removal (e.g., "Selexol"). Operation of the system at pipeline pressure (69 atm) is desirable from an energy conservation viewpoint. Preliminary studies have shown that both the stripper and the absorber can be operated in that pressure region, although the pressure (70 atm) may be at the lower edge of the efficient operation region for some catalytic gasification reactors. The pressure drop in the train of columns will minimize pumping and allow operation of condensers in the region of $-20°C$ with small cooling loads, thus minimizing refrigeration requirements.

The foregoing discussion was based upon preliminary process evaluations, using the ASPEN^{TM} process simulator and phase equilibrium information available on those components for which data were available in the open literature. The thermodynamic information is incomplete and only preliminary attempts have been made to optimize the process variables. In addition to the lack of complete information is the uncertainty of predicting multicomponent vapor-liquid

equilibria (VLE) in the vapor-liquid critical region, especially when high mole fractions of the solute are present in the liquid phase. Because of this uncertainty, thermodynamic studies are considered to be essential in the development of this process.

Given the typical coal gasification reactor effluent shown in Table 1, one can envision VLE measurements of each of the combinations of compounds to predict the behavior of this six component stream. This would obviously be an enormous task. Recent thermodynamic developments have yielded new equations of state that have resulted in better prediction of thermodynamic properties of multicomponent systems. These equations of state require only binary data in order to predict these multicomponent systems, with remarkable accuracy in some cases.

Table 1. Coal gasification reactor effluent composition.

Component	Mole %
H_2	3.0
CO	5.0
CO_2	55.0
CH_4	33.0
H_2S	3.0
COS	1.0

Because of the reported successes of the cubic equations of state and because of the uncertainty of their accuracy near the vapor-liquid critical region, the applicability of the cubic equations of state to the process conditions mentioned earlier was examined. More specifically, the purpose of this study was to build an apparatus and to collect VLE data which were applicable to the mixture shown in Table 1 that have not been previously reported. The CH_4–CO_2–H_2S system was chosen to be the ternary system to study. The reason for its selection was (1) the critical regions of CO_2 and H_2S exist at moderate pressures (72.8 and 88.2 atm, respectively), (2) the CO_2–CH_4 system was well documented, so results from the experiment could be compared to the literature; (3) the CH_4–H_2S and CO_2–CH_4–H_2S systems are not well documented in the temperature and pressure ranges of interest in this study; and (4) these compounds are of primary importance in the process noted earlier. A combination of literature data and data collected in this study was used to test the ability of the cubic equations to predict the ternary phase behavior from the binary properties near the vapor-liquid critical region. One of the cubic equations of state being considered in this test was chosen to model the proposed ORNL process because of its higher accuracy in predicting the ternary phase behavior. Parameters for this equation that were determined in this study were then used in updating the ASPEN™ simulation of the ORNL process.

2. THEORETICAL BACKGROUND

2.1 Equations of State.

The development of an equation of state capable of predicting dense gas or liquid properties with desired accuracy has been a difficult task. Nevertheless, scientists have continued the struggle using the fundamental theories of thermodynamics in tandem with more sophisticated equations of state to obtain more accurate results. Almost a century after the development of the ideal gas law, van der Waals' equation,

$$\left(P + \frac{n^2 a}{V^2}\right)(V - nb) = nRT \tag{6}$$

where

P = absolute pressure,

V = total volume,

n = total number of moles,

R = universal gas constant, and

T = absolute temperature,

was published. Van der Waals attempted to improve the ideal gas law by adding a term,

$$\frac{n^2 a}{V^2} \tag{7}$$

where a is an empirical constant, to account for the attractive intermolecular forces. He reasoned that the pressure on the vessel would decrease as the at-

tractive forces increased, as they would at high density. He also subtracted a term , nb, from the system volume to account for the volume occupied by the molecules themselves. The constant b, called the excluded volume for a pair of molecules and illustrated in Figure 2, is given by the equation

$$b = \frac{4}{3}\pi l^3, \tag{8}$$

where l is the molecular diameter. This is four times the molecular volume. Van der Waals' equation, written in the pressure explicit form is as follows:

$$P = \frac{nRT}{(V - nb)} - \frac{n^2 a}{V^2}. \tag{9}$$

Although this equation is not very accurate at high densities, its development was monumental in that the empirical constants have a basis in physical reality. Rearrangement of equation 6 yields a cubic form in volume,

$$V^3 - \left(nb + \frac{nRT}{P}\right) V^2 - \frac{n^2 a}{P} V - \frac{n^3 ab}{P} = 0. \tag{10}$$

While the van der Waals' equation is the simplest of the cubic equations of state, the nontrival nature of the mathematics involved in seeking roots can be recognized. In order to solve for the constants a and b, a least-squares fit of experimental data was required. However, since a and b have a physical basis, it is possible to predict them from fundamental properties. All equations of state should satisfy the law of mechanical stability (Prausnitz 1969; Martin and Hou 1955) at the critical point,

$$\frac{\partial P}{\partial v} = \frac{\partial^2 P}{\partial v^2} = 0. \tag{11}$$

It is also obvious that at the critical point

$$v = v_c. \tag{12}$$

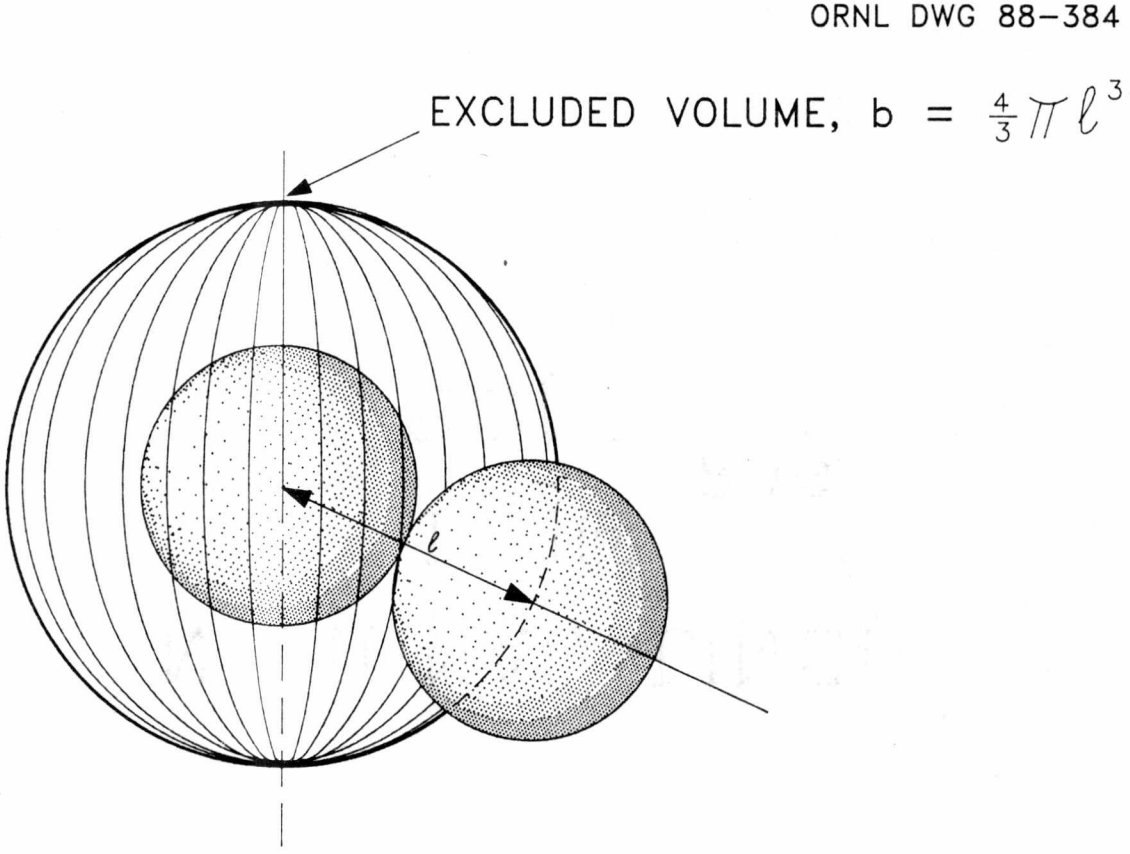


Figure 2. Van der Waals' excluded volume.

Equations 11 and 12, when applied to equation 10, led to the following generalizations:

$$a = \frac{27R^2T_c^2}{64P_c} \tag{13}$$

and

$$b = \frac{RT_c}{8P_c}. \tag{14}$$

These generalizations transformed van der Waals' equation into a useful two-constant equation of state that did not require volumes of VLE experimental data to predict pure component properties.

The van der Waals equation was also found to be applicable to gas mixtures. Van der Waals proposed mathematical combinations of the pure component properties, called mixing rules, that would allow the prediction of mixture properties. As would be expected since the theoretical bases of a and b are different, the mixing rules for these two constants are not the same. The mixing rule for the constant predicting attractive forces, a, is given as

$$a_{\text{mix}} = \sum_i \sum_j x_i x_j \left(a_i a_j\right)^{0.5}. \tag{15}$$

The term a_{ij} was shown to be equal to the geometric mean of the pure component constants.

$$a_{ij} = \sqrt{a_{ii}a_{jj}} \tag{16}$$

Although van der Waals' choice of the geometric mean was determined empirically, studies in quantum mechanics have given Eq. 16 some theoretical basis. This application of quantum mechanics to the study of intermolecular forces, as described by Prausnitz (1969), determined that the attractive potential between

two dissimilar molecules, Γ_{ij}, is approximately given as the geometric mean, as shown in Equation 17.

$$\Gamma_{ij} = \sqrt{\Gamma_{ii}\Gamma_{jj}} \tag{17}$$

This hypothesis, called the "geometric-mean rule", is frequently used in modern equations for explaining the attractive forces of mixtures, as is Eq. 15. It is also possible to make reasonable predictions for the distance or volume-rated mixing rules. The simplistic assumption of averaging the distance and volume-rated properties of unlike molecules is used frequently. For example, the intermolecular seperation for dissimilar molecules at zero potential energy, σ_{ij} using the hard-sphere model of molecular interaction is given as

$$\sigma_{ij} = \frac{1}{2}\left(\sigma_{ii} + \sigma_{jj}\right). \tag{18}$$

Because mixing rules like Eq. 18 have been shown to provide good results (Prausnitz 1969), the arithmetic mean is often used for volume or distance related properties. Therefore, the relationship proposed by van der Waals for the term explaining repulsive forces,

$$b_{\text{mix}} = \sum_i x_i b_i. \tag{19}$$

is also used widely in the more modern equations of state for predicting repulsive forces at low densities.

The next major step in the development of cubic equations was the Redlich–Kwong equation of state (Redlich and Kwong 1949). The pressure explicit form,

$$P = \frac{RT}{v-b} - \frac{a}{T^{0.5}v\left(v+b\right)} \tag{20}$$

where,

$$a = \frac{0.4278 R^2 T_c^{2.5}}{P_c} \tag{21}$$

and

$$b = \frac{0.0867 R T_c}{P_c} \tag{22}$$

appears to be similar to the van der Waals equation. The improvements proposed by Redlich and Kwong affected only the term to the right of the minus sign which explains the attractive interaction. The introduction of a temperature dependence to explain this phenomenon greatly increased the accuracy to the equation. Although many mixing rules can be considered with this equation of state, as discussed by Reid, Prausnitz, and Sherwood (1977), the mixing rules chosen for the van der Waals equations, Eqs. 15 and 18, are the used most frequently. The simplicity and improved accuracy of the Redlich-Kwong equation of state have led many to offer improvements.

Many thermodynamicists, aware of the success of the Redlich-Kwong equation, have pursued the study of the cubic equations of state. These polynomial equations of state are capable of yielding the ideal gas equation as the molar volume approaches infinity and of representing both liquid and vapor volumes at sufficiently low temperatures for many gas mixtures. The general pressure explicit form of the cubic equation of state may be written as follows (Abbott 1979):

$$P = \frac{RT}{v - b} - \frac{\varsigma (v - \eta)}{(v - b)(v^2 + \delta v + \epsilon)}. \tag{23}$$

Equation 23 can be considered a generalization of the van der Waals' equation of state where b, δ, ϵ, ς, and η depend upon temperature, composition, and

the chemical species of which the system is comprised. The first term to the right of the equal sign describes the repulsive forces between molecules and is identical to the van der Waals' repulsive term. The second term on the right side of the equation describes the attractive forces between molecules. It is interesting to note that the cubic equations of state offer no improvement to van der Waals' assumptions regarding the repulsive interaction inspite of its being shown to be incorrect (Carnahan and Starling 1972). Nevertheless, the simplicity of computerized data regression and the many reported successes of some recent cubic equations of state have led to their frequent use.

The choice of mixing rules while partially explained or supported by theory is often more empirical in nature. In order to understand the uncertainty of these mixing rules, one must consider the virial equation

$$Z = \frac{PV}{RT} = 1 + \frac{B}{V} + \frac{C}{V^2} + \frac{D}{V^3} + \ldots \tag{24}$$

Here, Z is the compressibility factor, B is the second virial coefficient, C the third, and so on. The second virial coefficient for a mixture of m components is given by

$$B_{\text{mix}} = \sum_{i=1}^{m} \sum_{j=1}^{m} y_i y_j B_{ij}. \tag{25}$$

In words, the second virial coefficient explains the two body interactions in a mixture. This mixing rule, Eq. 25 is thermodynamically rigorous. Similarly, the third coefficient explains the three body interactions, etc. In order to rigorously predict the properties of gas or liquid mixtures, regardless of their complexity, one must be able to accurately predict the m body interactions. This presents a great deal of difficulty since engineers cannot, with a high degree of confidence, predict molecular interactions above second order for some of the more complex

mixtures. Fortunately, the two body interactions are the largest contributor at lower densities as is evident from the success of the virial equation truncated after the second virial term. As densities increase, the higher level interactions become more important.

The cubic equations of state, like the virial equation truncated after the second virial term, only account for two-body interactions. Therefore, as Abbott (1979) explains, all of the mixing used in the study of cubic equations are variations of the general quadratic mixing rule

$$Q_{\text{mix}} = \sum_i \sum_j x_i x_j Q_{ij}. \tag{26}$$

Although totally empirical, Eq. 26 has become widely accepted as successful. This equation states that any parameter of a mixture, Q, can be determined from binary interactions. Q_{ij} represents the interaction between two dissimilar molecules. If $i = j$, then $Q_{ij} = Q_{ii} \equiv Q_i$. This is the parameter for the pure component. However, if $i \neq j$, the prediction of Q_{ij} becomes more difficult. The rationale presented in explaining equations 15 and 18 along with purely mathematical reasoning have led to the basic adoption of these equations. This is especially true with the b term, since engineers consistently use the same assumption as van der Waals.

The more recent cubic equations of state, while accepting that this reasoning is sound, offer an improvement to predict the attractive interaction parameters, given here as Q_{ij}.

$$Q_{ij} = (1 - k_{ij}) \sqrt{Q_i Q_j}. \tag{27}$$

The term k_{ij}, called the interaction parameter, describes the two-body interaction. $k_{ij} = 0$ if $i = j$ and is usually a small number. This new parameter gives

improved accuracy to the cubic equations of state, but requires that experimental binary data be at hand. This data must also be accurate as the cubic equations are very sensitive to the interaction parameter. Nevertheless, the acceptance of Eqs. 18 and 26 allow one to predict the properties of multicomponent systems with no more than binary data.

One of the more recent cubic equations of interest in this study is the three-constant Redlich–Kwong–Soave (RKS) equation of state (Soave 1972). The RKS equation of state for pure substances is given as

$$P = \frac{RT}{v-b} - \frac{a(T)}{v(v+b)}, \tag{28}$$

where

$$a_i(T_{c_i}) = a_{c_i} = 0.42747\frac{R^2T_{c_i}^2}{P_{c_i}}, \tag{29}$$

$$b_i = 0.08664\frac{RT_{c_i}}{P_{c_i}}, \tag{30}$$

$$a_i(T) = a_{c_i}\alpha_i(T), \tag{31}$$

$$\alpha_i^{0.5} = 1 + m_i\left(1 - T_{r_i}^{0.5}\right), \tag{32}$$

$$m_i = 0.480 + 1.574\omega_i - 0.176\omega_i^2, \tag{33}$$

and ω_i = accentric factor of component i.

In order to extend this equation to binary mixtures, Eq. 28 may be used along with the following mixing rules.

$$a_{\text{mix}} = \sum_i \sum_j x_i x_j \left(a_i a_j\right)^{0.5}\left(1 - k_{ij}\right) \tag{34}$$

and

$$b_{\text{mix}} = \sum_i x_i b_i \tag{35}$$

The quantity k_{ij} is an empirical correction factor which must be determined experimentally for each binary pair in the mixture. No higher interaction terms are required. For simple hydrocarbon mixtures, the interaction parameter is taken as zero. Also because of its simplicity and accuracy, the RKS equation of state was chosen by Huron, Dufour, and Vidal (1978), to study hydrocarbon systems containing hydrogen sulfide or carbon dioxide. In that study, it was concluded that critical points and liquid-vapor equilibria are correctly represented by the Soave equation in the entire range of vapor-liquid co-existence for these mixtures.

Another cubic equation of state of interest is the Peng-Robinson (PR) equation of state (Peng and Robinson 1976). The equation is given as

$$P = \frac{RT}{v-b} - \frac{a(T)}{v(v+b)+b(v-b)}, \tag{36}$$

where

$$a_i(T_{c_i}) = a_{c_i} = 0.45724\frac{R^2T_{c_i}^2}{P_{c_i}}, \tag{37}$$

$$b_i = 0.07780\frac{RT_{c_i}}{P_{c_i}}, \tag{38}$$

$$a_i(T) = a_{c_i}\alpha_i(T), \tag{39}$$

$$\alpha_i^{0.5} = 1 + m_i\left(1 - T_{r_i}^{0.5}\right), \tag{40}$$

$$m_i = 0.3746 + 1.5423\omega_i - 0.2699\omega_i^2$$

$$\text{for} \quad 0 < \omega_i < 0.5, \tag{41}$$

and

$$m_i = 0.3796 + 1.4850\omega_i - 0.1644\omega_i^2 + 0.01667\omega_i^3$$

$$\text{for} \quad 0.2 < \omega_i < 2.0. \tag{42}$$

Both Eq. 41 and 42 yield the same result when $0.2 < \omega < 0.5$.

In order to extend the PR equation to systems of more than one component, the following mixing rules are suggested.

$$a_{\text{mix}} = \sum_i \sum_j x_i x_j \left(a_i a_j\right)^{0.5} \left(1 - k_{ij}\right). \tag{43}$$

and

$$b_{\text{mix}} = \sum_i x_i b_i \tag{44}$$

where k_{ij} ,here, is the fitted parameter characteristic of the ij two-body molecular interaction.

The success of the PR equation of state for a chemically similar system to that of interest in this study was demonstrated by Mathias and Stein (1983). In their study, the PR equation of state was used as a phase equilibrium model for the SRC-1 coal liquefaction process. They state the accuracy and reliability of the PR equation of state for nonpolar mixtures, the superiority of the PR equation of state over the RKS equation in determining liquid densities, and the favorable computational characteristics as reasons for choosing the PR equation of state. Because of the success of Mathias and Stein, along with the chemical similarity of the system studied in their work, the PR equation of state was chosen to study the CO_2–CH_4–H_2S system in addition to the RKS equation.

The study of cubic equations of state has become a fast growing field. Many modifications have already been proposed to the improved cubic equations of state. One such example is the improved Peng–Robinson equation of state proposed by Stryjek and Vera, namely the Peng–Robinson–Stryjek–Vera (PRSV)

equation of state (Stryjek and Vera 1986). Considerable errors are realized in predicting phase behavior for all compounds with large accentric factors with the original PR equation at all temperatures. This led to the following improvement to the PR equation of state,

$$m_i = m_{0_i} + m_{1_i} \left(1 + T_{r_i}^{0.5}\right) \left(0.7 - T_{r_i}\right) \tag{45}$$

with m_{0_i} and m_{1_i} being adjustable parameters for each pure compound. At reduced temperatures above 0.7, the PRSV falls back to essentially the PR equation. Because the low accentric factor of the compounds of interest in the current study, the PRSV equation of state has not been applied to the current work.

Equations of state are also being introduced that better predict the properties of gases at higher densities. These equations range in complexity from the Carnahan and Starling (1972) equation, which suggests using the correct hard-sphere equation of state as the repulsive term in the Redlich–Kwong equation of state, to the work of Whiting (1982). Whiting has assumed that the repulsive forces of the molecular-interaction could be explained by the hard-sphere equation of state, the attractive forces by the square-well equation, and that the rotational and vibrational degrees of freedom were density dependent. Works, such as these, are drawing the study of gases and liquids closer together.

2.2 Thermodynamic Consistency.

Before developing or testing a new equation of state for vapor-liquid equilibrium calculations, two very important things must be accomplished. First, the

necessary vapor-liquid equilibrium data must be obtained and, secondly, these data must be tested for thermodynamic consistency. In order to prove that data are thermodynamically consistent, they must satisfy the Gibbs-Duhem equation. The Gibbs-Duhem equation states that at constant temperature and pressure,

$$\sum_i x_i dM = 0, \tag{46}$$

where M is any partial molar property. If the data satisfy this equation, they are not necessarily correct. However, failure to satisfy the equation means that the data are incorrect.

Thermodynamic consistency tests have been proposed (Redlich and Kister 1948; Herington 1947) for low pressure isothermal data. Since, in this study, we were approaching the critical point of the gas mixtures, a method proposed by Chueh, Muirbrook, and Prausnitz (1965) was used. Prausnitz (1969) shows how this useful method was derived. He first wrote the Gibbs-Duhem equation as follows for a binary mixture

$$x_1 d\ln f_1 + x_2 d\ln f_2 = \frac{v^L dP}{RT} \tag{47}$$

where

x = mole fraction of the liquid phase,

f = fugacity,

v^L = molar volume of the liquid phase,

and subscript 2 refers to the light component in the mixture. Using the identity $x_1 d\ln x_1 + x_2 d\ln x_2 = 0$, he rewrote the equation,

$$\ln\frac{f_2/x_2}{f_1/x_1} dx_2 + \frac{v^L dP}{RT} = d\left[\ln\frac{f_1}{x_1} + x_2 \ln\frac{f_2/x_2}{f_1/x_1}\right]. \tag{48}$$

We can further modify the equation by using the fugacity coefficients, φ, and K factors, where $K_i = y_i/x_i$, to obtain

$$\left(\ln\frac{\varphi_2}{\varphi_1} + \ln\frac{K_2}{K_1}\right) dx_2 + \frac{v^L dP}{RT} = d\left[\ln K_1 + \ln\varphi_1 P + x_2\left(\ln\frac{\varphi_2}{\varphi_1} + \ln\frac{K_2}{K_1}\right)\right]. \tag{49}$$

A useful equation can be obtained by applying the following boundary conditions at $x_2 = 0$:

$$\varphi_1 = \varphi_1^s, P = P_1^s, \text{ and } K_1 = 1$$

where the s refers to saturation. Given these conditions, equation 48 can be integrated to yield

$$\text{Area I} + \text{Area II} + \text{Area III} = \left[\ln K_1 + \ln\frac{\varphi_1 P}{\varphi_1^s P_1^s} + x_2\left(\ln\frac{\varphi_2}{\varphi_1} + \ln\frac{K_2}{K_1}\right)\right] \quad (\text{at } x_2) \tag{50}$$

where

$$\text{Area I} = \int_{x_2=0}^{x_2} \ln\frac{K_2}{K_1} dx_2 \tag{51}$$

$$\text{Area II} = \int_{x_2=0}^{x_2} \ln\frac{\varphi_2}{\varphi_1} dx_2 \tag{52}$$

$$\text{Area III} = \frac{1}{RT}\int_{x_2=0}^{x_2} v^L dP. \tag{53}$$

Equations 51 to 53 apply for compositions of $x_2 = 0$ to $x_2 = x_2$, whereas, the right side of equation 50 deals only with the composition at $x_2 = x_2$. The data gathered for this study consists of temperature, mole fractions, and pressures. Therefore, to use equations 50 to 53, equations of state must be used to calculate

the molar volume of the liquid, the fugacity coefficients, and the saturation properties. The difference between the right and left sides of equation 50 is then compared to the mathematical mean to determine the inconsistency.

3. EXPERIMENTAL

3.1 Apparatus.

High pressure vapor-liquid equilibrium experiments can be divided into two categories according to the method with which the material compositions are determined. The first of these, the synthetic method, employs mixtures of known composition and mass balances in such a way that eliminates the need for analysis of the equilibrium phases. As discussed by Adams (1986), the synthetic methods are catagorized according to whether (a) the equilibrium cell has a constant volume and contains a constant quantity of the mixture being studied, or (b) the volume or quantity of material in the equilibrium cell is varied. In the constant volume cell, carefully prepared samples are placed in the transparent cell and the temperature and pressure are varied until a phase transition is observed. In the latter case, either the volume or quantity of material is varied at constant temperature. A plot of pressure versus volume or composition will be smooth until a phase transition takes place. The synthetic method, as stated earlier, does not require measurement of the various phases at equilibrium. This is attractive because in many cases measurements of the vapor and liquid phases can upset equilibrium. However, a great deal of time is consumed in the preparation of the samples being charged into the equilibrium cell and the synthetic method has been shown to be inaccurate for measuring the dew point of very dilute gas mixtures.

The second type of VLE method, the analytic method, determines material compositions through sampling of the vapor and liquid phases at equilib-

rium conditions. The analytic method can be further classified into the static, dynamic, and circulation categories according to the way in which the phases are brought into contact (Adams 1986). In the static method, the two fluids are placed in a constant volume container and equilibrated through an internal mixer or by rocking the entire container. The dynamic method brings the materials together in a central contacting vessel which has a known residence time and flow pattern. The circulation method, which has been chosen in this work, contains the advantages of the static and dynamic methods. In this type of system, one or both of the phases are recirculated through the other.

The apparatus chosen in this work, shown in Figure 3, is similar in concept and design to that described by Nasir, Martin, and Kobayashi (1980). However, this static volume VLE apparatus has been modified to study the CH_4–CO_2–H_2S systems near the vapor-liquid critical region and to allow for a more workable operating procedure.

The apparatus, while seeming complicated because of the complex one-eighth inch 316 stainless steel tubing network, is actually quite simple. A schematic diagram of the experimental apparatus may be seen in Figure 4. The heart of the system is a static-volume-equilibrium cell (EC). The EC is a standard 300 cc AUTOCLAVE^{TM} made of 316 stainless steel. Modifications were completed to accommodate vapor and liquid sample ports, a vacuum line, a vapor recycle line, and a platinum resistance thermometer (PRT).

The vapor-liquid mixtures to be studied were added to the EC and allowed to reach thermal equilibrium before samples were taken. In order to hasten the establishment of equilibrium, a Ruska Instrument Corporation (RIC) model 2330-802 magnetic pump was installed to circulate the vapor phase through

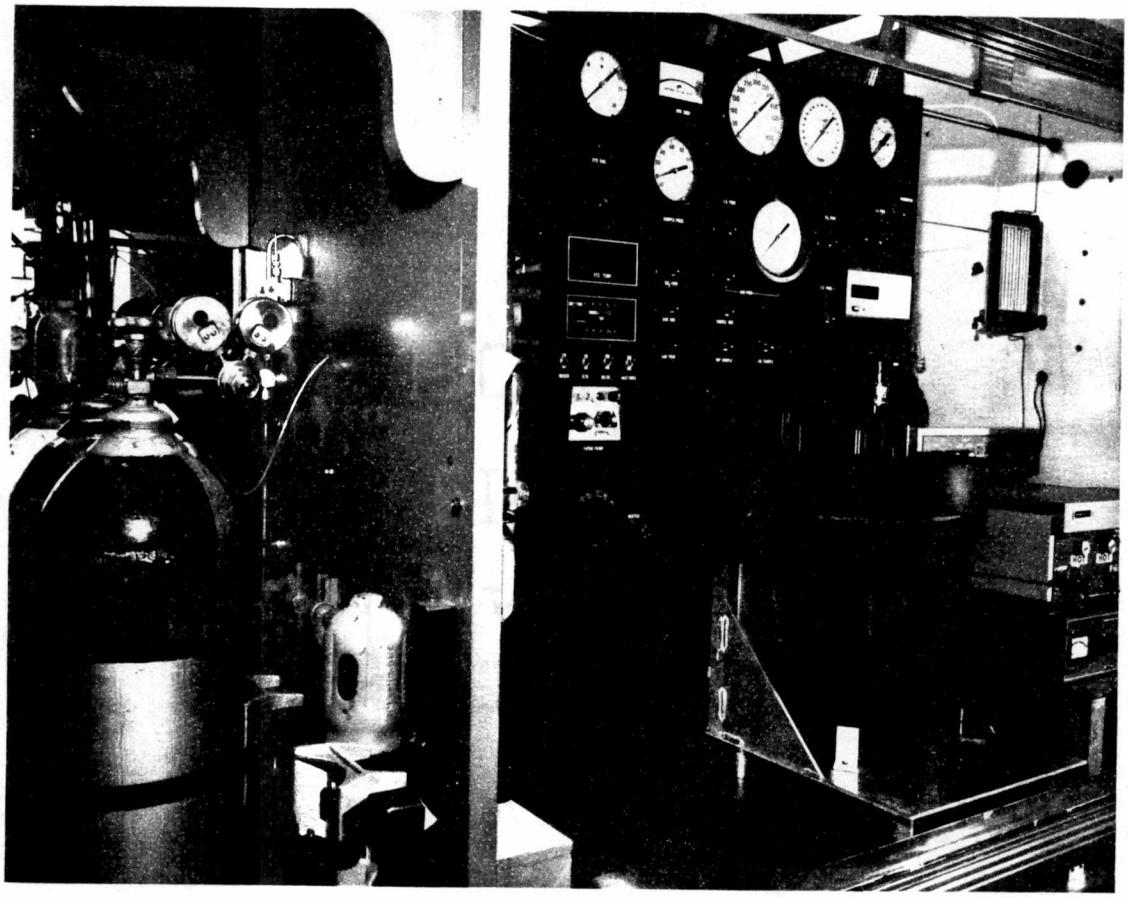


Figure 3. Photograph of VLE apparatus.

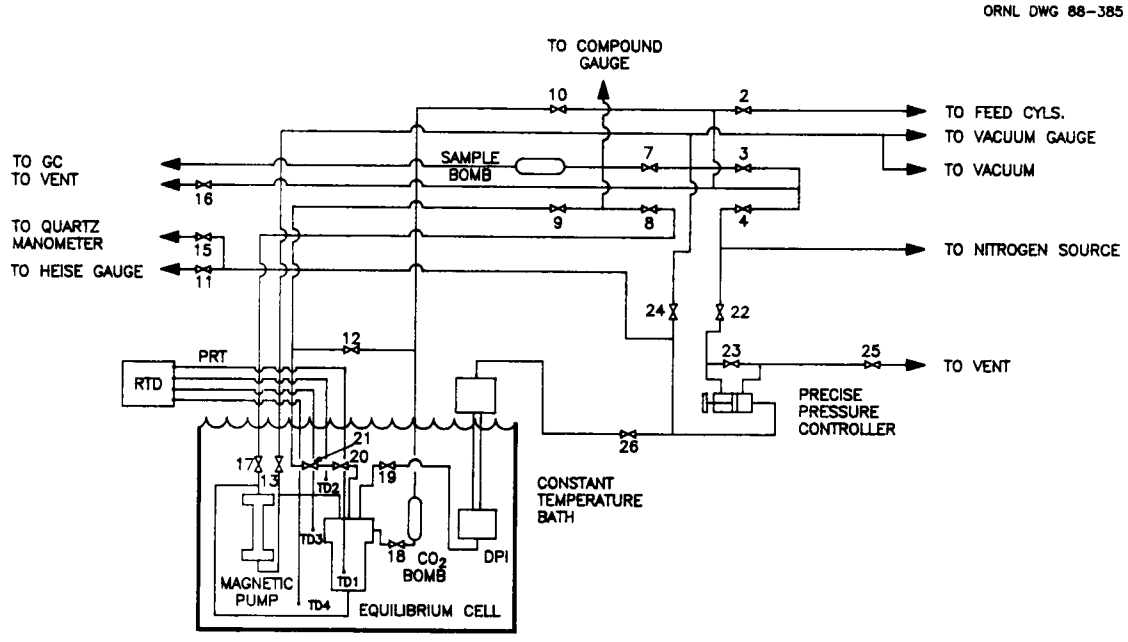


Figure 4. Schematic of the experimental apparatus.

the liquid phase. Early experiments revealed malfunctions of this pump, which were later attributed to expansion of a teflon sleeve at temperatures less than approximately $-35°C$. This limitation fixed the lower temperature limit of these studies. Further, the sensitivity of the electronic pressure instrumentation, described later, was such that sampling of the material was impossible when the pump was in operation. To prevent this interference, the pump was turned off prior to any sampling. This had no deleterious effects on the system's operation.

To prevent exposure of corrosive materials to the pressure instrumentation, the apparatus was equipped with a RIC Model 2439-702-41000 differential pressure null transducer (DPI). This device consisted of a diaphragm separating the corrosive sample mixture and an inert gas. An analog signal, which is proportional to the size of the diaphram deflection, is sent to the RIC Model 2416-711 differential pressure null indicator. When the inert gas pressure equals the pressure of the sample mixture, the deflection of the diaphram is at a minimum, and the null indicator signals zero deflection. This combination of equipment resulted in high sensitivity as pressure differentials of 6.0×10^{-4} psia could be detected. Fine adjustments in the inert gas are accomplished by using a RIC Model 3893-801 Precise Pressure Controller. Finally, the inert gas pressure of the DPI diaphragm was measured by a Mensor Corporation Model 10100-001 quartz manometer (QM). The quartz manometer, which was calibrated using a dead-weight gauge, provided a maximum error of 0.01 percent.

A temperature bath was constructed to house the parts of the apparatus containing the sample mixtures. The bath was made up of a 5-gallon carboy covered with two inch polyurethane insulation. The bath temperature was controlled by a FTS Systems Inc. FLEXI-COOL^{TM} cooler. This two-stage "freon"

system is capable of obtaining temperatures to -100°C. However, because of the large volume and high inertia of the bath and the less than acceptable control sensitivity of the FLEXI-COOL^{TM} cooler, the bath could only be controlled to about ±3°C of the desired temperatures of this study, when no special precautions were taken. The bath temperature was, however, controlled to ±0.1°C during the experimentation by manually operating the cooler controls. This technique involved manually controlling the bath and EC temperatures to about 0.1°C below the desired temperature, allowing the bath to slowly heat to the desired temperature, then recording the pressure measurement and taking samples when the digital temperature display hesitated for about five seconds at the desired temperature. The bath medium used in this study was approximately 50 volume percent ethylene glycol in water. A 250-watt Calrod heater was installed to hasten the bath temperature changes. A photograph of the EC and magnetic pump as they are mounted in the bath is shown in Figure 5.

The bath and EC temperatures were measured with a Doric Scientific Model 400A resistance temperature detectors (RTD) with PRT located in the EC and in the top, middle, and bottom of the bath. The accuracy of the temperature measurement equipment when calibrated with liquid nitrogen and boiling water was about ±0.1°C. During the experimentation, the temperature gradient measured by the four PRTs was less than or equal 0.1°C.

The collection of sample compositions was accomplished by using several components. The vapor samples were removed from the EC and directly expanded into the 75cc sample bomb. The liquid sample was also expanded in this vessel, but was first trapped in a small one-eighth (.464cc) inch tubing loop. This sample bomb was equipped with a compound pressure gauge. While

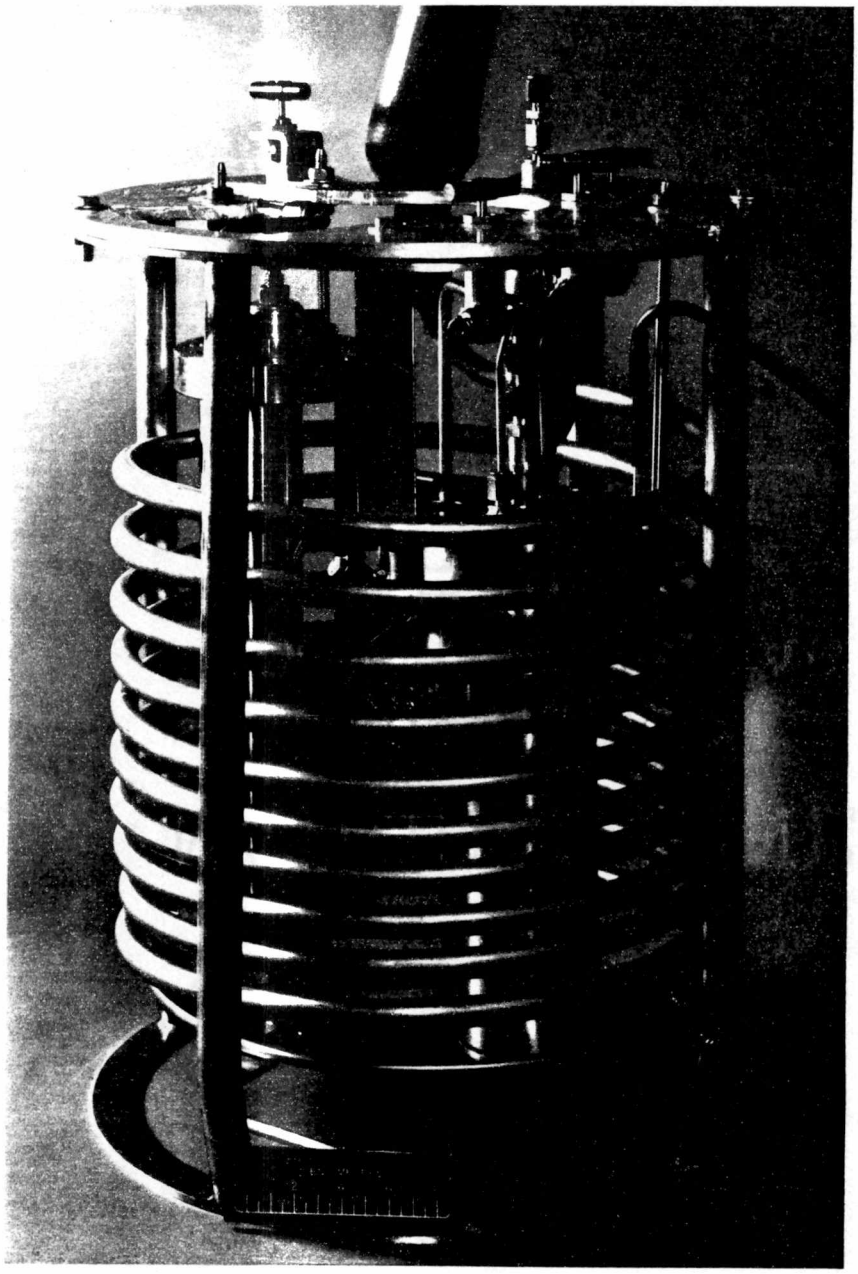


Figure 5. Photograph of EC and magnetic pump.

some VLE work has been conducted using spectrophotometry (Konrad, Swaid, and Schneider 1983; Swaid, Nickel, and Schneider 1985), gas chromatography has been more widely used analytical tool. In this study, the vapor and liquid compositions were measured by a Carle Instrumentation, Inc. Model 111-H analytical gas chromatograph (GC) which is equipped with a thermal conductivity detector. The integration of the chromatograms was accomplished using a Spectra-Physics Model SP4100 computing integrator. A discussion of the accuracy of the composition measurements is included in Section 4.5.

Finally, any discussion of the apparatus would be incomplete without some discussion of the valves. Frequent manipulations of the valves, extremely cold temperatures upon discharge of the system, and possible over tightening of the valve seats upon closing eventually led to leakages through the first valves used in the system, which contained stainless steel seats. After considerable experimentation, NUPRO^{TM} bellows seal valves with replaceable teflon seats were employed. Two models were installed, cat. no. SS-2BK in the temperature bath and cat. no. SS-2H elsewhere. The former valves were chosen for the temperature bath rather than the latter simply because they could be fitted with a valve stem extension which could penetrate the bath insulation. The highest pressure measurement capability of this apparatus was limited because these valves are rated only to 1000 psig.

3.2 Generalized Procedure.

Three experimental procedures were performed on the VLE apparatus. The first and most simple experiment was to collect vapor pressure data. Several

data points were taken with CO_2 to confirm the calibration of the pressure and temperature instruments. In order to collect this data, the following steps were followed. First, the temperature control setting on the FLEXI-COOL™ cooler was adjusted to the desired temperature and time was allowed for the bath to equilibrate. While allowing the bath temperature to adjust, the sample side of the system was purged with the feed gas. The liquid charge was then introduced to and isolated in the 75cc liquid bomb before being fed into the EC. This step prevented a waste of the liquid materials and allowed the stepwise pressurization of the cell required by the DPI. Next, nitrogen was introduced to the instrument side of the DPI and the liquid charge was bled into the EC in approximately 100 psia increments until no change in pressure was detected upon sample introduction. At this point, the magnetic pump was turned on, adjustments were made to the differential pressure null indicator, and the sample was allowed to equilibrate. Additional liquid was charged to the liquid bomb and subsequently to the EC and the system was allowed to equilibrate to assure that liquid did exist in the system before recording the data. Finally, the magnetic pump was turned off, the differential pressure null indicator was adjusted by the precise pressure controller, and the pressure was recorded from the quartz manometer.

The majority of experimental data collected with this apparatus were on binary systems, in particular the CO_2–CH_4 and CH_4–H_2S systems. A considerable amount of liquid was required in the EC because of vaporization of the liquid phase upon the addition of the more volatile component. Since the equilibrium cell contents could not be observed, two experimental techniques were used to determine if the amount of liquid present would be adequate after addi-

tion of the more volatile material. First, the vapor pressure of the liquid phase was measured after charging the system as described above. If the pressure of the system was the same as the vapor pressure of the liquid phase, the presence of a liquid phase was confirmed. However, the mere existence of this phase was not adequate. Some measurement of the quantity of liquid was needed to give some assurance that enough liquid would be present after adding the more volatile component. After considerable experimentation, the second technique was developed. This technique involved trapping a liquid sample in the tubing loop and expanding this sample into the sample bomb. A pressure of 40 to 60 psig on the compound gauge upon expansion of this liquid sample was an indication that the liquid phase level, at least, reached the liquid sample inlet. At this point the more volatile gas was added. If the pressure appeared to be lower than expected vapor pressure or a liquid sample expansion in the sample bomb resulted in a pressure of less than 40 psig, the system was purged and more liquid was introduced to the EC as described earlier. Upon confirming that the liquid phase was present at the liquid sample inlet, the liquid bomb and associated piping were vented and purged with the lighter constituent. The feed cylinder containing the more volatile component was then opened directly to the liquid bomb and introduced to the EC until the desired pressure had been obtained. Again, a liquid sample was taken and its pressure measured to ensure that adequate liquid was available to begin sampling. If not, the system was vented and liquid was once again added. Finally, the magnetic pump was turned on and the system was allowed to equilibrate. To begin the sampling of the binary systems, the magnetic pump was turned off and both the vapor and liquid tubing between the EC and sample bomb were purged. This lengthy

process consisted of alternately expanding 40 to 60 psig quantities of liquid and vapor samples into the sample bomb and determining the compositions on the GC. A leveling or reduction of the less volatile constituent composition in the sample gas indicated that the lines were purged. The binary data reported in this work were those collected as the light component composition reached a maximum.

The final data collected were three data points for the CH_4–CO_2–H_2S system. Because H_2S was desired to be a minor constituent, piping modifications to the system allowed the H_2S to be introduced to the EC via the liquid sample loop (i.e. the H_2S entered the EC via valves 2, 10, 12, 20, and 21). This allowed the H_2S to be added in small quantities. After the addition of the H_2S, the procedure became similar to that described above for binary mixtures. The CO_2 was added just as it was for the binary CO_2–CH_4 studies, as was the CH_4.

3.3 Materials.

The compressed feed gases, with the exception of methane, were obtained from the Alphagaz Specialty Gases Division of Liquid Air Corporation. The methane was purchased from the Linde Division of Union Carbide Corporation. The methane and hydrogen sulfide was of C.P. grade while the carbon dioxide was Bone Dry Grade. The minimum purity of the feed gases were given as: methane, 99.5 percent; hydrogen sulfide, 99.6 percent; and carbon dioxide, 99.8 percent.

The gas standards used to calibrate the gas chromatograph were both "certified standards". Mixtures of carbon dioxide and methane were obtained from

Matheson Gas Corporation for calibration of the chromatograph for the binary tests involving these constituents, while ternary mixtures of carbon dioxide, methane, and hydrogen sulfide were obtained from Liquid Air Corporation for the tests involving the CH_4–H_2S and the CH_4–CO_2–H_2S systems. The analytical accuracy of these gas standards was reported to be ± 2 percent of the measured components.

4. RESULTS AND DISCUSSION

The experimental plan consisted of three parts. First, the accurate measurement of pressure was to be demonstrated by collecting carbon dioxide vapor pressure data and comparing the results with the literature. The methods for acquiring accurate mole fraction data would, then, be developed and demonstrated by collecting VLE data for the CO_2–CH_4 system and comparing these with the literature. After demonstrating some competency at acquiring these measurements, the experiment focused on expanding the database. Measurements of VLE data not sighted in the literature were collected for the CO_2–CH_4 and CH_4–H_2S systems and a few points for the CO_2–CH_4–H_2S were also obtained. Binary interaction parameters were regressed from the data and the predictions of the PR and RKS equations were compared with the experimental data. Thermodynamic consistency tests were performed on this VLE data and the measurement error was determined.

As stated earlier, one of the benefits of using cubic equations of state is the prediction of multicomponent properties from the binary properties. In order to test this for the CO_2–CH_4–H_2S system, binary interaction parameters were obtained for the CO_2–H_2S system using the data in the literature, these parameters were combined with the binary parameters of the CH_4–CO_2 and CH_4–H_2S systems, and ternary properties were calculated.

4.1 Carbon Dioxide Vapor Pressure.

The first experimentation performed with the VLE apparatus was vapor

pressure measurements of carbon dioxide. The accuracy of the pressure measurement is influenced by the pressure instrumentation. However, it is also greatly affected by the experimental technique. Small variations in temperature could result in increased pressure measurement error. Since the temperature measurement appeared to be accurate to about $\pm 0.1^{o}$C this experiment was designed to determine the accuracy of the pressure measuring equipment and the method of collecting this data.

The results of this work are shown graphically in Fig. 6, along with the results of Donnelly (1954) and Stull (1947). As is shown the temperature range covered in this study ranged from 243.2 K to 298.2 K. Excellent agreement is demonstrated with the literature. In order to quantitatively analyze the accuracy of the data, the results obtained in this study were compared with predicted vapor pressure data from the Huang (1984) equation of state for carbon dioxide. This twenty-seven constant equation has been shown to provide accurate VLE data for carbon dioxide in the entire fluid region and at the phase boundaries. In comparison with vapor pressure data in the 217.2 K to 304.2 K range (Michels et al. 1937, 1950), the predictions from this equation were found to deviate from the experimental data by less than ± 0.15 percent.

The comparison of the experimental vapor pressure data from the current work with the Huang equation is shown in Table 2. With the exception of the last value in this table, the percent deviation of the calculated value to the experimental value is less than 0.5 percent, with the predictions of the equation being slightly lower than the experimental data in most cases. The reproducibility of the pressure measurements is demonstrated with the duplicate samples taken at 283.2 K and 288.2 K. Vapor pressure differences of 0.7 and 0.2 psia were ob-

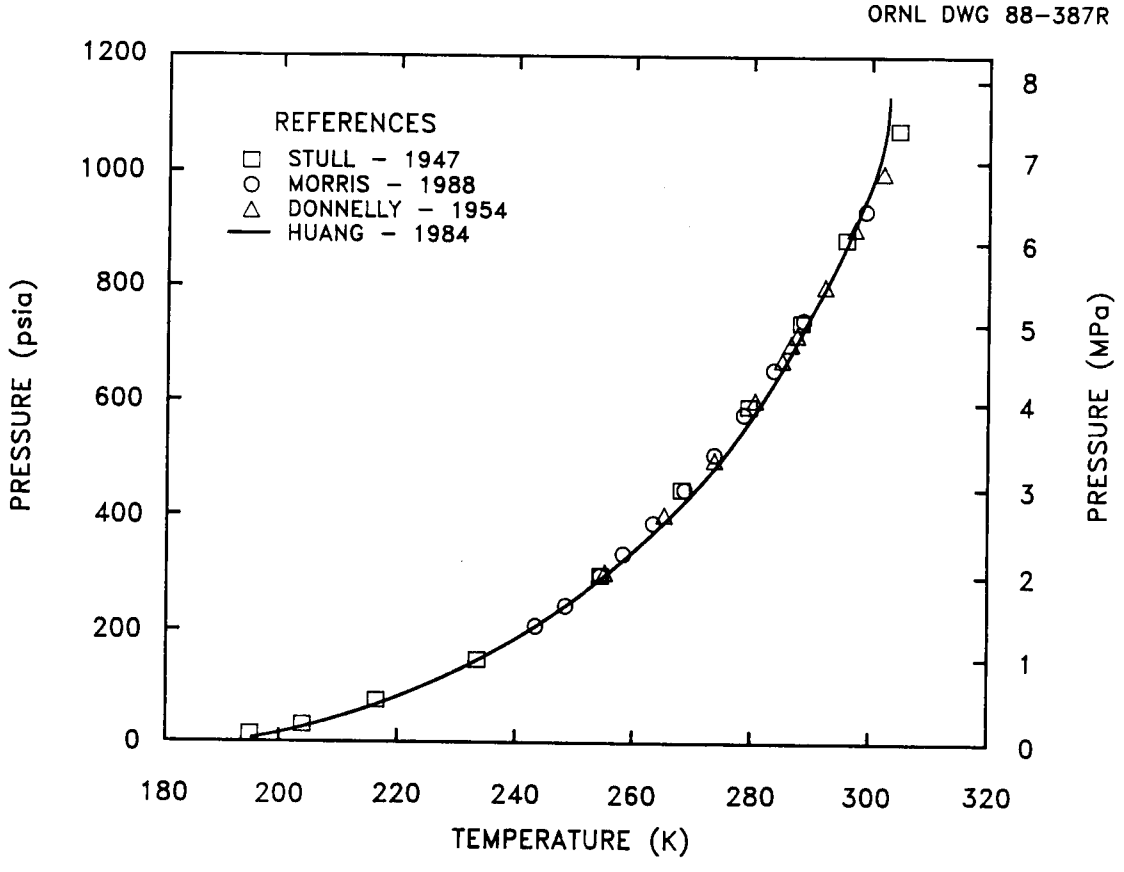


Figure 6. Carbon dioxide vapor pressure data.

Table 2. Carbon dioxide vapor pressure results.

Temp.	Vapor Pressure (psia)		Deviation
(K)	Expr.	Calc.	(percent)
243.2	207.3	207.1	-0.0965
248.2	243.9	244.4	0.2052
254.2	295.6	294.6	-0.3383
258.2	332.7	332.3	-0.1202
263.2	385.0	384.0	-0.2597
268.2	442.6	441.4	-0.2711
270.0	465.1	464.8	-0.0645
273.2	507.1	505.0	-0.4141
278.2	577.0	575.2	-0.3120
283.2	654.6	652.4	-0.3361
283.2	653.9	652.4	-0.2294
288.2	738.5	737.4	-0.1490
288.2	738.7	737.4	-0.1760
293.2	831.4	830.3	-0.1323
298.2	925.4	933.3	0.8537

served at 283.2 K and 288.2 K, respectively. The vapor pressure measurement at 298.2 K was difficult to obtain because the carbon dioxide feed tank was at or below this temperature. Since this situation existed, it was not certain that the equilibrium cell actually contained any liquid carbon dioxide. If this were true, then the pressure would be expected to be low. Because no heat supply was available for the CO_2 feed cylinder, the upper temperature limit of the apparatus was determined to be room temperature, approximately 25°C. Overall, the pressure detection equipment and the experimental technique proved to provide good results.

4.2 Carbon Dioxide–Methane.

With the successful measurement of carbon dioxide vapor pressure, the accurate measurement of liquid and vapor compositions became the only variables left to demonstrate. The procedure used to obtain these data was described in Section 3.2. Two isotherms were chosen to explore. The first isotherm, 270.0 K, was chosen because considerable literature data existed (Davalos, Anderson, and Kidnay 1976; Somait and Kidnay 1978). Data were also collected at 288.2 K isotherm in order to expand the literature database.

The results of the VLE measurements at 270.0 K and 288.2 K are shown in Table 3. In Fig. 7, the data taken at 270.0 K, are shown with the data of Davalos, Anderson, and Kidnay (1976) and the data of Somait and Kidnay (1978), along with the predicted curves of the PR and RKS equations of state. The results at 288.2 K along with the predictions of the PR and RKS equations are shown in Fig. 8.

Table 3. Experimental phase equilibrium measurements for carbon dioxide–methane.

		Mole Fraction			
Temp.	Press.	Liquid Phase		Vapor Phase	
(K)	(psia)	CO_2	CH_4	CO_2	CH_4
270.0	465.1	1.0000	0.0000	1.0000	0.0000
	629.3	0.9581	0.0419	0.8085	0.1915
	738.3	0.9275	0.0725	0.7210	0.2790
	807.0	0.9084	0.0916	0.6815	0.3185
	907.5	0.8705	0.1295	0.6404	0.3596
	904.7	0.8744	0.1256	0.6387	0.3613
	996.4	0.8423	0.1577	0.6218	0.3782
	993.7	0.8445	0.1555	0.6204	0.3796
288.2	738.4	1.0000	0.0000	1.0000	0.0000
	822.0	0.9741	0.0259	0.9318	0.0682
	820.0	0.9749	0.0251	0.9314	0.0686
	884.0	0.9584	0.0416	0.8840	0.1160
	881.9	0.9579	0.0421	0.8850	0.1150
	1003.1	0.9246	0.0754	0.8374	0.1626
	997.6	0.9243	0.0757	0.8389	0.1611

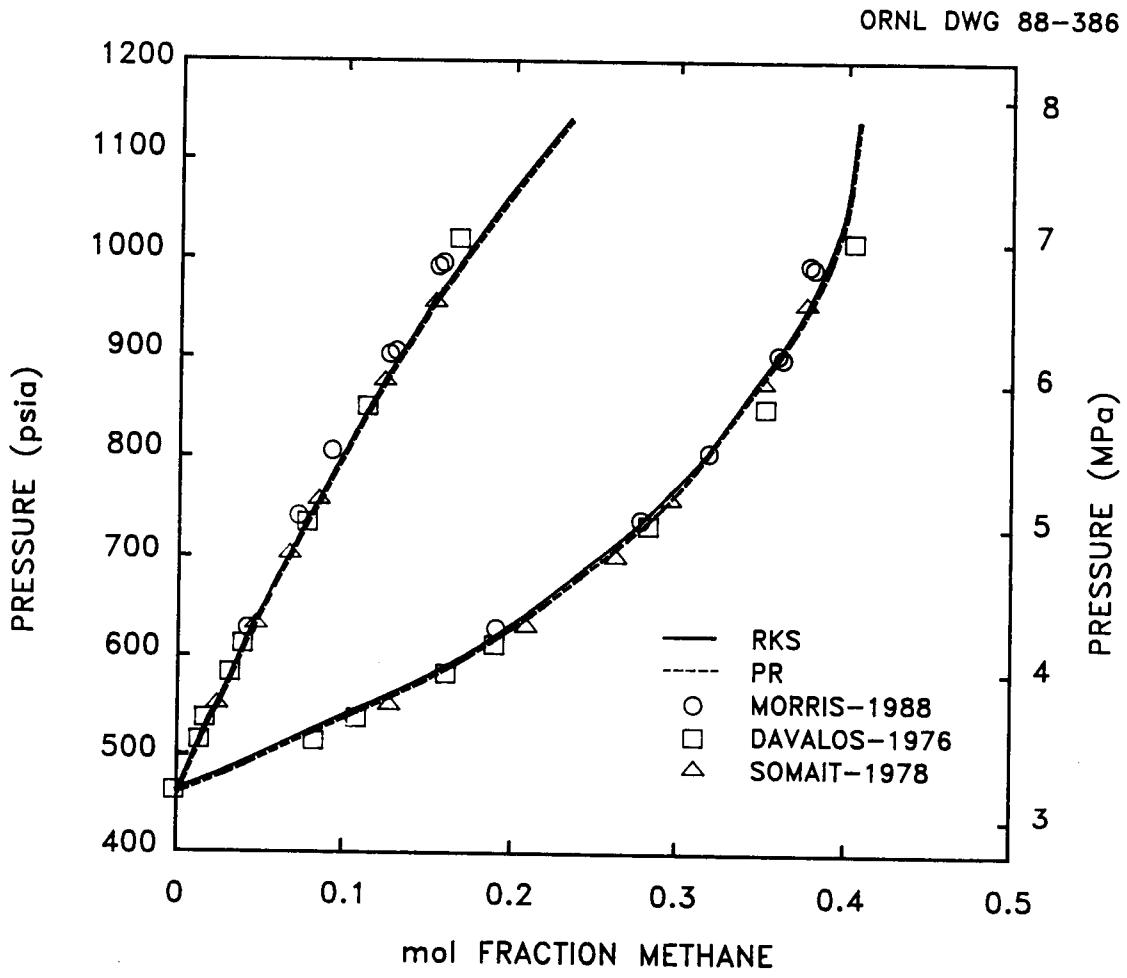


Figure 7. Pressure versus composition for carbon dioxide–methane at 270.0 K.

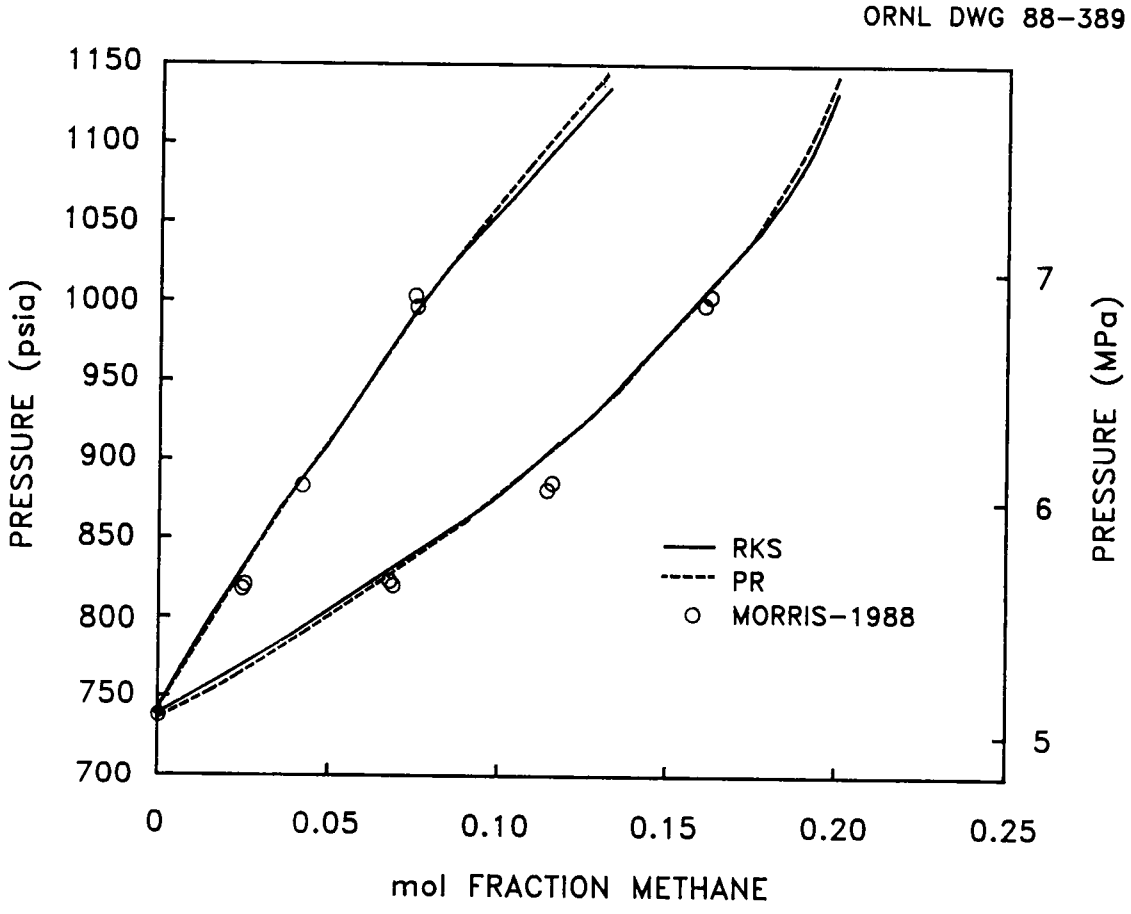


Figure 8. Pressure versus composition for carbon dioxide–methane at 288.2 K.

The curves in Figs. 7 and 8 were generated using the ASPEN^{TM} simulator. The calculation of the data for these curves involved a two step process. First, the data regression system (DRS) was used to generate the binary interaction parameters, k_{ij}, for each of the equations of state. The DRS utilizes the generalized least-squares algorithm, proposed by Britt and Luecke (1973), in the calculation of selected parameters from inputed data. In order to calculate the binary interaction parameters for PR and RKS equations, experimental data consisting of temperature, pressure, and compositions of the liquid and vapor equilibrium phases were input (An example DRS input file and report for determination of the RKS binary interaction parameter for the CH_4–CO_2 system is shown in Appendix II). All available data (Davalos, Anderson, and Phelps 1976; Donnelly and Datz 1954; Somait and Kidnay 1978) in the 270.0 K to 288.2 K temperature range and pressures to 1200 psia were included in the input file to generate the binary interaction parameters. The binary interaction parameter for the PR equation of state was calculated to be 1.001×10^{-1} with a standard deviation of 2.962×10^{-3}. The Soave equation's binary interaction parameter for carbon dioxide-methane was found to be 1.032×10^{-1} with a standard deviation of 3.244×10^{-3}.

The calculation of the VLE data in Figs. 7 and 8 was not straightforward because the molar volume or molar density was not measured in this experiment. An iterative process employing the principles of equal fugacities and pressures for each phase is required to determine the molar volume, and subsequently pressure, of each phase. In order to hasten this activity, another function of the ASPEN^{TM} simulator was employed. The equilibrium phase compositions and pressures shown in Figs. 7 and 8 were obtained by using the ASPEN^{TM}

FLASH2 model. FLASH2 determines the compositions and conditions of one vapor and one liquid outlet stream when any number of feed streams are flashed. The vapor-liquid equilibrium flash calculations used in this model were proposed by Boston and Britt (1978). In the generation of the curves in Figs. 7 and 8, a model of one inlet stream and two outlet streams, one vapor and one liquid, was used. The binary interaction parameters, temperatures of the inlet and outlet streams, and composition of the feed stream were input (See Appendix III for an example of an input file and report for FLASH2). The inlet stream temperature was set near the temperature of interest in this study and the composition of the inlet stream was set so that the outlet vapor stream was identical to the vapor composition obtained experimentally. The temperature of the outlet stream was designated to be the 270.0 K or 288.2 K. By setting the vapor stream equal to the experimental values, the calculated pressure and liquid phase compositions could be compared to the experimental results.

The data presented in Tables 4 and 5 provide a quantitive comparison of the data collected in this study to the calculations of the RKS and PR equations of state, respectively. The comparison of the RKS calculations with the experimental data in Table 4 shows excellent agreement exists for pressures below 900 psia at 270.0 K, with deviations below 1 percent. An error of 3.38 percent was realized in the pressure calculation when the experimental measurement was 996.4 psia. Likewise, excellent agreement in the experimental and calculated pressures are seen at 288.2 K. The deviation in liquid phase composition calculations versus the experimental results is less than 15 percent at both 270.0 K and 288.2 K. Very similar results are observed in the PR equation calculations in Table 5. Overall, the results of the PR and RKS equations of state accurately

Table 4. RKS calculations versus experimental results for the CH_4–CO_2 system.

	Vapor	Pressure			Liquid Phase		
	Mole	RKS			Mole Fraction CH_4		
Temp.	Frac.	Expr.	Calc.	Dev.		RKS	Dev.
(K)	CH_4	(psia)	(psia)	(%)	Expr.	Calc.	(%)
270.0	0.0000	465.1	467.2	0.4515	0.0000	0.0000	0.00
	0.1915	629.3	623.1	-0.9852	0.0419	0.0419	0.00
	0.2790	738.3	738.7	0.0542	0.0725	0.0764	5.38
	0.3185	807.0	809.3	0.2850	0.0916	0.0989	7.97
	0.3596	907.5	905.3	-0.2424	0.1295	0.1319	1.85
	0.3782	996.4	962.7	-3.3822	0.1577	0.1531	-2.92
288.2	0.0000	738.4	743.5	0.6907	0.0000	0.0000	0.00
	0.0682	822.0	830.6	1.0462	0.0259	0.0244	-5.79
	0.1160	884.0	908.2	2.7376	0.0416	0.0475	14.18
	0.1626	1003.1	1007.0	0.3888	0.0754	0.0798	5.84

Table 5. PR calculations versus experimental results for the CH_4–CO_2 system.

	Vapor	Pressure			Liquid Phase		
	Mole	PR			Mole Fraction CH_4		
Temp.	Frac.	Expr.	Calc.	Dev.		PR	Dev.
(K)	CH_4	(psia)	(psia)	(%)	Expr.	Calc.	(%)
270.0	0.0000	465.1	462.0	-0.6665	0.0000	0.0000	0.00
	0.1915	629.3	617.9	-1.8115	0.0419	0.0419	0.00
	0.2790	738.3	734.2	-0.5553	0.0725	0.0760	4.83
	0.3185	807.0	806.2	-0.0991	0.0916	0.0986	7.64
	0.3596	907.5	905.1	-0.2645	0.1295	0.1320	1.93
	0.3782	996.4	965.2	-3.1313	0.1577	0.1539	-2.41
288.2	0.0000	738.4	738.5	0.0135	0.0000	0.0000	0.00
	0.0682	822.0	826.6	0.0056	0.0259	0.0241	-6.95
	0.1160	884.0	905.4	2.4208	0.0416	0.0471	13.22
	0.1626	1003.1	1006.0	0.2891	0.0754	0.0796	5.57

predict the results published in the literature and those presented in this work for the CH_4–CO_2 system.

The previous discussion would have been meaningless if the data were found to be thermodynamically inconsistent. The data required for the thermodynamic consistency test (fugacity coefficents, molar volume, and K-factors) were produced by using another of the ASPEN^{TM} simulator's functions, the table generation system (TGS). The TGS provides tables of calculated physical properties as functions of temperature, pressure, vapor fraction and composition, for pure components, mixtures, or streams generated in a process simulation. Three types of tables can be generated (1) single phase properties, (2) properties of points on a flash curve, and (3) properties of points along a vapor fraction line of a P-T envelope. The TGS can be utilized at the end of a DRS run, in the middle of a simulation, or in a stand-alone mode. The later of these (the stand-alone mode) was used to generate a P–T envelope for various vapor phase compositions for both of the equations of state (See the example TGS input file and report in Appendix IV). The values used in the thermodynamic consistency test were determined through interpolation of the TGS output data to obtain values at 270.0 K and 288.2 K. For the CH_4–CO_2 system, the binary interaction parameters for each of the equations of state and the desired vapor phase composition were added to the input file. The output tables included various equilibrium properties along the P–T envelope. Because the RKS equation fit the data so well and no significant difference existed between the two equations' predictions, values using the RKS equation of state at 270.0 K and 288.2 K were used to generate the curves for the left-hand-side of equation 49 (page 23). Examples plots used in the graphical integration are shown in Figs. 9 to 11.

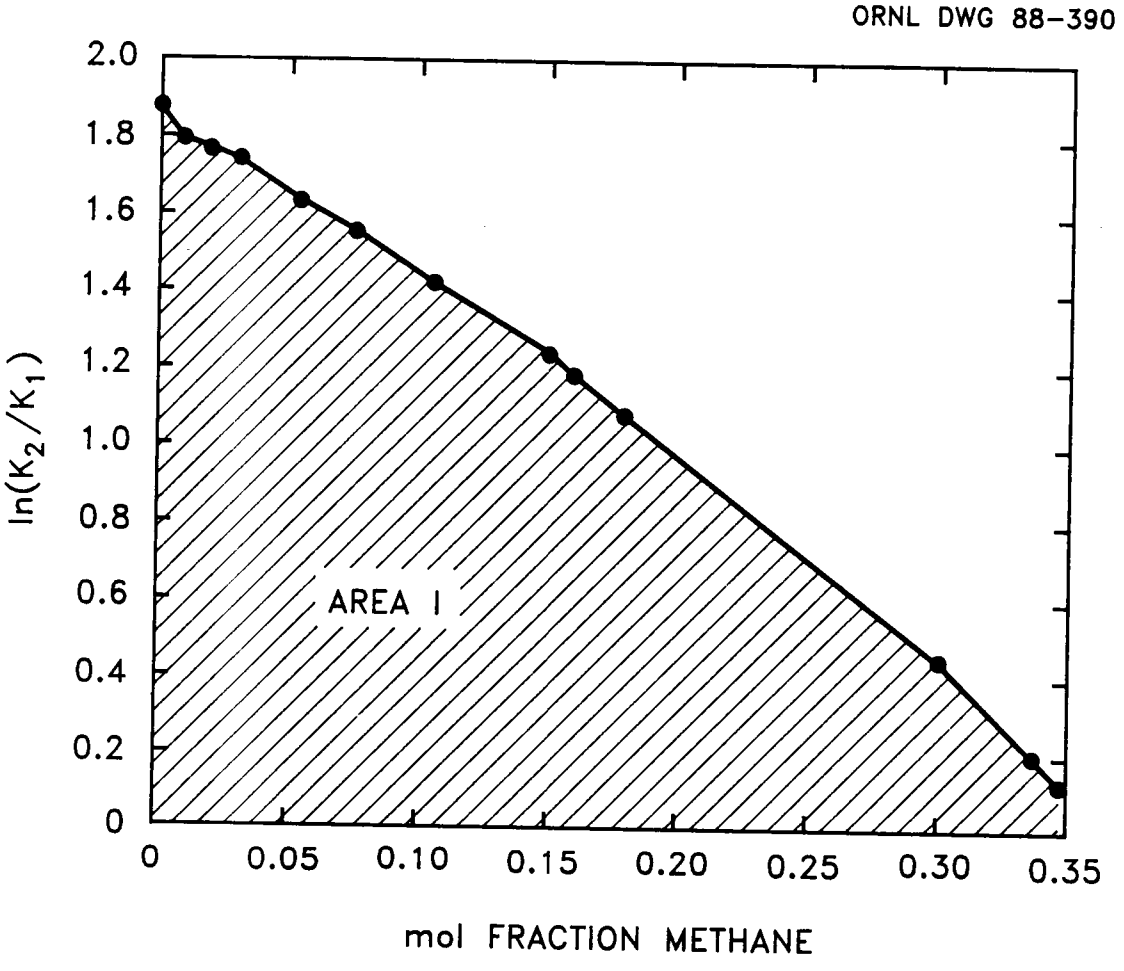


Figure 9. Thermodynamic consistency test–Area I.

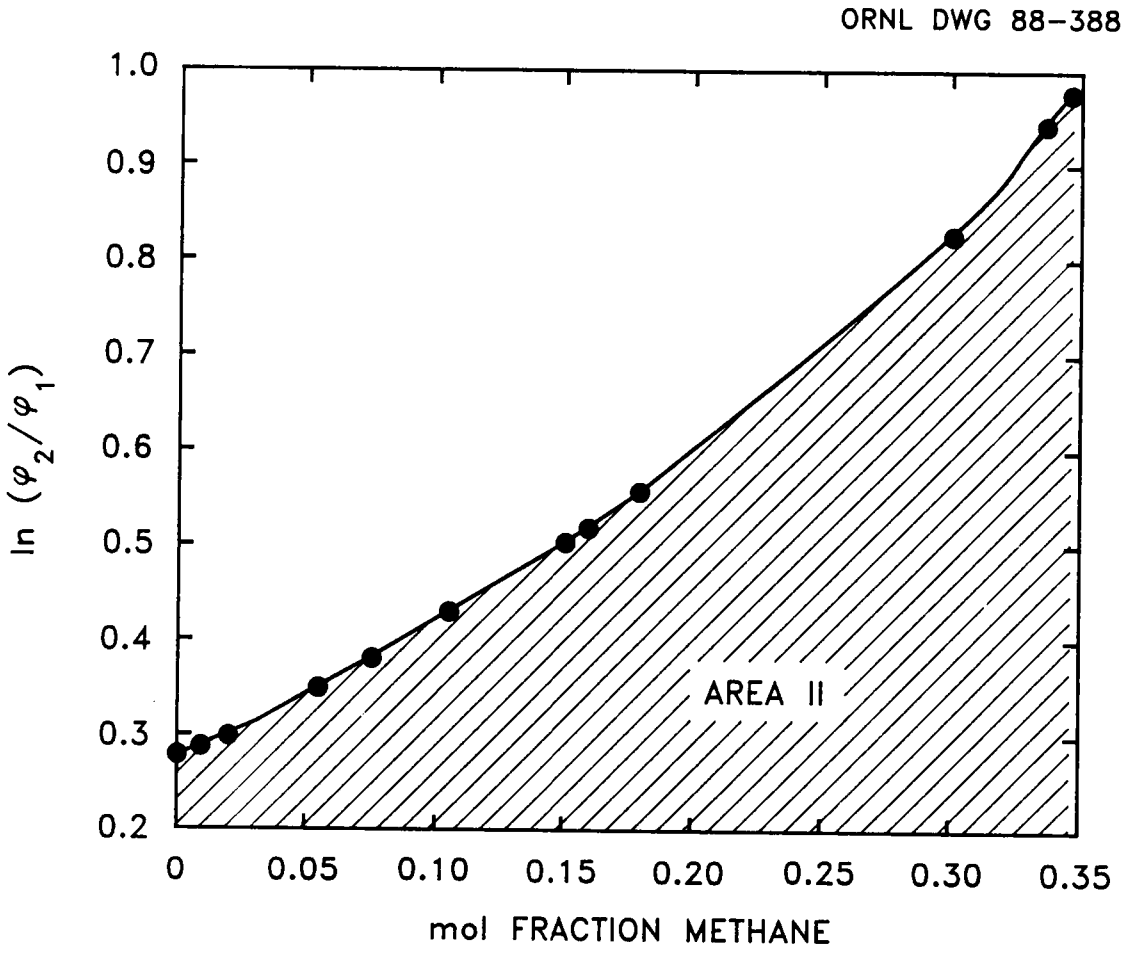


Figure 10. Thermodynamic consistency test–Area II.

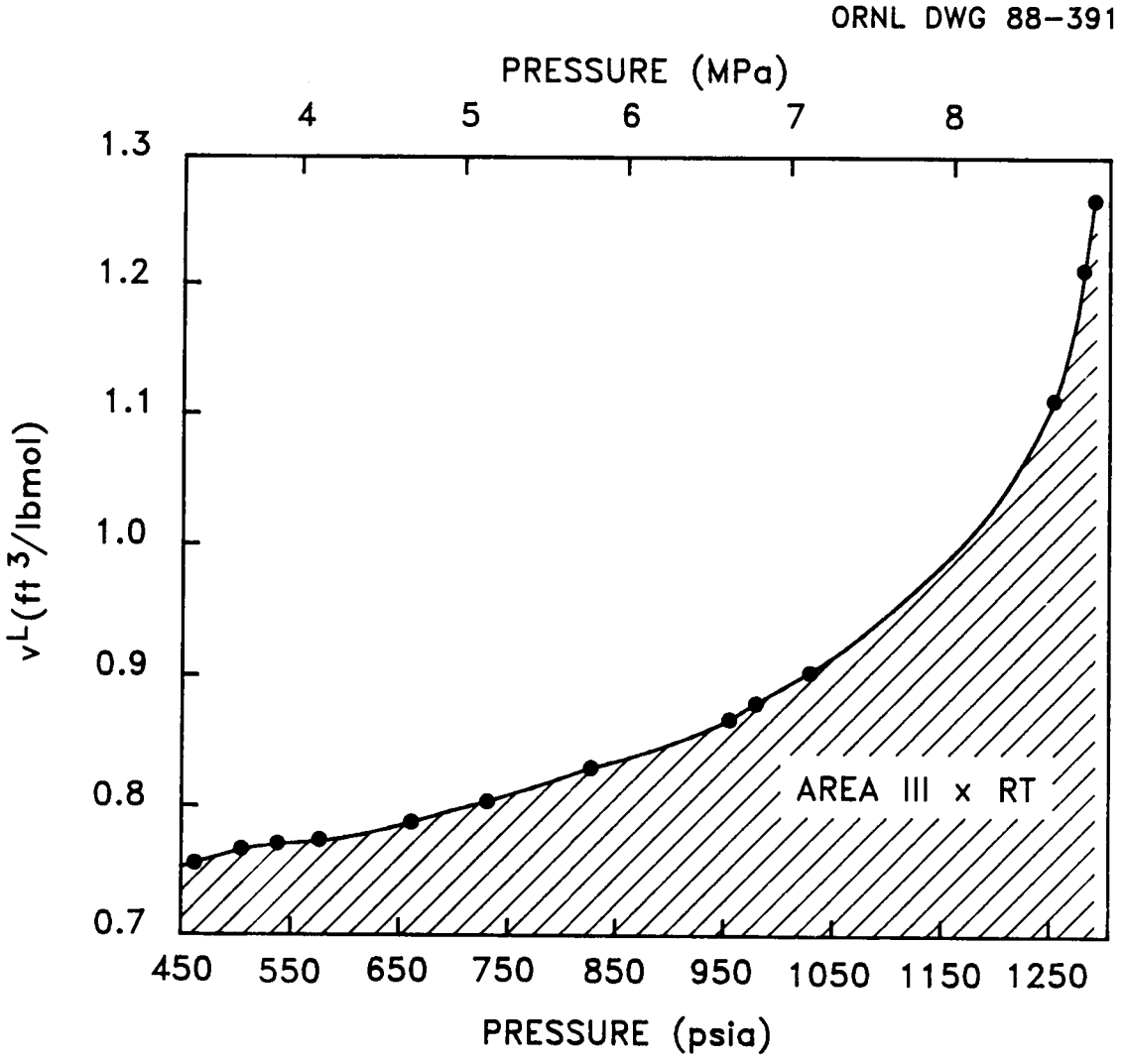


Figure 11. Thermodynamic consistency test–Area III × RT.

The results of this analysis, Table 6, show that the thermodynamic inconsistency was 1.93 percent for the 270.0 K isotherm in the pressure range of this study. Somewhat higher inconsistency, 5.76 percent, was shown for the 288.2 K isotherm. The inconsistency of the data is within the measurement error of this experiment. Therefore, the data are considered to be internally consistent.

4.3 Methane–Hydrogen Sulfide.

Little literature data exist for the methane-hydrogen sulfide system in the 270.0 K to 288.2 K range. The data recorded in the literature at 277.6 K (Kohn and Kurata 1958; Reamer, Sage, and Lacey 1951) was felt to require confirmation and supplementation because of the small quantity of data and because hydrogen sulfide gas compositions are difficult analyze. The tendency of H_2S to adsorb to container and piping surfaces was recognized as a possible problem in sampling and analysis. Studies of this system would reflect the applicability of using a circulating VLE apparatus in conjunction with GC analysis in the study of hydrogen sulfide systems. Additional gas standards for the gas chromatograph calibration and the addition of scrubbers on the vent were the only significant changes made to the experiment in order to perform this work.

The experimental results obtained in this work are shown in Table 7. As was done with the CH_4–CO_2 results, binary interaction parameters were regressed using the ASPEN^{TM} data regression system with the data from this study and the literature results in the desired 270.0 K to 288.2 K range. The binary interaction parameter for the PR equation of state was determined to be 8.672 $\times 10^{-2}$ with a standard deviation of 3.189 $\times 10^{-3}$, while the RKS equation

Table 6. Thermodynamic consistency test for CH_4–CO_2 using results from the PR equation.

	Temperature (K)	
	270.0	288.2
x_2	0.347	0.133
P @ x_2	1291.	1145.
φ_1 @ x_2	0.421	0.578
K_1 @ x_2	0.950	0.922
φ_1^s	0.782	0.724
P_1^s	467.2	743.5
Area I	0.375	0.114
Area II	0.186	0.075
Area III	0.156	0.081
LHS = $\sum$	0.717	0.270
ln K_1	-0.051	-0.081
$\ln\left[\frac{\varphi_1 P}{\varphi_1^s P_1^s}\right]$ =	0.397	0.207
$x_2\left[\ln\frac{\varphi_2}{\varphi_1}+\ln\frac{K_2}{K_1}\right]$	0.385	0.160
RHS = $\sum$	0.731	0.286
% Inconsistency	1.93	5.76

Table 7. Experimental phase equilibrium measurements for methane–hydrogen sulfide.

		Mole Fraction			
Temp.	Press.	Liquid Phase		Vapor Phase	
(K)	(psia)	H_2S	CH_4	H_2S	CH_4
270.0	263.5	*	*	0.6151	0.3849
	250.1	*	*	0.6282	0.3718
	461.9	0.9776	0.0224	0.3845	0.6155
	450.6	0.9806	0.0195	0.3906	0.6094
	690.0	0.9516	0.0484	0.2824	0.7176
	675.0	0.9525	0.0475	0.2958	0.7042
	842.0	0.9215	0.0785	0.2644	0.7356
	818.0	0.9249	0.0751	0.2677	0.7323
288.2	231.6	1.0000	0.0000	1.0000	0.0000
	376.0	0.9992	0.0008	0.7087	0.2913
	370.9	0.9994	0.0006	0.7117	0.2883
	613.0	0.9729	0.0271	0.4911	0.5089
	608.6	0.9679	0.0321	0.4958	0.5042
	796.9	0.9397	0.0603	0.4168	0.5832
	792.3	0.9423	0.0577	0.4281	0.5719
	1012.9	0.9005	0.0995	0.3614	0.6386

* methane composition below the detection limit of the gas chromatograph

yielded a binary interaction parameter of 8.261×10^{-2} with a standard deviation of 3.435×10^{-3}. Figs. 12 and 13 show the experimental results and the calculated data of the PR and RKS equations at 270.0 K and 288.2 K, respectively. A quantative comparison of the RKS and PR calculations are shown respectively versus the experimental results of this work in Tables 8 and 9. As can be seen, the PR and the RKS calculations compare well with one another. However, the fit of these equations to the experimental data of this study reflect some differences.

Tables 8 and 9 show the calculated liquid phase composition and the equilibrium pressure for the RKS and PR equations given the vapor phase composition and temperature obtained experimentally. As can be seen, for both equations, the deviation of the calculated and experimental pressures is less than 12 percent at both temperatures. However, very large differences are observed in the liquid phase compositions when the system pressures are below about 800 psia. Above this pressure, the deviations for both equations are within 17 percent. As was mentioned above, no significant difference can be observed in the ability of the PR or RKS equations to fit the data. Because of the large differences at pressures below 800 psia in the calculated liquid phase composition and the experimental results, a comparison of the experimental results of this work and the literature data was undertaken.

A comparison of the experimental results to the literature Kohn et al. (1958) and Reamer et al. (1951) are shown in Figs. 14 and 15. The vapor phase measurements from the present work compare well with the literature. As shown in Fig. 14, the vapor phase data from the current work at 270.0 K falls between the literature curves at 255.4 K and 277.6 K and the data at 288.2

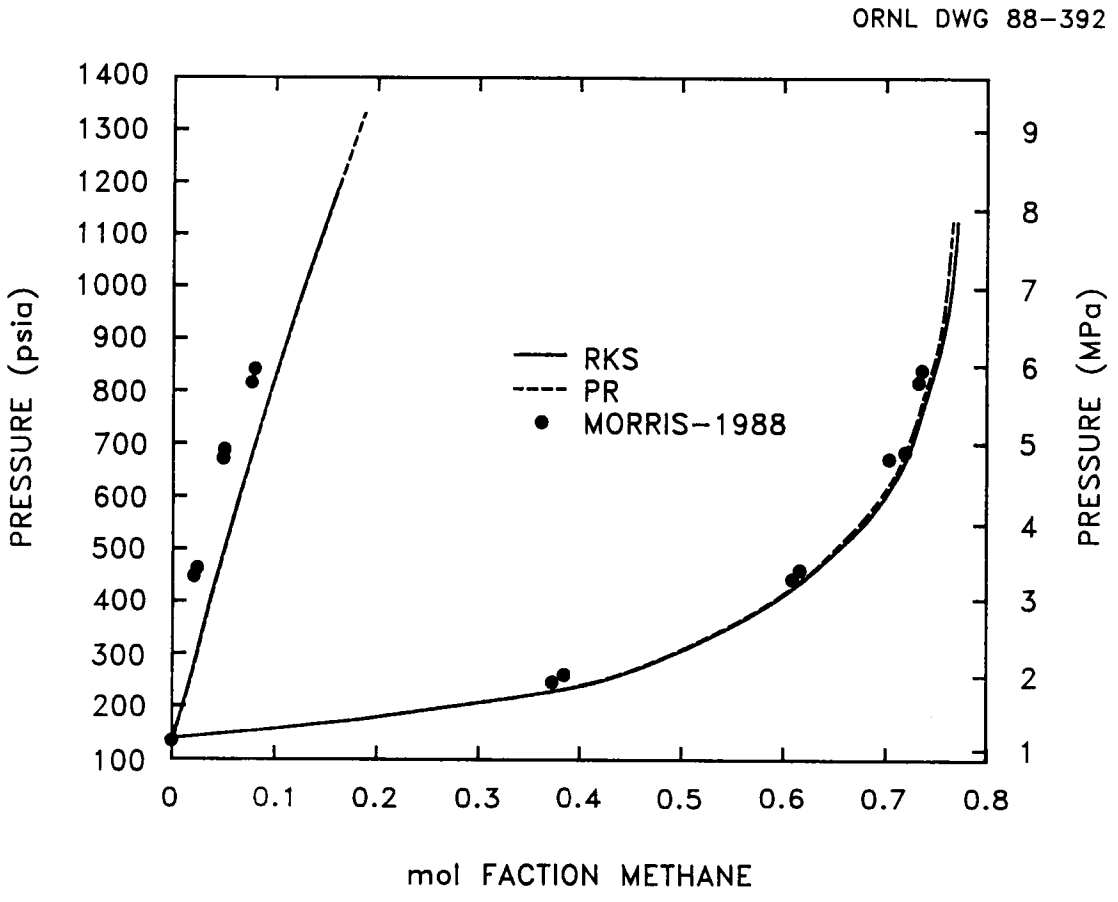


Figure 12. Pressure versus composition for methane–hydrogen sulfide at 270.0 K.

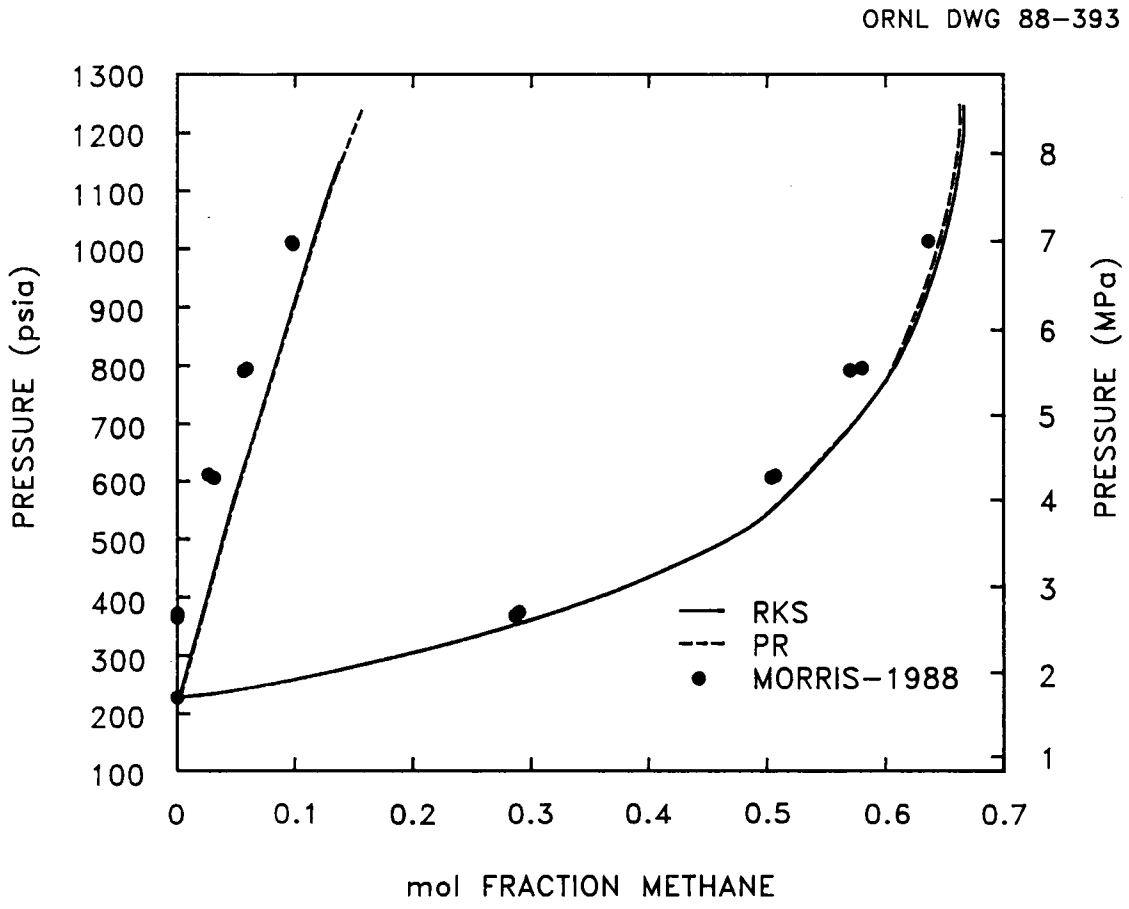


Figure 13. Pressure versus composition for methane–hydrogen sulfide at 288.2 K.

Table 8. RKS calculations versus experimental results for the CH_4–H_2S system.

	Vapor		Pressure		Liquid Phase		
	Mole		RKS		Mole Fraction CH_4		
Temp.	Frac.	Expr.	Calc.	Dev.		RKS	Dev.
(K)	CH_4	(psia)	(psia)	(%)	Expr.	Calc.	(%)
270.0	0.3849	263.5	234.0	-11.20	*	0.0136	—
	0.6155	461.9	417.3	- 9.65	0.0224	0.0381	70.09
	0.7176	690.0	658.7	- 4.54	0.0484	0.0730	50.08
	0.7356	842.0	742.7	-11.79	0.0785	0.0858	9.30
288.2	0.0000	231.6	226.3	- 2.29	0.0000	0.0000	0.00
	0.2913	376.0	341.3	- 9.23	0.0008	0.0150	1775.
	0.5089	613.0	551.2	-10.08	0.0271	0.0437	61.25
	0.5832	796.9	706.1	-11.39	0.0577	0.0659	14.21
	0.6386	1012.9	917.3	- 9.44	0.0995	0.0981	-1.41

* methane composition below the detection limit of the gas chromatograph

Table 9. PR calculations versus experimental results for the CH_4–H_2S system.

	Vapor		Pressure		Liquid Phase		
	Mole		PR		Mole Fraction CH_4		
Temp.	Frac.	Expr.	Calc.	Dev.		PR	Dev.
(K)	CH_4	(psia)	(psia)	(%)	Expr.	Calc.	(%)
270.0	0.3849	263.5	234.7	-10.93	*	0.0134	—
	0.6155	461.9	421.0	- 8.85	0.0224	0.0392	75.00
	0.7176	690.0	672.3	- 2.57	0.0484	0.0759	56.82
	0.7356	842.0	762.6	- 9.43	0.0785	0.0897	14.27
288.2	0.0000	231.6	225.2	- 2.76	0.0000	0.0000	0.00
	0.2913	376.0	340.5	- 9.44	0.0008	0.0152	1800.
	0.5089	613.0	552.9	- 9.80	0.0271	0.0443	63.47
	0.5832	796.9	712.3	-10.62	0.0577	0.0672	16.46
	0.6386	1012.9	936.6	- 7.53	0.0995	0.1013	-1.81

* methane composition below the detection limit of the gas chromatograph

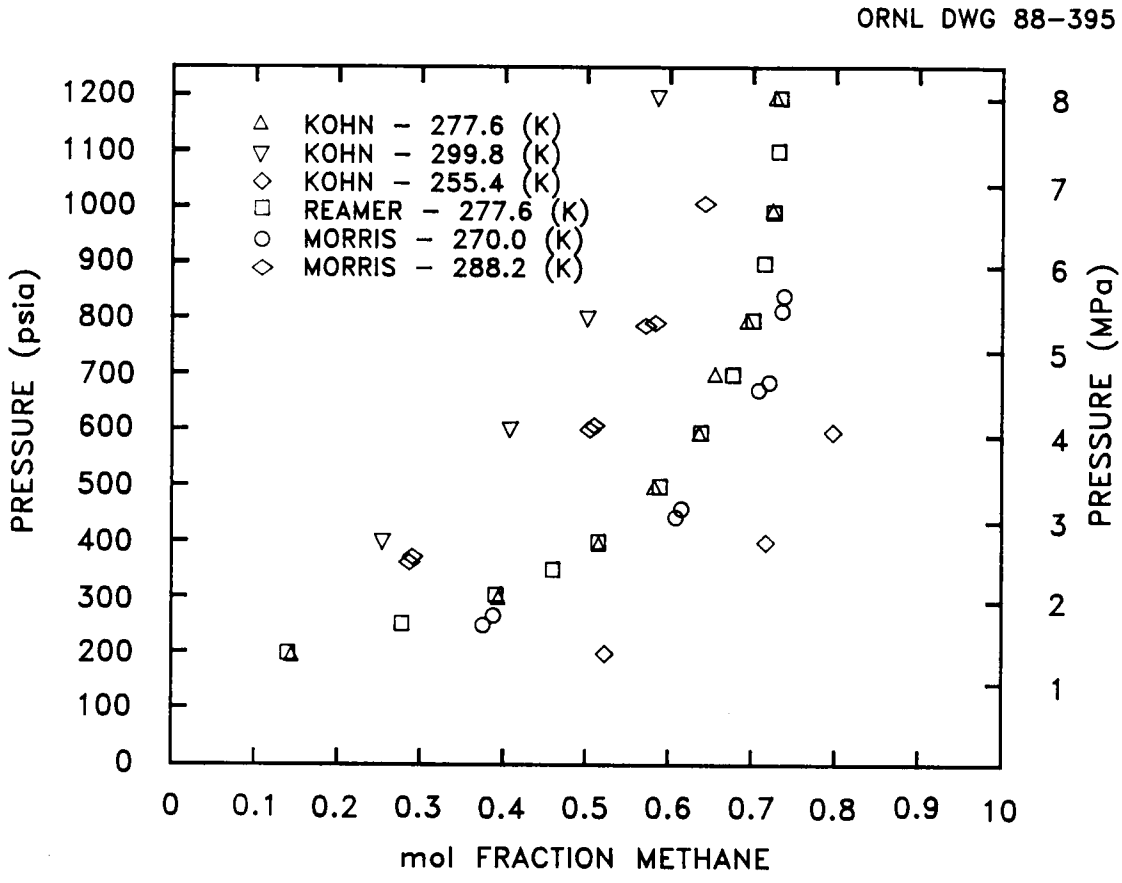


Figure 14. Methane–hydrogen sulfide vapor phase measurements versus the literature.

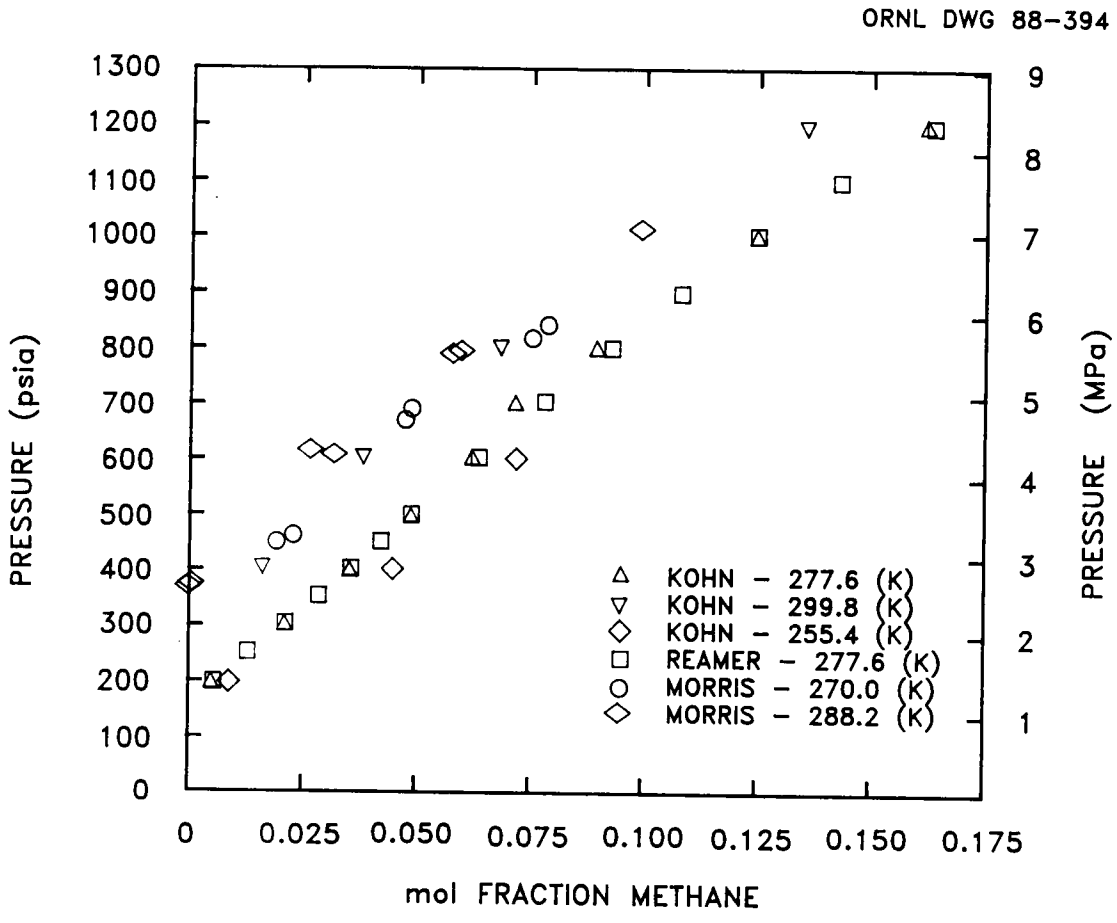


Figure 15. Methane–hydrogen sulfide liquid phase measurements versus the literature.

K falls between the literature values at 277.6 K and 299.8 K. However, comparison of the liquid phase data, in Fig. 15, reveals a discrepancy. The liquid composition data collected in this work do not follow the trends of the literature, as both isotherms appear to be approximately 2.5 mole percent lower than the literature measurements.

A quantitive comparison of the PR and RKS calculations versus the data of Reamer et al. (1951) at 277.6 K is shown in Table 10. A notable difference in the PR and RKS equations' ability to fit this data is shown. The RKS equation compares slightly better to the experimental data, 3.10 percent to 9.50 percent at the highest deviation. A more significant difference is seen in the liquid composition comparison. The RKS equation better predicts the liquid phase composition at 200 psia, however, the PR equation yields much better results above that point. Between 200 and 1000 psia, the PR equation yields results within $\pm$ 12.71 percent of the experimental data, while the RKS equation's calculations differ by up to 56.40 percent.

It is interesting to note that the PR equation compares well to both the literature and the current experimental results as the system pressure approaches 1000 psia. However, a disturbing trend, which does not become evident in Table 9, is suggested in Table 10. As can be seen, the deviation between the calculated and the experimental results is increasing with increased pressure. This trend should be further explored if the PR equation is to be used at pressures above 1000 psia with the binary interaction parameter stated above.

Thermodynamic consistency tests were performed on the data to determine if either the data from the literature or the data presented here could be discounted. Thermodynamic consistency tests conducted for the experimental

Table 10. RKS and PR calculations versus literature data for the CH_4–H_2S system at 277.6 K.

EOS	Vapor Mole Frac. CH_4	Pressure Expr.* (psia)	Pressure Calc. (psia)	Dev. (%)	Liquid Phase Mole Fraction CH_4 Expr.*	Liquid Phase Mole Fraction CH_4 Calc.	Dev. (%)
RKS	0.0000	169.0	168.9	-0.059	0.0000	0.0000	0.00
	0.1371	200.0	199.4	-0.300	0.0057	0.0059	3.51
	0.5126	400.0	393.7	-1.575	0.0354	0.0447	26.27
	0.6394	600.0	597.5	-0.417	0.0636	0.0885	39.15
	0.6989	800.0	819.2	2.400	0.0930	0.1403	33.71
	0.7242	1000.0	1031.0	3.100	0.1250	0.1955	56.40
PR	0.0000	169.0	168.6	-0.237	0.0000	0.0000	0.00
	0.1371	200.0	199.6	-0.200	0.0057	0.0041	-28.07
	0.5126	400.0	398.1	-0.475	0.0354	0.0309	-12.71
	0.6394	600.0	609.6	1.600	0.0636	0.0610	- 4.09
	0.6989	800.0	846.1	5.448	0.0930	0.0966	3.89
	0.7242	1000.0	1091.0	9.500	0.1250	0.1364	9.12

* Reamer, Sage, and Lacey (1951)

data generated in this study and for the literature data all resulted in an inconsistency of approximately 10 percent. Because no significant differences in the thermodynamic consistency tests were detected, a further evaluation of the measurement error in the present work and its effects will be discussed in Section 4.5.

4.4 Carbon Dioxide–Hydrogen Sulfide.

The carbon dioxide-hydrogen sulfide system was the third binary mixture for which parameters were needed prior to predicting ternary properties. No experimental data were obtained in this work because adequate data in the temperature and pressure ranges of interest were contained in the literature (Bierlein and Kay 1953; Sobocinski and Kurata 1959).

All available data in the 270.0 K to 288.2 K range were employed to determine binary interaction parameters of 9.894×10^{-2} with a standard deviation of 1.247×10^{-3} and 9.968×10^{-2} with a standard deviation of 1.349×10^{-3} for the PR and RKS equations, respectively. A plot of the literature data at 283.2 K is shown in Fig. 16. Table 11 shows the comparison of the calculated and literature data of Sobocinski and Kurata (1959). The agreement of the calculated values and literature values is excellent with the pressure deviations of less than 2 percent over the entire range of liquid-vapor coexistence. The liquid phase composition is quite good as well, with a maximum deviation of 12.9 percent. Both equations of state adequately fit the data and no significant difference can be detected between the two equations' results. The thermodynamic consistency

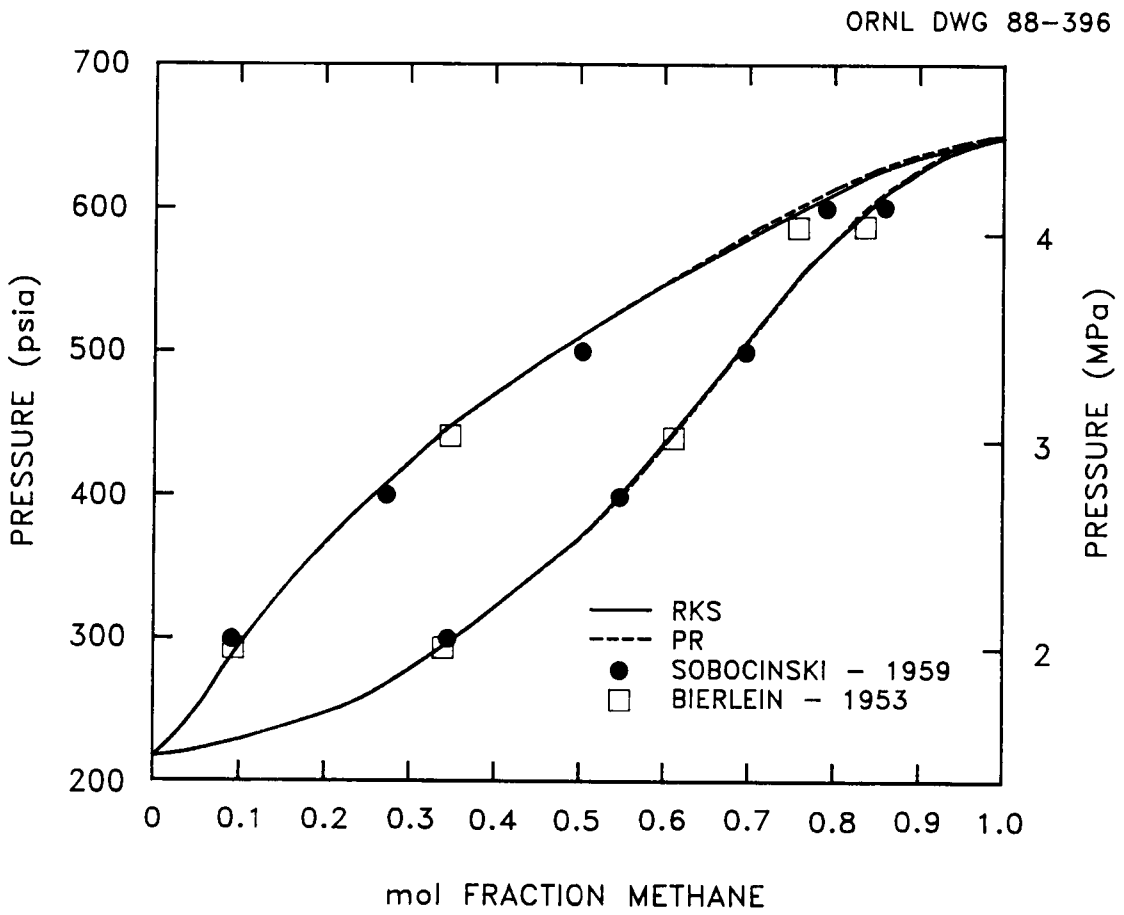


Figure 16. Pressure versus composition for carbon dioxide–hydrogen sulfide at 283.2 K.

Table 11. RKS and PR calculations versus literature data for the CO_2–H_2S system at 283.2 K.

EOS	Vapor Mole Frac. CH_4	Expr.* (psia)	Calc. (psia)	Dev. (%)	Liquid Phase Mole Fraction CH_4 Expr.*	Calc.	Dev. (%)
RKS	0.349	300.0	295.3	1.567	0.093	0.105	-12.90
	0.551	400.0	400.2	-0.050	0.275	0.262	4.73
	0.697	500.0	504.2	-0.840	0.503	0.497	1.19
	0.860	600.0	606.8	-1.133	0.791	0.804	- 1.64
PR	0.349	300.0	295.3	1.567	0.093	0.104	-11.80
	0.551	400.0	401.3	-0.325	0.275	0.263	4.36
	0.697	500.0	505.9	-1.180	0.503	0.502	0.20
	0.860	600.0	605.6	-0.933	0.791	0.807	- 2.02

* Sobocinski and Kurata (1959)

test revealed an inconsistency of 1.17 percent for the RKS equation data results, which also indicates the literature data are excellent.

4.5 Error Analysis.

Because of the deviation from the literature vapor-liquid equilibrium data for the CH_4–H_2S system, a closer examination of the measurement error of the present work was undertaken. This analysis consisted of comparing the calibration runs and measurement experience obtained from the CO_2–CH_4 and CH_4–H_2S studies, determining the expected measurement error expected from this analysis, and finally determining the effect of this error on the prediction of the equations of state.

The methane concentration of the standard gas samples used to calibrate the gas chromatograph for the carbon dioxide-methane system ranged from 4.65 to 75 mole percent. The response curves, area versus concentration, of both carbon dioxide and methane exhibited a high degree of linearity. The response factor, peak area divided by concentration, could be used to calculate the expected error measurements for these two gases because the linearity of the curves resulted in a response factor which revolved about a mean value regardless of the gas concentration. The relative standard deviation (RSD) of the response factor for both carbon dioxide and methane was less than 1.3 percent. From the RSD, which is the standard deviation divided by the mean times 100, one can anticipate a larger error being generated at either extreme of the concentration range. Another influence on the error measurement is the normalization of the concentrations performed prior to reporting. Taking this into account

and assuming that the gas compositions reported by the vendor were exact, the composition of a 75 mole percent methane in carbon dioxide sample to range from 75.00 to 76.03 mole percent methane. This equates to an error of 0.00 to +1.37 percent. Similarly, for a mixture of 1 mole percent methane in carbon dioxide, the resulting methane composition could be expected to range from 1.000 to 1.259 mole percent, for an error range of 0.00 to +25.90 percent.

Ternary gas standards were purchased to calibrate the GC for the CH_4–H_2S and CH_4–CO_2–H_2S studies. A notable difference from the CH_4–CO_2 calibration was observed during this calibration, as the carbon dioxide response curve exhibited second order polynomial characteristics. The same error analysis was conducted as above, however, because both the hydrogen sulfide and methane response curves were linear. Two calibrations were conducted, one at the beginning of the experiment and another near the end of the binary measurements. This analysis revealed a RSD of 3.99 percent and 0.87 percent for the CH_4 and H_2S response factors, respectively. For a gas mixture of 1.84 mole percent CH_4 in H_2S one would expect the composition to vary between 1.74 and 1.91 mole percent, an error of less than $\pm$ 5 percent. The actual experience disputes this analysis, however, as the methane composition measurements, as compared to the literature appear, to be orders of magnitude lower than expected.

Inconsistent flowrates in the gas chromatograph, low quality gas standards used in calibration, or inaccurate results in the literature could be responsible for the difference between the literature data and the data presented here. It should be pointed out, however, that Reamer, Sage, and Lacey (1951) reported methane mole fraction measurement error of less than 0.3 percent. This is hard to dispute since their synthetic method experiment appeared to be very accurate. A more

reasonable explanation for the lower than expected methane compositions, in this work, is the choice of analytical technique for determining hydrogen sulfide compositions. H_2S is known to adsorb to equipment surfaces. This was observed firsthand in this experiment. Because of the elevated temperatures and constant purging of the columns in the GC, H_2S adsorption and deadsorption could be resulting in increased error.

The effects of this composition discrepancy on the Peng–Robinson and Soave equations were examined. A difference in the binary interaction parameter was realized for both equations of state when only the literature data were used in the parameters' determination. The binary interaction parameter for the PR equation, using only the data in the literature, is 8.099×10^{-2} with a standard deviation of 9.306×10^{-4}. The resulting interaction parameter for the RKS equation is 7.645×10^{-2} with a standard deviation of 1.153×10^{-3}. Likewise, the root mean squares deviation of the calculated variables versus the experimental values (temperature, pressure, and composition) generated in the ASPEN^{TM} data regression were greatly reduced when only the literature data were input. This means that the PR and RKS equations of state better predict the literature data when only the literature data are used, but does not give an indication as to the accuracy of either sets of data.

Another important measurement error often experienced in VLE experiments using static volume systems is the upset of equilibrium when samples are obtained. This could have been a more significant problem in this experiment, given the size of the sample bombs, if the possibility had not been recognized. Given the present system, the size of the liquid sample is set by the volume of the tubing loop, so the experimenter had no control when taking liquid samples.

The experimenter maintains some control in the amount of vapor sample taken, so the quantities of this sample were held to a minimum. Nevertheless, perturbation in the mixture composition occurred with each sample. A pressure drop of approximately 1 psia could be expected after obtaining any set of samples (a set of samples consists of a vapor and a liquid phase sample) taken up to 600 psia. While the pressure deviation would be expected to be as high as 3 to 5 psia in the 600 to 1000 psia range. This held true for all binary mixtures at all temperatures except for the CH_4–H_2S 270.0 K isotherm. Here, pressure drops of approximately 5 psia were observed below 400 psia, 10 psia pressure drops were observed at 600 psia, and pressure drops up to 30 psia could be expected above 800 psia. Therefore, pressure measurement error in this experiment could be as high at 3 percent even though the measurement is capable of less than 1 percent.

4.6 Carbon Dioxide–Methane–Hydrogen Sulfide.

The binary interaction parameters for the PR and RKS equations were used to predict ternary properties shown in Table 12. A comparison of the predicted ternary properties and the actual results determined by experiment are shown in Table 13. Three samples, were collected at 270.0 K in the 595.8 to 933.8 psia pressure range. The ASPEN^{TM} simulator was again employed to generate equilibrium data near the range of interest. In this simulation, three flash calculations were performed with each of the equations of state to predict the liquid phase composition, given the vapor phase composition and temperature results obtained in the experiment. The data in Table 13 reveal a

Table 12. Binary interaction parameters for CH_4, CO_2, and H_2S binary systems.

Binary System	Equation of State	
	PR	RKS
CH_4–CO_2	1.001×10^{-1}	1.032×10^{-1}
CO_2–H_2S	9.894×10^{-2}	9.968×10^{-2}
CH_4–H_2S	8.672×10^{-2}	8.261×10^{-2}

Table 13. Phase equilibrium properties for CH_4–CO_2–H_2S at 270.0 K.

Source	Press.	Mole Fraction					
		Liquid Phase			Vapor Phase		
	(psia)	CO_2	H_2S	CH_4	CO_2	H_2S	CH_4
Expr.	595.8	0.6630	0.2951	0.0419	0.6264	0.1485	0.2251
	743.7	0.6887	0.2315	0.0798	0.6080	0.1129	0.2791
	933.8	0.6869	0.1970	0.1161	0.4825	0.1119	0.4056
PR	573.6	0.6764	0.2797	0.0439	0.6264	0.1485	0.2251
	660.9	0.7252	0.2086	0.0662	0.6080	0.1129	0.2791
	883.6	0.6372	0.2228	0.1399	0.4825	0.1119	0.4056
RKS	460.5	0.6130	0.3494	0.0376	0.6264	0.1485	0.2251
	537.1	0.6620	0.2799	0.0581	0.6080	0.1129	0.2791
	665.6	0.5953	0.2989	0.1058	0.4825	0.1119	0.4056

major difference in the capability of the equations of state to predict the ternary system. The liquid phase compostion predictions of the PR equation compare acceptably to those gathered in the experiment with the greatest deviation being in the methane composition at the highest pressure (21 percent). The pressure predictions are accurate to 12 percent of the experimental value. However, the same does not hold true for the RKS equation's predictions. The predicted pressure in, all cases, differs greatly from the experimental results. This translates in a discrepancy of -23 to -29 percent from the measured pressure. Likewise, the liquid composition when compared to the experimental results shows much more error. These finding suggest that the PR equation of state is superior to the RKS equation for prediction of the ternary system properties in the limited temperature and pressure range of interest in this study.

5. CONCLUSIONS AND RECOMMENDATIONS

5.1 Conclusions.

The apparatus designed, constructed, and tested in this work has been demonstrated to provide acceptable vapor-liquid equilibrium data for both binary and multicomponent systems. Excellent agreement with the literature obtained from the measurement of CO_2 vapor pressure and CO_2–CH_4 vapor-liquid equilibrium data, has shown that this equipment and the methods utilized in this work are capable of providing good pressure, temperature, and composition results for this system. The analytical results for systems containing H_2S are questionable and should be further studied. Vapor phase compositions for the CH_4–H_2S system appear to compare well with literature data; however, the liquid phase measurements reveal a disagreement when compared with literature results.

The Peng–Robinson and Redlich–Kwong–Soave equations of state both accurately predict binary properties of the CO_2–CH_4 and CO_2–H_2S systems. No significant differences appeared to be evident in the results of these two equations for this CO_2–CH_4 and CO_2–H_2S binary properties at the temperatures and pressures studied in this report. PR equation calculations better compare to experimental phase equilibrium properties of the CH_4–H_2S system at pressures of 800 to 1000 psia. It has also been suggested that the PR equation is superior to the RKS equation in the prediction of the ternary properties at the conditions of interest in this study. Given a choice between these two equations,

the PR equation should be used in the simulation of the absorption-fractionation process proposed by the Oak Ridge National Laboratory.

5.2 Recommendations for Future Work.

The apparatus designed, constructed, and tested in this work has been demonstrated to provide acceptable vapor-liquid equilibrium data for both binary and multicomponent systems. Excellent agreement of experimental and literature CO_2 vapor pressure and CO_2-CH_4 vapor- liquid equilibrium data, has shown that this equipment and the methods utilized in this work are capable of providing good pressure, temperature, and composition results. However, improvements to the apparatus can easily be implemented to enhance the pressure measurement, reduce the disturbance of equilibrium conditions during sampling, and improve the measurement of mixture compositions.

Although the pressure measurement instrumentation has shown to provide very good sensitivity and accuracy, the sampling system of this apparatus could be modified to greatly reduce the pressure measurement error and to reduce the upset of equilibrium while samples are taken. As was stated earlier, the phase samples were expanded into a sample bomb prior to introduction to the gas chromatograph. The liquid sample was trapped in a 0.464 cc tubing loop prior to being introduced to the chromatograph. This sampling technique consistently produced pressures of 40 to 60 psig in the expansion bomb and resulted in pressure reductions of 0.5 psia up to 5 psia in the equilibrium cell. The size of this tubing loop could be reduced to one-third its present volume for the materials studied in this work and still provide enough material for the chromatograph.

The size of this loop should be carefully chosen to provide the minimum sample volume consistent with analytical sensitivity. The vapor sample is introduced directly to the sample bomb. Improved valving should be provided to better control the quantity of sample taken as the present configuration could result in equilibrium cell pressure reductions of 1 to 50 psia, with the experimentalist having little control.

The control of temperature appeared to be adequate, in this experiment, although manual operation of the cooler was required to operate to within $\pm 0.1^{\circ}C$ of the desired temperature. Because the FLEXI–COOL^{TM} system required frequent maintenance activities, and because of the manual operation was burdensome, an upgrade of this system or a replacement should precede further studies. Temperature gradients in the bath were kept to approximately $0.1^{\circ}C$, indicating that the mixing by air agitation appeared to be adequate. However, a cooling system in which the bath medium is recirculated may prove to be superior to the existing system.

Prior to collecting data at a new temperature or a new pressure, the vapor and liquid sample systems were purged. This process consisted of acquiring samples and analyzing their compositions as described earlier. When the least volatile gas concentration reached a maximum, the sample line was known to be purged. Because each chromatogram required approximately 15 minutes and because several samples were required to purge each sample line, the amount of time to perform this operation was not inconsequential. The length of time required to purge the vapor sample system was much longer than for the liquid sample system. A solution to this problem and the problem of controlling the amount of vapor phase sample might be the inclusion of a multi-port injection

valve in the vapor recirculation line. This valve could be introduced to the GC directly or to a vaporization system that allows for sample expansion, homogenization, and dilution before being analyzed as suggested by Adams (1986).

In regard to future studies for this apparatus, two areas of interest come to mind. First, the systems studied in this work need to be explored at higher pressure and temperature ranges. Hardware limitation prevented study of the critical region in the current work. In expanding the data of the CH_4–CO_2–H_2S system, great care should be given to the analytical technique for measuring vapor and liquid phase compositions. Secondly, systems containing annhydrous NH_3 should be explored. The vapor-liquid equilibrium behavior of systems containing NH_3 should be interesting because of the NH_3 molecule's similarity to water.

LIST OF REFERENCES

LIST OF REFERENCES

W. R. Adams, "A New Apparatus for Measuring Supercritical Fluid-Liquid Phase Equilibria and Results for the Systems Carbon Dioxide + Decane, Carbon Dioxide + Dodecane, Carbon Dioxide + Methyl Linoleate, and Ethane + Methyl Linoleate", Ph. D. Dissertation [microfilm], Univ. Microfilms, Ann Arbor, Mich., 1986; Publication 8628416.

M. M. Abbott, "Cubic Equations of State: An Interpretive Review", Equations of State in Engineering and Research, ACS Series 182, eds. K. C. Chao and R. L. Robinson, 47-70, American Chemical Society, Washington D. C., 1979

J. A. Bierlein, and W. B. Kay, "Phase Equilibrium Properties of System Carbon Dioxide–Hydrogen Sulfide", Industrial and Engineering Chemistry, **43**, 3, 618, (1953).

J. F. Boston, and H. I. Britt, "A Radically Different Formulation and Solution of the Single-Stage Flash Problem", Computers and Chemical Engineering, **2**, 109, (1978).

H. I. Britt, and H. Lueke, "The Estimation of Parameters in Non-Linear Implicit Models", Technometrics, **15**, 233, (1973).

N. F. Carnahan, and A. T. Starling, "Intermolecular Repulsions and the Equation of State for Fluids", AIChE J., **18**, 1184, (1972).

P. L. Chueh, N. K. Muirbook, and J. M. Praunitz, "Thermodynamic Analysis", AIChE J., **11**, 1097, (1965).

J. Davalos, W. R. Anderson, R. E. Phelps, and A. Kidnay, "Liquid-Vapor Equilibria at 250 K for Systems Containing Methane, Ethane, and Carbon Dioxide." Journal of Chemical and Engineering Data, **21**, 1, 81, (1976).

H. G. Donnelly, and D. L. Katz, "Phase Equilibria in the Carbon Dioxide–Methane System", Industrial and Engineering Chemistry, **46**, 511, (1954).

M. A. Elliot, ed., Chemistry of Coal Utilization, Second Supplementary VXol., John Wiley, 1981.

T. M. Gilliam, "Development of the Krypton Absorption in Liquid CO_2 (KALC) Process: Mass Transfer Efficiencies of Packed Columns", Nuclear Technology, **43**, 75, (1979).

A. J. Grant, "Applications of the Woodall–Duckham Two-stage Coal Gasification," paper prepared for presentation at the 3rd Ann. Int. Conf. Coal Conversion, Pittsburg, August 3-5, (1976).

E. F. G. Herington, "A Thermodynamic Test for the Internal Consistency of Experimental Data on Volatility Ratios",Nature, **160**, 610, (1947).

F. H. Huang, M. H. LI, L. L. Lee, and K. E. Starling, "An Accurate Equation of State for Carbon Dioxide", Journal of Chemical Engineering of Japan, **18**, 6, 490, (1985).

M. J. Huron, G. N. Dufour, and J. Vidal, "Vapor–Liquid Equilibrium and Critical Locus Curve Calculations with the Soave Equation for Hydrocarbon Systems with Carbon Dioxide and Hydrogen Sulfide," Fluid Phase Equil., **1**, 247, (1978).

J. P. Kohn, and F. Kurata, "Heterogenous Phase Equilibria of the Methane–Hydrogen Sulfide System", AIChE J., **4**, 2, 211, (1958).

R. Konrad, I. Swaid, and G. M. Schneider, "High-Pressure Phase Studies on fluid Mixtures of Low-Volatile Organic Substances With Supercritical Carbon Dioxide", Fluid Phase Equil., **10**, 307, (1983).

Martin, and Hou, AIChE Journal, **142**, 1, (1955).

P. M. Mathias, and F. P. Stein, Phase Equilibrium Studies, **DOE/OR/03054-67 (DE 84014932)**, September 1983.

A. Michels, B. Blaisse, and C. Michels, Proc. Roy. Soc. (London), **A160**, 358, (1937).

A. Michels, T. Wassenaar, T. Zweitering, and P. Smits, Physica, **16**, 5, 501, (1950).

P. Nasir, R. J. Martin, and R. Kobayashi, "A Novel Apparatus for the Measurement of Phase and Volumetric Behavior at High Temperatures and Pressures and Its Application to Study VLE in the Hydrogen–Tetralin System", Fluid Phase Equil., **5**, 279, (1981).

D. Y. Peng, and D. B. Robinson, "A New Two-Constant Equation of State," Industrial and Engineering Chemistry Fundundamentals, **15**, 54, (1976).

J. M. Prausnitz, Molecular Thermodynamics of Fluid-Phase Equilibria, Prentice-Hall, Englewood Cliffs, N. J., (1969).

H. H. Reamer, B. H. Sage, and W. N. Lacey, "Phase Equilibria in Hydrocarbon Systems", Industrial and Engineering Chemistry, **43**, 4, 976, (1951).

O. Redlich, and A. T. Kister, "Algebraic Representation of Thermodynamic Properties and the Classification of Solutions", Industrial and Engineering Chemistry, **40**, 345, (1948).

O. Redlich, and J. N. S. Kwong, "An Equation of State. Fugacities of Gaseous Compounds.", Chem. Rev., **44**, 233, (1949).

R. C. Reid, J. M. Prausnitz, and T. K. Sherwood, The Properties of Gases and Liquids, McGraw Hill, New York, 1977.

G. Soave, "Equilibrium Constants From a Modified Redlich–Kwong Equation of State", Chem. Engr. Sci., **27**, 1197, (1972).

D. P. Sobocinski, and F. Kurata, "Heterogeneous Phase Equilibria of the Hydrogen Sulfide–Carbon Dioxide System", AIChE J., **5**, 4, 545, (1959).

F. A. Somait, and A. J. Kidnay, "Liquid-Vapor equilibria at 270.00 K for Systems Containing Nitrogen, Methane, and Carbon Dioxide", Journal of Chemical Engineering Data, **23**, 4, 301, (1978).

R. Stryjek, and J. H. Vera, "PRSV: An Improved Peng–Robinson Equation of State for Pure Components and Mixtures", Can. J. Chem. Engr., **64**, 323, (1986).

R. Stryjek, and J. H. Vera, "PRSV: An Improved Peng–Robinson Equation of State with New Mixing Rules for Strongly Nonideal Mixtures", Can. J. Chem. Engr., **64**, 334, (1986).

D. R. Stull, "Vapor Pressure of Pure Substances", Industrial and Engineering Chemistry, **39**, 517, (1947).

I. Swaid, D. Nickel, and G. M. Schneider, "NIR–Spectroscopic Investigations on Phase Behavior of Low-Volatile Organic Substances in Critical Carbon Dioxide", Fluid Phase Equil., **21**, 95, (1985).

W. B. Whiting, "High Pressure Vapor-Liquid Equilibria for Asymmetric Mixtures", Ph. D. Dissertation [microfilm], Univ. Microfilms, Ann Arbor, Mich., 1982; Publication 8300704.

APPENDICES

APPENDIX I

OPERATING INSTRUCTIONS FOR THE ORNL VAPOR–LIQUID EQUILIBRIUM APPARATUS

The valving configuration at start-up should be as follows: the chromatograph sample valve and valves 2, 3, 4, 13, 17, 20, 24 should be closed All other valves should be open.

A. Charging the equilibrium cell with carbon dioxide

(1) Note that the zero indicator on the Differential Pressure (DPI) at maximum gain.

(2) Close valves 22 and 25

(3) Open the valve on the nitrogen cylinder. The regulator can be set to any pressure. It is convenient to set the regulator to 1000 psia.

(4) By slightly opening valve 22, add 100 psig of N_2.

(5) Close valve 22.

(6) The DPI zero is a function of pressure. Note the difference in the zero at 100 psi and make necessary adjustments.

(7) Close valve 16.

(8) Open the valve on the CO_2 cylinder.

(9) Slowly open valve 2 to introduce CO_2 to the remainder of the system. Watch the DPI. Before opening valve 2, the needle will be pegged to the right of zero. When the CO_2 pressure has reached 100 psi, the needle will move to zero. A small overshoot may occur, as the DPI is extremely sensitive.

(10) Close valve 2 when the proper amount of CO_2 has been added.

(11) Repeat steps 9 and 10, then close the CO_2 cylinder valve.

(12) Allow the system a little time to mix.

(13) Open valve 16.

(14) Open valve 25.

(15) Check the zero of the DPI. If the zero does not return to the original

setting within 5 minutes, close valve 25 and repeat steps 3 to 14.

(16) If the zero is repeated, add 100 psi of N_2 as in steps 2 to 4. Then add 100 psi of CO_2 and vent several times to purge the system of air.

(17) Close valves 16, 18, and 19.

(18) Open valve 2 and allow approximately 5 minutes for the expansion bomb to equilibrate with the CO_2 cylinder.

(19) Close valve 2 and the valve on the CO_2 cylinder.

(20) Open valve 18. Allow the temperature to return to the desired value.

(21) Close valve 18. This has charged the EC with liquid.

(22) Repeat steps 17 to 21.

(23) Open valve 22 and allow an additional 100 psi of N_2 to enter the top chamber of the DPI.

(24) Close valve 22.

(25) Reduce the DPI zero to correspond with the new pressure.

(26) Repeat steps 13 through 15 until the N_2 pressure remains greater than the equilibrium cell pressure. In other words, continue steps 13 through 15 until the DPI needle remains pegged to the right when valve 19 is fully open.

(27) Open valve 25 allowing N_2 to escape until the DPI has been zeroed.

(28) Close valve 23 and keep the DPI zeroed by using the Precise Pressure Controller. The DPI is extremely sensitive to temperature.

(29) Allow the temperature to stabilize. The barometric pressure plus the manometer pressure is now the vapor pressure of CO_2.

B. Charging the equilibrium cell with methane

(1) Open valve 16 to vent excess CO_2 from part A. Close valve 16 when the system has been vented.

(2) Open the CH_4 cylinder valve with the regulator at 100 psi. Allow the gas in the manifold to mix for a few minutes. Close the CH_4 cylinder valve and open valve 16. Continue this several times to prevent air contamination.

(3) Close valves 16 and 19.

(4) Increase the CH_4 regulator pressure to the desired system pressure. This should be above the vapor pressure of the liquid, of course.

(5) Open valve 18 until the system temperature has returned to the desired level. This assures that an adequate CH_4 charge has been added.

(6) Close valve 18.

(7) Increase the DPI pressure to that of the EC in the step-by-step manner outlined earlier.

(8) Turn on the magnetic pump and allow the system to mix.

C. Taking vapor and liquid samples

The system refrigerator controls $\pm$ 0.5°C about the desired temperature. When samples are taken, a $\pm$ 0.1°C difference is desired. For this reason, one must allow the system to cool about 0.2°C below the desired temperature before taking a sample. Once the temperature has "undershot" the desired temperature, manually close the solenoid valve and allow the system to warm. Using this method gives a tighter temperature control as the system warms slowly and evenly.

(1) Once the temperature is as desired, close valves 7 and 21.

(2) Slowly open valve 17. Close when the compound gauge on the sampling system is approximately 10 psi. This traps the vapor sample

(3) The system has now cooled about 0.1°C. Allow the system to warm to the desired temperature.

(4) Open valve 20. Close after about 30 seconds.

(5) Open the valve leading to the GC and start the analysis of the vapor sample.

(6) When the vapor sample has been vented, close the GC valve and open valve 7 to evacuate the sample system.

(7) Open the GC valve and begin the analysis of the liquid sample.

(8) After the liquid sample has been vented, close the GC valve and open valve 7 to evacuate the sample system.

APPENDIX II

EXAMPLE OF AN ASPEN DRS INPUT FILE AND REPORT

```
NEW DRS
;-----------------------------------------------------------------
;
;                          OAK RIDGE NATIONAL LABORATORY
;
;    AUTHOR        : James S. Morris          Date:   April 17, 1988
;
;    SHORT TITLE   : DRS RUN FOR THE METHANE - CARBON DIOXIDE SYSTEM
;
;    DESCRIPTION   : REGRESSION OF EXPERIMENTAL AND LITERATURE DATA
;                    FOR PR BINARY INTERACTION PARAMETER IN THE RANGE
;                    OF 270 K TO 288.2 K.
;
;-----------------------------------------------------------------

;
TITLE 'DATA REGRESSION FOR METHANE-CARBON DIOXIDE SYSTEM'
IN-UNITS SI PRES=PSIA
OUT-UNITS SI PRES=PSIA
HISTORY MSG-LEVEL PROPERTIES=2
RUN-CONTROL MAX-ERRORS=250
COMPONENTS C1 CH4/C2 CO2
PROPERTIES SYSOP3; REDLICH-KWONG-SOAVE
;
PARAMETERS
  BIPARAMETER 1 RKSKIJ C1 C2 1 -1.0 -1.05 0.564
;
DATA-GROUP G1
  SYSTEM-DEF TPXY C1 C2
  PHASE-EQ VL C1 C2
  STD-DEV  1  1.0  2.0  0.002  0.0005
;
;-------------------------------------------------
;    EXPERIMENTAL RESULTS - MORRIS (1988)
;-------------------------------------------------
;              T        P         X         Y
;
  DATA  1   288.15    822.0    0.02586   0.06825/
        2   288.15    820.0    0.02510   0.06857/
        3   288.15    884.0    0.04157   0.11602/
        4   288.15    881.9    0.04210   0.11505/
        5   288.15   1003.1    0.07536   0.16260/
        6   288.15    997.6    0.07569   0.16113/
        7   270.0     629.3    0.04188   0.19153/
        8   270.0     738.3    0.07253   0.27905/
        9   270.0     807.0    0.09158   0.31846/
       10   270.0     907.5    0.12954   0.35961/
       11   270.0     904.7    0.12555   0.36128/
       12   270.0     996.4    0.15769   0.37822/
       13   270.0     993.7    0.15553   0.37964/
;-------------------------------------------------
```

```
;-------------------------------------------------
;    LITERATURE DATA - DAVALOS, ET AL (1976)
;-------------------------------------------------
;              T         P          X          Y
;
       14    270.0     515.7     0.01400    0.08300/
       15    270.0     536.8     0.01800    0.10800/
       16    270.0     584.2     0.03200    0.16200/
       17    270.0     611.2     0.04000    0.19000/
       18    270.0     734.4     0.07700    0.28200/
       19    270.0     849.6     0.11300    0.35300/
       20    270.0    1018.3     0.16600    0.40500/
       21    270.0    1169.5     0.26000    0.41100/
;-------------------------------------------------
;    LITERATURE DATA - KIDNAY, ET AL (1978)
;-------------------------------------------------
;              T         P          X          Y
;
       22    270.0     556.2     0.02370    0.12690/
       23    270.0     637.1     0.04550    0.20820/
       24    270.0     707.6     0.06660    0.26290/
       25    270.0     764.2     0.08380    0.29620/
       26    270.0     881.8     0.12260    0.35190/
       27    270.0     961.1     0.15330    0.37740/
       28    270.0    1116.9     0.22240    0.40060/
       29    270.0    1196.2     0.27400    0.38950/
;-------------------------------------------------
;    LITERATURE DATA - DONNELLY, ET AL (1954)
;-------------------------------------------------
;              T         P          X          Y
;
       30    271.5     733.0     0.06750    0.25300/
       31    271.5     811.0     0.08400    0.30000/
       32    271.5     870.0     0.10300    0.32900/
       33    271.5     988.0     0.16000    0.36700/
       34    271.5     992.0     0.15700    0.36900/
       35    271.5    1052.0     0.16500    0.38700/
       36    271.5    1108.0     0.19100    0.39000
;
CASE C1
  PARAMETERS BINARY =1
  DATA-GROUPS G1
  PROPERTIES SYSOP3
  ALGORITHM MAXIT=100 IDEM=-1
```

RUN CONTROL INFORMATION

TYPE OF RUN: NEW

INPUT FILE NAME: DRSB

INPUT PROBLEM DATA FILE NAME: DRSB UPDATE NO. 0

MAIN CALLING PROGRAM NAME: DRSB

DRS ONLY RUN

DATA REGRESSION FOR METHANE-CARBON DIOXIDE SYSTEM

TABLE OF CONTENTS

PHYSICAL PROPERTIES SECTION..... 1
COMPONENTS..... 1
OPTION SETS..... 1

DATA REGRESSION SECTION..... 2
SUBSECTION: CASE C1..... 2

DATA REGRESSION FOR METHANE-CARBON DIOXIDE SYSTEM

PHYSICAL PROPERTIES SECTION

COMPONENTS

ID	TYPE	FORMULA	DATABANK REFERENCE	ALIAS
C1	C	CH4	CH4	CH4
C2	C	CO2	CO2	CO2

OPTION SETS

SYSOP0

MAJOR PROPERTY ROUTE ID						
	PHILMX	HVMX	HLMX	GVMX	GLMX	SVMX
	PHILMX00	HVMX00	HLMX00	GVMX00	GLMX00	SVMX00
	SLMX	VVMX	VLMX	MUVMX	MULMX	KVMX
	SLMX00	VVMX00	VLMX01	MUVMX01	MULMX01	KVMX01
	KLMX	DVMX	DLMX	SIGLMX	PHIV	PHIL
	KLMX01	DVMX01	DLMX01	SIGLMX01	PHIV01	PHIL00
	HV	HL	GV	GL	SV	SL
	HV00	HL00	GV00	GL00	SV00	SL00
	VV	VL	KS	VS	PHISMX	HSMX
	VV00	VL01	KS01	VS01	PHISMX02	HSMX02
	GSMX	SSMX	VSMX	KSMX	PHIS	HS
	GSMX02	SSMX01	VSMX02	KSMX01	PHIS02	HS02
	GS	SS				
	GS02	SS02				

SYSOP3

MAJOR PROPERTY ROUTE ID						
	PHIVMX	PHILMX	HVMX	HLMX	GVMX	GLMX
	PHIVMX03	PHILMX03	HVMX03	HLMX03	GVMX03	GLMX03
	SVMX	SLMX	VVMX	VLMX	PHIV	PHIL
	SVMX03	SLMX03	VVMX03	VLMX03	PHIV03P	PHIL03P
	HV	HL	GV	GL	SV	SL
	HV03	HL03	GV03	GL03	SV03	SL03
	VV	VL	MUVMX	MULMX	KVMX	KLMX
	VV03	VL03	MUVMX02	MULMX02	KVMX02	KLMX01
	DVMX	DLMX	SIGLMX			
	DVMX02	DLMX01	SIGLMX01			

DATA REGRESSION FOR METHANE-CARBON DIOXIDE SYSTEM

DATA REGRESSION SECTION

SUBSECTION: CASE C1

PARAMETER NAME	ELEMENT NUMBER	COMPONENT OR PAIR		PARAMETER ESTIMATE	STANDARD DEVIATION
RKSKIJ	1	C1	C2	.1031594	.3243551E-02

NUMBER OF ITERATIONS 1

DATA REGRESSION FOR METHANE-CARBON DIOXIDE SYSTEM

DATA REGRESSION SECTION

SUBSECTION: CASE C1 (CONTINUED)

DATA-GROUP G1 VARIABLE: TEMPERATURE
UNITS : K

MEASURED	ESTIMATED	STD-DEVIATION	ADJUSTMENTS	% ADJUSTMENTS
288.1500	287.7836	1.0000	-.36645	-.12717
288.1500	287.6704	1.0000	-.47962	-.16645
288.1500	287.1987	1.0000	-.95135	-.33016
288.1500	287.1898	1.0000	-.96015	-.33321
288.1500	288.0738	1.0000	-.76238E-01	-.26458E-01
288.1500	288.0272	1.0000	-.12281	-.42619E-01
270.0000	270.3307	1.0000	.33075	.12250
270.0000	269.9660	1.0000	-.34037E-01	-.12606E-01
270.0000	269.8802	1.0000	-.11981	-.44376E-01
270.0000	270.0439	1.0000	.43892E-01	.16256E-01
270.0000	269.8103	1.0000	-.18969	-.70254E-01
270.0000	270.7568	1.0000	.75681	.28030
270.0000	270.5665	1.0000	.56648	.20981
270.0000	269.4532	1.0000	-.54679	-.20251
270.0000	269.5505	1.0000	-.44948	-.16647
270.0000	269.5281	1.0000	-.47185	-.17476
270.0000	269.4479	1.0000	-.55205	-.20446
270.0000	269.6308	1.0000	-.36918	-.13673
270.0000	268.8034	1.0000	-1.1966	-.44317
270.0000	268.8695	1.0000	-1.1305	-.41870
270.0000	270.1186	1.0000	.11860	.43925E-01
270.0000	269.7804	1.0000	-.21958	-.81326E-01
270.0000	269.7465	1.0000	-.25354	-.93905E-01
270.0000	269.7231	1.0000	-.27693	-.10257
270.0000	269.8710	1.0000	-.12897	-.47766E-01
270.0000	269.9024	1.0000	-.97638E-01	-.36162E-01
270.0000	270.0372	1.0000	.37249E-01	.13796E-01
270.0000	270.8072	1.0000	.80717	.29895
270.0000	272.2651	1.0000	2.2651	.83892
271.5000	271.4928	1.0000	-.72007E-02	-.26522E-02
271.5000	271.3213	1.0000	-.17868	-.65813E-01
271.5000	271.2087	1.0000	-.29133	-.10730
271.5000	271.5315	1.0000	.31535E-01	.11615E-01
271.5000	271.4392	1.0000	-.60810E-01	-.22398E-01
271.5000	270.9903	1.0000	-.50973	-.18775
271.5000	271.5942	1.0000	.94222E-01	.34704E-01

ROOT MEAN SQUARES DEVIATION = .6134215
AVERAGE ABSOLUTE DEVIATION = .4192431
MAXIMUM DEVIATION = 2.265082

DATA REGRESSION FOR METHANE-CARBON DIOXIDE SYSTEM

DATA REGRESSION SECTION

SUBSECTION: CASE C1 (CONTINUED)

DATA-GROUP G1 VARIABLE: PRESSURE
UNITS : PSIA

MEASURED	ESTIMATED	STD-DEVIATION	ADJUSTMENTS	% ADJUSTMENTS
822.0000	822.1910	2.0000	.19101	.23237E-01
820.0000	820.1633	2.0000	.16328	.19912E-01
884.0000	883.8697	2.0000	-.13026	-.14736E-01
881.9000	881.8557	2.0000	-.44331E-01	-.50267E-02
1003.100	1002.532	2.0000	-.56750	-.56575E-01
997.6000	997.3074	2.0000	-.29259	-.29329E-01
629.3000	629.1542	2.0000	-.14576	-.23162E-01
738.3000	737.8066	2.0000	-.49336	-.66824E-01
807.0000	805.9838	2.0000	-1.0162	-.12593
907.5000	906.8877	2.0000	-.61225	-.67466E-01
904.7000	903.3968	2.0000	-1.3032	-.14405
996.4000	995.1714	2.0000	-1.2286	-.12331
993.7000	992.0639	2.0000	-1.6361	-.16465
515.7000	515.8327	2.0000	.13270	.25731E-01
536.8000	536.8425	2.0000	.42510E-01	.79191E-02
584.2000	584.2443	2.0000	.44304E-01	.75837E-02
611.2000	611.2528	2.0000	.52813E-01	.86409E-02
734.4000	734.5203	2.0000	.12033	.16384E-01
849.6000	848.9551	2.0000	-.64487	-.75903E-01
1018.300	1015.073	2.0000	-3.2271	-.31691
1169.500	1177.720	2.0000	8.2201	.70288
556.2000	556.2191	2.0000	.19110E-01	.34358E-02
637.1000	637.0033	2.0000	-.96748E-01	-.15186E-01
707.6000	707.4713	2.0000	-.12872	-.18191E-01
764.2000	764.0463	2.0000	-.15367	-.20109E-01
881.8000	881.5340	2.0000	-.26598	-.30163E-01
961.1000	961.3145	2.0000	.21453	.22321E-01
1116.900	1119.917	2.0000	3.0173	.27015
1196.200	1216.076	2.0000	19.876	1.6616
733.0000	732.8247	2.0000	-.17528	-.23913E-01
811.0000	809.7269	2.0000	-1.2731	-.15697
870.0000	868.3354	2.0000	-1.6646	-.19133
988.0000	989.1504	2.0000	1.1504	.11643
992.0000	991.7958	2.0000	-.20416	-.20581E-01
1052.000	1047.925	2.0000	-4.0753	-.38738
1108.000	1104.055	2.0000	-3.9450	-.35605

ROOT MEAN SQUARES DEVIATION = 3.832435
AVERAGE ABSOLUTE DEVIATION = 1.571351
MAXIMUM DEVIATION = 19.87554

DATA REGRESSION FOR METHANE-CARBON DIOXIDE SYSTEM

DATA REGRESSION SECTION

SUBSECTION: CASE C1 (CONTINUED)

DATA-GROUP G1 VARIABLE: COMPOSITION LIQUID C1
UNITS : MOL-FR

MEASURED	ESTIMATED	STD-DEVIATION	ADJUSTMENTS	% ADJUSTMENTS
.2586000E-01	.2391669E-01	.20000E-02	-.19433E-02	-7.5147
.2510000E-01	.2391574E-01	.20000E-02	-.11843E-02	-4.7182
.4157000E-01	.4497369E-01	.20000E-02	.34037E-02	8.1878
.4210000E-01	.4445084E-01	.20000E-02	.23508E-02	5.5839
.7536000E-01	.7899669E-01	.20000E-02	.36367E-02	4.8257
.7569000E-01	.7755734E-01	.20000E-02	.18673E-02	2.4671
.4188000E-01	.4274823E-01	.20000E-02	.86823E-03	2.0731
.7253000E-01	.7628011E-01	.20000E-02	.37501E-02	5.1704
.9158000E-01	.9816371E-01	.20000E-02	.65837E-02	7.1890
.1295400	.1322476	.20000E-02	.27076E-02	2.0902
.1255500	.1318546	.20000E-02	.63046E-02	5.0216
.1576900	.1620495	.20000E-02	.43595E-02	2.7646
.1555300	.1616465	.20000E-02	.61165E-02	3.9327
.1400000E-01	.1457927E-01	.20000E-02	.57927E-03	4.1377
.1800000E-01	.1986805E-01	.20000E-02	.18680E-02	10.378
.3200000E-01	.3295585E-01	.20000E-02	.95585E-03	2.9870
.4000000E-01	.4081989E-01	.20000E-02	.81989E-03	2.0497
.7700000E-01	.7661625E-01	.20000E-02	-.38375E-03	-.49838
.1130000	.1170535	.20000E-02	.40535E-02	3.5871
.1660000	.1784921	.20000E-02	.12492E-01	7.5253
.2600000	.2486661	.20000E-02	-.11334E-01	-4.3592
.2370000E-01	.2436831E-01	.20000E-02	.66831E-03	2.8199
.4550000E-01	.4710313E-01	.20000E-02	.16031E-02	3.5234
.6660000E-01	.6798435E-01	.20000E-02	.13843E-02	2.0786
.8380000E-01	.8491525E-01	.20000E-02	.11152E-02	1.3308
.1226000	.1238809	.20000E-02	.12809E-02	1.0448
.1533000	.1525085	.20000E-02	-.79152E-03	-.51632
.2224000	.2160581	.20000E-02	-.63419E-02	-2.8516
.2740000	.2562728	.20000E-02	-.17727E-01	-6.4698
.6750000E-01	.6886852E-01	.20000E-02	.13685E-02	2.0274
.8400000E-01	.9325937E-01	.20000E-02	.92594E-02	11.023
.1030000	.1131514	.20000E-02	.10151E-01	9.8557
.1600000	.1561847	.20000E-02	-.38153E-02	-2.3845
.1570000	.1577429	.20000E-02	.74293E-03	.47321
.1650000	.1810360	.20000E-02	.16036E-01	9.7188
.1910000	.2032488	.20000E-02	.12249E-01	6.4130

ROOT MEAN SQUARES DEVIATION = .6418357E-02
AVERAGE ABSOLUTE DEVIATION = .4502710E-02
MAXIMUM DEVIATION = -.1772721E-01

DATA REGRESSION FOR METHANE-CARBON DIOXIDE SYSTEM

DATA REGRESSION SECTION

SUBSECTION: CASE C1 (CONTINUED)

DATA-GROUP G1 VARIABLE: COMPOSITION VAPOR C1
UNITS : MOL-FR

MEASURED	ESTIMATED	STD-DEVIATION	ADJUSTMENTS	% ADJUSTMENTS
.6825000E-01	.6829017E-01	.50000E-03	.40169E-04	.58856E-01
.6857000E-01	.6858863E-01	.50000E-03	.18634E-04	.27176E-01
.1160200	.1159366	.50000E-03	-.83405E-04	-.71888E-01
.1150500	.1149850	.50000E-03	-.64977E-04	-.56477E-01
.1626000	.1625123	.50000E-03	-.87654E-04	-.53908E-01
.1611300	.1610817	.50000E-03	-.48284E-04	-.29966E-01
.1915300	.1915236	.50000E-03	-.64090E-05	-.33462E-02
.2790500	.2789936	.50000E-03	-.56408E-04	-.20214E-01
.3184600	.3183523	.50000E-03	-.10773E-03	-.33827E-01
.3596100	.3595548	.50000E-03	-.55207E-04	-.15352E-01
.3612800	.3611539	.50000E-03	-.12607E-03	-.34897E-01
.3782200	.3781321	.50000E-03	-.87877E-04	-.23234E-01
.3796400	.3795110	.50000E-03	-.12903E-03	-.33989E-01
.8300000E-01	.8298694E-01	.50000E-03	-.13059E-04	-.15734E-01
.1080000	.1079758	.50000E-03	-.24178E-04	-.22387E-01
.1620000	.1619820	.50000E-03	-.18034E-04	-.11132E-01
.1900000	.1899815	.50000E-03	-.18490E-04	-.97318E-02
.2820000	.2820000	.50000E-03	.83784E-08	.29711E-05
.3530000	.3529039	.50000E-03	-.96145E-04	-.27237E-01
.4050000	.4047064	.50000E-03	-.29357E-03	-.72486E-01
.4110000	.4114496	.50000E-03	.44964E-03	.10940
.1269000	.1268895	.50000E-03	-.10527E-04	-.82954E-02
.2082000	.2081755	.50000E-03	-.24496E-04	-.11765E-01
.2629000	.2628748	.50000E-03	-.25159E-04	-.95697E-02
.2962000	.2961792	.50000E-03	-.20752E-04	-.70060E-02
.3519000	.3518722	.50000E-03	-.27812E-04	-.79035E-02
.3774000	.3774196	.50000E-03	.19645E-04	.52055E-02
.4006000	.4008311	.50000E-03	.23109E-03	.57687E-01
.3895000	.3902286	.50000E-03	.72860E-03	.18706
.2530000	.2529785	.50000E-03	-.21466E-04	-.84847E-02
.3000000	.2998572	.50000E-03	-.14284E-03	-.47613E-01
.3290000	.3288245	.50000E-03	-.17546E-03	-.53333E-01
.3670000	.3670986	.50000E-03	.98613E-04	.26870E-01
.3690000	.3689807	.50000E-03	-.19259E-04	-.52194E-02
.3870000	.3866419	.50000E-03	-.35815E-03	-.92544E-01
.3900000	.3896902	.50000E-03	-.30979E-03	-.79432E-01

ROOT MEAN SQUARES DEVIATION = .1866002E-03
AVERAGE ABSOLUTE DEVIATION = .1121846E-03
MAXIMUM DEVIATION = .7286033E-03

DATA REGRESSION FOR METHANE-CARBON DIOXIDE SYSTEM

DATA REGRESSION SECTION

SUBSECTION: CASE C1 (CONTINUED)

PARAMETER CORRELATION MATRIX

1.0000000

APPENDIX III

EXAMPLE OF AN ASPEN FLASH2 INPUT FILE AND REPORT

```
NEW
;-----------------------------------------------------------------------
;
;                          OAK RIDGE NATIONAL LABORATORY
;
;    AUTHOR        : James S. Morris          Date:   April 2, 1988
;
;    SHORT TITLE   : FLASH CALCULATION FOR THE CO2 - CH4 - H2S SYSTEM
;
;    DESCRIPTION   : IN THIS CALCUATION THE VAPOR PHASE IS HELD TO
;                    NEAR THE EXPERIMENTAL COMPOSITION AND THE LIQUID
;                    PHASE COMPOSITION AND PRESSURE ARE DETERMINED
;                    USING THE RKS EQUATION OF STATE.
;-----------------------------------------------------------------------
TITLE 'FLASH CALCULATION'
IN-UNITS SI PRES=PSIA
OUT-UNITS SI PRES=PSIA
HISTORY MSG-LEVEL PROPERTIES=2
RUN-CONTROL MAX-ERRORS=250
COMPONENTS C1 CH4/C2 CO2/C3 H2S
PROPERTIES SYSOP3 GLOBAL ; REDLICH-KWONG-SOAVE
;
PROP-DATA
  PROP-LIST RKSIJ
  BPVAL C1 C2 0.1032
  BPVAL C2 C3 0.09968
  BPVAL C1 C3 0.08261
;
FLOWSHEET
  F1  IN=S1  OUT=S2 S3
;
STREAM S1 TEMP=300.0 V=0
  MOLE-FLOW C1 .4057/C2 .4825/C3 .1119
;
BLOCK F1 FLASH2 TEMP=270.0 V=0.999
```

RUN CONTROL INFORMATION

TYPE OF RUN: NEW

INPUT FILE NAME: FL3

INPUT PROBLEM DATA FILE NAME: FL3 UPDATE NO. 0

MAIN CALLING PROGRAM NAME: FL3

SIMULATION REQUESTED FOR ENTIRE FLOWSHEET

FLASH CALCULATION
TABLE OF CONTENTS

FLOWSHEET SECTION..... 1
FLOWSHEET CONNECTIVITY BY STREAMS..... 1
FLOWSHEET CONNECTIVITY BY BLOCKS..... 1
COMPUTATIONAL SEQUENCE USED..... 1
OVERALL FLOWSHEET BALANCE..... 1

PHYSICAL PROPERTIES SECTION..... 2
COMPONENTS..... 2
OPTION SETS..... 2

UNIT OPERATION BLOCK SECTION..... 3
FLASH:2-OUTL (FLASH2): F1..... 3
FLASH UNIT SUMMARY..... 4

STREAM SECTION..... 5
S2 S3 S1..... 5

FLASH CALCULATION
FLOWSHEET SECTION

FLOWSHEET CONNECTIVITY BY STREAMS

STREAM	SOURCE	DESTINATION	STREAM	SOURCE	DESTINATION
S2	F1	----	S3	F1	----
S1	----	F1			

FLOWSHEET CONNECTIVITY BY BLOCKS

BLOCK	INLETS	OUTLETS
F1	S1	S2 S3

COMPUTATIONAL SEQUENCE USED

F1

OVERALL FLOWSHEET BALANCE

*** MASS AND ENERGY BALANCE ***

	IN	OUT	RELATIVE DIFF.
CONVENTIONAL COMPONENTS (KMOL/SEC)			
C1	.405700	.405700	-.128348E-06
C2	.482500	.482500	.407186E-07
C3	.111900	.111900	.289760E-06
TOTAL BALANCE			
MOLE(KMOL/SEC)	1.00010	1.00010	.000000E+00
MASS(KG/SEC)	31.5570	31.5570	.359443E-07
ENTHALPY(WATT)	-.227825E+09	-.225799E+09	-.889091E-02

CONVENTIONAL MASS BALANCE SATISFACTORY

FLASH CALCULATION
PHYSICAL PROPERTIES SECTION

COMPONENTS

ID	TYPE	FORMULA	DATABANK REFERENCE	ALIAS
C1	C	CH4	CH4	CH4
C2	C	CO2	CO2	CO2
C3	C	H2S	H2S	H2S

OPTION SETS

SYSOP0

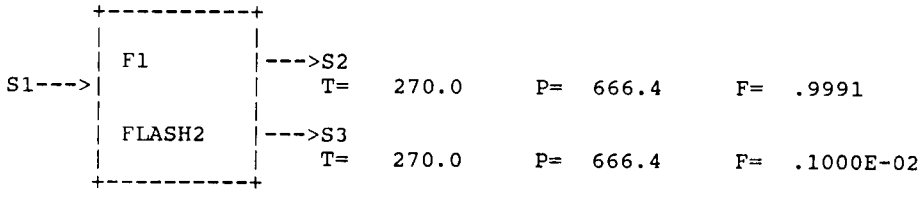
MAJOR PROPERTY ROUTE ID						
	PHILMX	HVMX	HLMX	GVMX	GLMX	SVMX
	PHILMX00	HVMX00	HLMX00	GVMX00	GLMX00	SVMX00
	SLMX	VVMX	VLMX	MUVMX	MULMX	KVMX
	SLMX00	VVMX00	VLMX01	MUVMX01	MULMX01	KVMX01
	KLMX	DVMX	DLMX	SIGLMX	PHIV	PHIL
	KLMX01	DVMX01	DLMX01	SIGLMX01	PHIV01	PHIL00
	HV	HL	GV	GL	SV	SL
	HV00	HL00	GV00	GL00	SV00	SL00
	VV	VL	KS	VS	PHISMX	HSMX
	VV00	VL01	KS01	VS01	PHISMX02	HSMX02
	GSMX	SSMX	VSMX	KSMX	PHIS	HS
	GSMX02	SSMX01	VSMX02	KSMX01	PHIS02	HS02
	GS	SS				
	GS02	SS02				

SYSOP3

MAJOR PROPERTY ROUTE ID						
	PHIVMX	PHILMX	HVMX	HLMX	GVMX	GLMX
	PHIVMX03	PHILMX03	HVMX03	HLMX03	GVMX03	GLMX03
	SVMX	SLMX	VVMX	VLMX	PHIV	PHIL
	SVMX03	SLMX03	VVMX03	VLMX03	PHIV03P	PHIL03P
	HV	HL	GV	GL	SV	SL
	HV03	HL03	GV03	GL03	SV03	SL03
	VV	VL	MUVMX	MULMX	KVMX	KLMX
	VV03	VL03	MUVMX02	MULMX02	KVMX02	KLMX01
	DVMX	DLMX	SIGLMX			
	DVMX02	DLMX01	SIGLMX01			

FLASH CALCULATION
UNIT OPERATION BLOCK SECTION

FLASH:2-OUTL (FLASH2): F1



PROPERTY OPTION SET: SYSOP3

CONVENTIONAL MASS BALANCE SATISFACTORY

*** INPUT DATA ***

2 PHASE TV FLASH	
SPECIFIED TEMPERATURE K	270.000
VAPOR FRACTION	0.99900
NO INITIAL PRESSURE GUESS	
MAXIMUM NUMBER OF ITERATIONS	30
CONVERGENCE TOLERANCE	0.00010000
LIQUID ENTRAINMENT	.00000E+00

*** RESULTS ***

OUTPUT TEMPERATURE	K	270.00
OUTPUT PRESSURE	PSIA	666.40
HEAT DUTY	WATT	.20256E+07
VAPOR FRACTION		.99900

V-L PHASE EQUILIBRIUM :

COMPONENT	F(I)	X(I)	Y(I)	K(I)
C1	.40566	.10603	.40596	3.8288
C2	.48245	.59551	.48234	.80988
C3	.11189	.29847	.11170	.37420

FLASH CALCULATION
UNIT OPERATION BLOCK SECTION

FLASH UNIT SUMMARY

BLOCK ID	F1
MODEL TYPE	FLASH2
OUTLET TEMPERATURE (K)	270.0000
OUTLET PRESSURE(PSIA)	666.4016
VAPOR FRACTION	0.9990
HEAT DUTY (WATT)	.20256+07
FLOW LIQUID1/FLOW LIQUID2	MISSING
VAPOR FLOW (KMOL/SEC)	0.9990
LIQUID1 FLOW (KMOL/SEC)	0.0010
LIQUID2 FLOW (KMOL/SEC)	
VAPOR VOL-FLOW(CUM/SEC)	0.3497
LIQ VOL-FLOW (CUM/SEC)	.50828-04
DENSITY RATIO	2.7044

FLASH CALCULATION
STREAM SECTION

S2 S3 S1 FLOW DETAILS	S2	S3	S1
COMPONENT FLOWS <KMOL/SEC>			
CH4	0.4055	.10604-03	0.4057
CO2	0.4819	.59557-03	0.4825
H2S	0.1116	.29850-03	0.1119
TOTAL	0.9990	0.0010	1.0001
PHASE SPLITS			
VAPOR FRACTION <MOLE BASIS>	1.0000	0.0	0.0
LIQUID FRACTION <MOLE BASIS>	0.0	1.0000	1.0000
SOLID FRACTION <MOLE BASIS>	0.0	0.0	0.0
INTENSIVE PROPERTIES			
TEMPERATURE <K>	270.0000	270.0000	300.0000
PRESSURE <PSIA>	666.4016	666.4016	1650.9491
MOLECULAR WEIGHT	31.5473	38.0810	31.5538
ENTHALPY <J/KMOL>	-.22574+09	-.26225+09	-.22780+09
ENTROPY <J/KMOL-K>	-.59554+05	-.63634+05	-.71227+05
DENSITY <KMOL/CUM>	2.8568	19.6763	8.6131

APPENDIX IV

EXAMPLE OF AN ASPEN TGS INPUT FILE AND REPORT

```
NEW TGS
;-------------------------------------------------------------------------
;
;                          OAK RIDGE NATIONAL LABORATORY
;
;    AUTHOR        : James S. Morris        Date:   April 2, 1988
;
;    SHORT TITLE   : TGS RUN FOR THE METHANE - HYDROGEN SULFIDE SYSTEM
;
;    DESCRIPTION   : THIS IS A TABLE GENERATION INPUT FILE AND REPORT
;                    USING THE PR EQUATION OF STATE.  THIS TABLE SHOWS
;                    A P-T ENVELOPE FOR A MIXTURE OF 72.5 PERCENT METHANE
;
;-------------------------------------------------------------------------
;
PROPERTIES   SYSOP4
TITLE 'TGS RUN FOR THE METHANE - H2S SYSTEM '
COMPONENTS   METHANE   CH4 / H2S H2S
OUT-UNITS ENG TEMP=K
PROP-DATA
 PROP-LIST PRKIJ
 BPVAL METHANE H2S 0.08672
REPORT   TABLES
PPTABLES   TABLE1   PTENVELOPE
     DESCRIPTION   'PT ENVELOPE USING PENG-ROBINSON EQU. OF STATE'
     SYSTEM    1   METHANE   .725/ H2S .275
     DEP-VAR   1   TEMP   PRES   MOLEFRAC   PHIVMX   VLMX   &
           COMP = METHANE H2S PHASES = VL
     INDEP-VAR   1   VFRAC
     RANGE   1   LIST = 1.0
     PARAM   1   MAXPT = 30   RED-T = 0.5
     TABLE   1   'VAP. FRACT. = 1.0/0.0 BRANCH' &
           SYST = 1   INDEP-VAR = 1   RANGE = 1   &
           PARAM = 1  DEP-VAR = 1
```

RUN CONTROL INFORMATION

TYPE OF RUN: NEW

INPUT FILE NAME: JTGS

INPUT PROBLEM DATA FILE NAME: JTGS UPDATE NO. 0

MAIN CALLING PROGRAM NAME: JTGS

TGS ONLY RUN

TGS RUN FOR THE METHANE - H2S SYSTEM
TABLE OF CONTENTS

PHYSICAL PROPERTIES SECTION..... 1
COMPONENTS..... 1
OPTION SETS..... 1

PHYSICAL PROPERTY TABLES SECTION..... 2
PPTABLES (PTENVELOPE): TABLE1..... 2

TGS RUN FOR THE METHANE - H2S SYSTEM
PHYSICAL PROPERTIES SECTION

COMPONENTS

ID	TYPE	FORMULA	DATABANK REFERENCE	ALIAS
METHANE	C	CH4	CH4	CH4
H2S	C	H2S	H2S	H2S

OPTION SETS

SYSOP0

MAJOR PROPERTY ROUTE ID						
	PHILMX	HVMX	HLMX	GVMX	GLMX	SVMX
	PHILMX00	HVMX00	HLMX00	GVMX00	GLMX00	SVMX00
	SLMX	VVMX	VLMX	MUVMX	MULMX	KVMX
	SLMX00	VVMX00	VLMX01	MUVMX01	MULMX01	KVMX01
	KLMX	DVMX	DLMX	SIGLMX	PHIV	PHIL
	KLMX01	DVMX01	DLMX01	SIGLMX01	PHIV01	PHIL00
	HV	HL	GV	GL	SV	SL
	HV00	HL00	GV00	GL00	SV00	SL00
	VV	VL	KS	VS	PHISMX	HSMX
	VV00	VL01	KS01	VS01	PHISMX02	HSMX02
	GSMX	SSMX	VSMX	KSMX	PHIS	HS
	GSMX02	SSMX01	VSMX02	KSMX01	PHIS02	HS02
	GS	SS				
	GS02	SS02				

SYSOP4

MAJOR PROPERTY ROUTE ID						
	PHIVMX	PHILMX	HVMX	HLMX	GVMX	GLMX
	PHIVMX04	PHILMX04	HVMX04	HLMX04	GVMX04	GLMX04
	SVMX	SLMX	VVMX	VLMX	MUVMX	MULMX
	SVMX04	SLMX04	VVMX04	VLMX04	MUVMX02	MULMX02
	KVMX	KLMX	DVMX	DLMX	SIGLMX	VV
	KVMX02	KLMX01	DVMX02	DLMX01	SIGLMX01	VV04
	VL	PHIV	PHIL	HV	HL	SV
	VL04	PHIV04P	PHIL04P	HV04	HL04	SV04
	SL	GV	GL			
	SL04	GV04	GL04			

TGS RUN FOR THE METHANE - H2S SYSTEM
PHYSICAL PROPERTY TABLES SECTION

PPTABLES (PTENVELOPE): TABLE1
PT ENVELOPE USING PENG-ROBINSON EQU. OF STATE
VAP. FRACT. = 1.0/0.0 BRANCH

V-FRAC	PHIVMX METHANE	PHIVMX H2S	X H2S MOL-FR	Y H2S MOL-FR	X METHANE MOL-FR
1.00000 00	9.92051-01	9.78725-01	9.98055-01	2.75000-01	1.94457-03
1.00000 00	9.91951-01	9.78451-01	9.98027-01	2.75000-01	1.97290-03
1.00000 00	9.90263-01	9.73801-01	9.97538-01	2.75000-01	2.46233-03
1.00000 00	9.88248-01	9.68207-01	9.96926-01	2.75000-01	3.07435-03
1.00000 00	9.84487-01	9.57658-01	9.95707-01	2.75000-01	4.29259-03
1.00000 00	9.76748-01	9.35544-01	9.92902-01	2.75000-01	7.09760-03
1.00000 00	9.58685-01	8.82053-01	9.84814-01	2.75000-01	1.51863-02
1.00000 00	9.30191-01	7.92518-01	9.67163-01	2.75000-01	3.28365-02
1.00000 00	8.89651-01	6.52711-01	9.27983-01	2.75000-01	7.20169-02
1.00000 00	8.65277-01	5.60134-01	8.92761-01	2.75000-01	1.07239-01
1.00000 00	8.52170-01	5.07614-01	8.69043-01	2.75000-01	1.30957-01
1.00000 00	8.38306-01	4.50606-01	8.40127-01	2.75000-01	1.59873-01
1.00000 00	8.23195-01	3.88488-01	8.05098-01	2.75000-01	1.94902-01
1.00000 00	8.05339-01	3.19405-01	7.63137-01	2.75000-01	2.36863-01
1.00000 00	7.78381-01	2.34547-01	7.13776-01	2.75000-01	2.86224-01
1.00000 00	7.66052-01	2.04879-01	7.00288-01	2.75000-01	2.99712-01
1.00000 00	7.56020-01	1.84562-01	6.93378-01	2.75000-01	3.06622-01
1.00000 00	7.47461-01	1.69594-01	6.89882-01	2.75000-01	3.10118-01
1.00000 00	7.38836-01	1.56415-01	6.88124-01	2.75000-01	3.11876-01
1.00000 00	7.37898-01	1.55104-01	6.87689-01	2.75000-01	3.12311-01
1.00000 00	7.19187-01	1.32151-01	6.87680-01	2.75000-01	3.12320-01
1.00000 00	7.08620-01	1.21677-01	6.90279-01	2.75000-01	3.09721-01
1.00000 00	7.02957-01	1.16652-01	6.91447-01	2.75000-01	3.08553-01
1.00000 00	6.95318-01	1.10428-01	6.93195-01	2.75000-01	3.06805-01
1.00000 00	6.88202-01	1.05132-01	6.94936-01	2.75000-01	3.05064-01
1.00000 00	6.81356-01	1.00437-01	6.96670-01	2.75000-01	3.03330-01
1.00000 00	6.74644-01	9.61690-02	6.98398-01	2.75000-01	3.01602-01
1.00000 00	6.67981-01	9.22230-02	7.00118-01	2.75000-01	2.99882-01
1.00000 00	6.57960-01	8.67654-02	7.02686-01	2.75000-01	2.97314-01
1.00000 00	6.42625-01	7.93467-02	7.06508-01	2.75000-01	2.93492-01

TGS RUN FOR THE METHANE - H2S SYSTEM
PHYSICAL PROPERTY TABLES SECTION

PPTABLES (PTENVELOPE): TABLE1 (CONTINUED)
VAP. FRACT. = 1.0/0.0 BRANCH

V-FRAC	Y METHANE MOL-FR	VLMX CUFT/LBM OLE	PRES PSIA	TEMP K
1.00000 00	7.25000-01	5.10410-01	1.46959+01	1.89543+02
1.00000 00	7.25000-01	5.10600-01	1.49341+01	1.89790+02
1.00000 00	7.25000-01	5.13628-01	1.90928+01	1.93656+02
1.00000 00	7.25000-01	5.16901-01	2.43989+01	1.97681+02
1.00000 00	7.25000-01	5.22332-01	3.52121+01	2.04030+02
1.00000 00	7.25000-01	5.31898-01	6.08666+01	2.14284+02
1.00000 00	7.25000-01	5.50548-01	1.36901+02	2.31305+02
1.00000 00	7.25000-01	5.76793-01	3.01290+02	2.49814+02
1.00000 00	7.25000-01	6.14363-01	6.35797+02	2.67713+02
1.00000 00	7.25000-01	6.38193-01	8.98107+02	2.74703+02
1.00000 00	7.25000-01	6.51040-01	1.05603+03	2.77094+02
1.00000 00	7.25000-01	6.63899-01	1.23019+03	2.78346+02
1.00000 00	7.25000-01	6.75663-01	1.41671+03	2.77987+02
1.00000 00	7.25000-01	6.83851-01	1.60885+03	2.75210+02
1.00000 00	7.25000-01	6.80680-01	1.79922+03	2.67696+02
1.00000 00	7.25000-01	6.74065-01	1.84853+03	2.63784+02
1.00000 00	7.25000-01	6.67368-01	1.87662+03	2.60654+02
1.00000 00	7.25000-01	6.61214-01	1.89471+03	2.58093+02
1.00000 00	7.25000-01	6.54924-01	1.90934+03	2.55648+02
1.00000 00	7.25000-01	6.54403-01	1.91094+03	2.55398+02
1.00000 00	7.25000-01	6.41627-01	1.93613+03	2.50644+02
1.00000 00	7.25000-01	6.34659-01	1.94948+03	2.48267+02
1.00000 00	7.25000-01	6.31336-01	1.95687+03	2.47078+02
1.00000 00	7.25000-01	6.27102-01	1.96730+03	2.45560+02
1.00000 00	7.25000-01	6.23406-01	1.97761+03	2.44228+02
1.00000 00	7.25000-01	6.20061-01	1.98817+03	2.43014+02
1.00000 00	7.25000-01	6.16969-01	1.99919+03	2.41883+02
1.00000 00	7.25000-01	6.14069-01	2.01084+03	2.40813+02
1.00000 00	7.25000-01	6.09995-01	2.02976+03	2.39294+02
1.00000 00	7.25000-01	6.04344-01	2.06212+03	2.37150+02

APPENDIX V

ASPEN SIMILATION OF PROPOSED METHANE PURIFICATION PROCESS

METHANE PURIFICATION PROCESS SIMULATION

The following are the input files, reports, and some selected plots of the ASPEN^{TM} simulation of the proposed methane purification process. The first input file, report, and chosen profiles are for the absorber, which contains two sections a fractionation section and a stripping section. The second input file and reports are dedicated to the H_2S stripper. These two computer programs were separated for convenience. They could easily be combined. No effort has been made to optimize the process profiles.

```
NEW
;
TITLE 'Sour Gas Stripper -- FRACTIONATION UNIT '
;
DESCRIPTION "A Syn-gas stream is purified by stripping with
  liquid CO2. The absorber requires a fractionation section and a
  stripping section, as well as a third unit which strips H2S. The per-
  performance of the first two units is evaluated here. From a computa-
  tional viewpoint the first two units are computed as a single unit. The
  third unit is computed in a separate program.  April 1988."
;
HISTORY MSG-LEVEL PROPERTIES=2
;
IN-UNITS TEMP=C
OUT-UNITS TEMP=C
RUN-CONTROL MAX-TIME=60
;
COMPONENTS H2 HYDROGEN/CO2 CARBON-DIOXIDE/CO CARBON-MONOXIDE/CH4 METHANE/
           H2S HYDROGEN-SULFIDE
;
FORMULA CO2 CO2/H2 H2/CO CO/CH4 CH4/H2S H2S
;
PROPERTIES SYSOP4 GLOBAL
;
PROP-DATA
    PROP-LIST PRKIJ
    BPVAL CO CO2 -0.0659 ; From Literature
    BPVAL H2 CO2 -0.0564 ; From Literature
    BPVAL CH4 CO2 0.1001 ; Our Experiments
    BPVAL CO CH4 0.01258 ; Literature Values
    BPVAL CO2 H2S 0.09894 ; Our Experiments
    BPVAL CH4 H2S 0.08672 ; Our Experiments
;
FLOWSHEET
   FRACTION IN=FD1 SRB8 OUT=RCY2 BTM5
;
STREAM FD1 V-FRAC=0.7 TEMP = 0
  MOLE-FLOW H2 3/CO2 56/CO 5/CH4 33/H2S 3
STREAM SRB8  TEMP= -10 PRES= 1000
  MOLE-FLOW CO2 540
;
BLOCK FRACTION RADFRC
  PARAM 25
  FEEDS FD1 13/SRB8 1
  PRODUCTS RCY2 1 1 /BTM5 25 0
  COL-SPECS RDV=1 BR=0.75 D=35
  P-SPEC 1 1000/25 1000
  T-EST 1 0/25 20
```

Sour Gas Stripper -- FRACTIONATION UNIT

DESCRIPTION

A Syn-gas stream is purified by stripping with liquid CO2. The absorber requires a fractionation section and a stripping section, as well as a third unit which strips H2S. The performance of the first two units is evaluated here. From a computational viewpoint, the first two units are computed as a single unit. The third unit is computed in a separate program. April 1988.

RUN CONTROL INFORMATION

TYPE OF RUN: NEW

INPUT FILE NAME: sour

INPUT PROBLEM DATA FILE NAME: sour UPDATE NO. 0

MAIN CALLING PROGRAM NAME: sour

SIMULATION REQUESTED FOR ENTIRE FLOWSHEET

Sour Gas Stripper -- FRACTIONATION UNIT

TABLE OF CONTENTS

FLOWSHEET SECTION..... 1
FLOWSHEET CONNECTIVITY BY STREAMS..... 1
FLOWSHEET CONNECTIVITY BY BLOCKS..... 1
COMPUTATIONAL SEQUENCE USED..... 1
OVERALL FLOWSHEET BALANCE..... 1

PHYSICAL PROPERTIES SECTION..... 2
COMPONENTS..... 2
OPTION SETS..... 2

UNIT OPERATION BLOCK SECTION..... 3
FRACTIONATIO (RADFRC): FRACTION..... 3
COLUMN SUMMARY..... 8

STREAM SECTION..... 9
RCY2 BTM5 FD1 SRB8..... 9

Sour Gas Stripper -- FRACTIONATION UNIT

FLOWSHEET SECTION

FLOWSHEET CONNECTIVITY BY STREAMS

STREAM	SOURCE	DESTINATION	STREAM	SOURCE	DESTINATION
RCY2	FRACTION	----	BTM5	FRACTION	----
FD1	----	FRACTION	SRB8	----	FRACTION

FLOWSHEET CONNECTIVITY BY BLOCKS

BLOCK	INLETS	OUTLETS
FRACTION	FD1 SRB8	RCY2 BTM5

COMPUTATIONAL SEQUENCE USED

FRACTION

OVERALL FLOWSHEET BALANCE

*** MASS AND ENERGY BALANCE ***

	IN	OUT	RELATIVE DIFF.
CONVENTIONAL COMPONENTS (LBMOL/HR)			
H2	3.00000	3.00000	.199929E-11
CO2	596.000	596.000	-.270865E-13
CO	5.00000	5.00000	.144436E-11
CH4	33.0000	33.0000	.945237E-13
H2S	3.00000	3.00000	-.115463E-12
TOTAL BALANCE			
MOLE(LBMOL/HR)	640.000	640.000	.000000E+00
MASS(LB/HR)	27007.7	27007.7	-.167030E-13
ENTHALPY(BTU/HR)	-.105854E+09	-.104756E+09	-.103717E-01

CONVENTIONAL MASS BALANCE SATISFACTORY

PHYSICAL PROPERTIES SECTION

COMPONENTS

ID	TYPE	FORMULA	DATABANK REFERENCE	ALIAS
H2	C	H2	HYDROGEN	H2
CO2	C	CO2	CARBON-DIOXIDE	CO2
CO	C	CO	CARBON-MONOXIDE	CO
CH4	C	CH4	METHANE	CH4
H2S	C	H2S	HYDROGEN-SULFIDE	H2S

OPTION SETS

SYSOP0

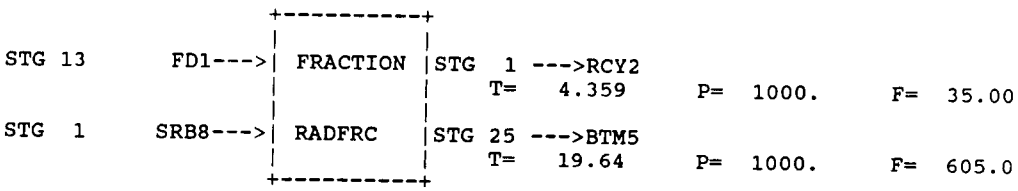
MAJOR PROPERTY ROUTE ID						
	PHILMX	HVMX	HLMX	GVMX	GLMX	SVMX
	PHILMX00	HVMX00	HLMX00	GVMX00	GLMX00	SVMX00
	SLMX	VVMX	VLMX	MUVMX	MULMX	KVMX
	SLMX00	VVMX00	VLMX01	MUVMX01	MULMX01	KVMX01
	KLMX	DVMX	DLMX	SIGLMX	PHIV	PHIL
	KLMX01	DVMX01	DLMX01	SIGLMX01	PHIV01	PHIL00
	HV	HL	GV	GL	SV	SL
	HV00	HL00	GV00	GL00	SV00	SL00
	VV	VL	KS	VS	PHISMX	HSMX
	VV00	VL01	KS01	VS01	PHISMX02	HSMX02
	GSMX	SSMX	VSMX	KSMX	PHIS	HS
	GSMX02	SSMX01	VSMX02	KSMX01	PHIS02	HS02
	GS	SS				
	GS02	SS02				

SYSOP4

MAJOR PROPERTY ROUTE ID						
	PHIVMX	PHILMX	HVMX	HLMX	GVMX	GLMX
	PHIVMX04	PHILMX04	HVMX04	HLMX04	GVMX04	GLMX04
	SVMX	SLMX	VVMX	VLMX	MUVMX	MULMX
	SVMX04	SLMX04	VVMX04	VLMX04	MUVMX02	MULMX02
	KVMX	KLMX	DVMX	DLMX	SIGLMX	VV
	KVMX02	KLMX01	DVMX02	DLMX01	SIGLMX01	VV04
	VL	PHIV	PHIL	HV	HL	SV
	VL04	PHIV04P	PHIL04P	HV04	HL04	SV04
	SL	GV	GL			
	SL04	GV04	GL04			

UNIT OPERATION BLOCK SECTION

FRACTIONATIO (RADFRC): FRACTION



PROPERTY OPTION SET: SYSOP4

*** INPUT DATA ***

**** INPUT PARAMETERS ****

NUMBER OF THEORETICAL STAGES	25

* ALGORITHM OPTIONS *

MAXIMUM OUTSIDE LOOPS	25
MAXIMUM INSIDE LOOPS PER OUTSIDE LOOP	10
MAXIMUM ITERATIONS FOR FEED FLASH	30
NONIDEAL OPTION	OFF
NUMBER OF INTERNAL DESIGN SPECS	0
BOUNDED WEGSTEIN MODULUS ON OUTSIDE LOOP NUMBER	1
ENTHALPY BALANCE OPTION CODE	MOLAR
INSIDE LOOP ITERATION METHOD	BROYDEN
KB UPDATING OPTION CODE	1
KB WEIGHTING OPTION CODE	Y/(1+K)
LIQUID PHASE STABILITY CHECKING	OFF

* CONVERGENCE METHOD VARIABLES *

FEED FLASH CONVERGENCE TOLERANCE	0.100000-05
OUTSIDE LOOP CONVERGENCE TOLERANCE	0.00010000
MINIMUM INSIDE LOOP CONV TOLERANCE	0.300000-05
INITIAL INSIDE LOOP CONV TOLERANCE	0.010000
INSIDE LOOP CONV TOL REDUCTION FACTOR	0.30000
INSIDE LOOP RMS ERR FOR JACOBIAN UPDATE	0.100000-05
COMPONENT MASS BALANCE CONV TOLERANCE	0.100000-06
SIMPLE MODEL SLOPE PARAMETER UPDATE TOLERANCE	0.050000
QMIN FOR BOUNDED WEGSTEIN IN OUTSIDE LOOP	0.0
QMAX FOR BOUNDED WEGSTEIN IN OUTSIDE LOOP	0.50000
BOUNDED WEGSTEIN SLOPE TOLERANCE	0.050000
QMIN FOR BOUNDED WEGSTEIN IN INSIDE LOOP	0.0
QMAX FOR BOUNDED WEGSTEIN IN INSIDE LOOP	0.50000

Sour Gas Stripper -- FRACTIONATION UNIT

UNIT OPERATION BLOCK SECTION

FRACTIONATIO (RADFRC): FRACTION (CONTINUED)

**** COL-SPECS ****

VAPOR DISTILLATE / TOTAL DISTILLATE (RDV)		1.00000
BOILUP RATIO		0.75000
DISTILLATE RATE	LBMOL/HR	35.0000

**** PROFILES ****

TEMP-EST	STAGE	1	TEMP, C	0.0
		25		20.0000
P-SPEC	STAGE	1	PRES, PSIA	1,000.000
		25		1,000.000

*** RESULTS ***

TOP TRAY TEMPERATURE	C	4.35904
BOTTOM TRAY TEMPERATURE	C	19.6432
TOP TRAY LIQUID FLOW	LBMOL/HR	755.697
BOTTOM TRAY LIQUID FLOW	LBMOL/HR	605.000
TOP TRAY VAPOR FLOW	LBMOL/HR	35.0000
BOTTOM TRAY VAPOR FLOW	LBMOL/HR	453.750
CONDENSER DUTY	BTU/HR	13,024.4
REBOILER DUTY	BTU/HR	1,084,810.

UNIT OPERATION BLOCK SECTION
FRACTIONATIO (RADFRC): FRACTION (CONTINUED)
**** PROFILES ****

STG	TEMPERATURE C	PRESSURE PSIA	FEED RATE LBMOL/HR LIQUID	FEED RATE LBMOL/HR VAPOR	PRODUCT RATE LBMOL/HR LIQUID	PRODUCT RATE LBMOL/HR VAPOR
1	4.3590	1000.0	540.0000			35.0000
2	6.2435	1000.0				
3	7.2449	1000.0				
4	7.6878	1000.0				
5	7.7583	1000.0				
6	7.5539	1000.0				
7	7.1207	1000.0				
8	6.4706	1000.0				
9	5.5889	1000.0				
10	4.4323	1000.0				
11	2.9215	1000.0				
12	.92443	1000.0		81.6321		
13	1.0907	1000.0	18.3679			
14	1.4214	1000.0				
15	1.7340	1000.0				
16	2.0679	1000.0				
17	2.4717	1000.0				
18	3.0105	1000.0				
19	3.7763	1000.0				
20	4.8936	1000.0				
21	6.5167	1000.0				
22	8.8003	1000.0				
23	11.831	1000.0				
24	15.538	1000.0				
25	19.643	1000.0			605.0000	

STG	TOTAL LIQUID FLOW LBMOL/HR	LB/HR	CUFT/HR	TOTAL VAPOR FLOW LBMOL/HR	LB/HR	CUFT/HR
1	755.70	31808.	646.37	35.000	1264.4	117.90
2	795.61	33415.	704.59	250.70	9307.2	808.74
3	822.22	34456.	744.01	290.61	10914.	912.16
4	838.72	35067.	768.45	317.22	11955.	978.90
5	847.88	35367.	781.78	333.72	12566.	1019.2
6	851.76	35440.	786.97	342.88	12866.	1040.7
7	851.64	35341.	785.95	346.76	12939.	1049.0
8	848.31	35099.	779.89	346.64	12840.	1047.2
9	842.15	34726.	769.37	343.31	12598.	1037.1
10	833.29	34223.	754.55	337.15	12225.	1019.5
11	821.59	33575.	735.22	328.29	11722.	994.51
12	807.39	32772.	711.36	316.59	11074.	961.18
13	835.51	33864.	740.38	220.76	7745.5	664.21
14	843.59	34176.	752.25	230.51	8120.8	688.36
15	850.60	34449.	762.62	238.59	8432.4	708.27

Sour Gas Stripper -- FRACTIONATION UNIT

UNIT OPERATION BLOCK SECTION

FRACTIONATIO (RADFRC): FRACTION (CONTINUED)

STG	TOTAL LIQUID FLOW LBMOL/HR	LB/HR	CUFT/HR	TOTAL VAPOR FLOW LBMOL/HR	LB/HR	CUFT/HR
16	857.16	34710.	772.43	245.60	8705.3	725.49
17	863.94	34989.	782.70	252.16	8966.3	741.66
18	871.77	35327.	794.74	258.94	9246.0	758.50
19	881.73	35778.	810.32	266.77	9584.1	778.11
20	895.44	36424.	832.08	276.73	10035.	803.20
21	915.39	37388.	864.10	290.44	10680.	837.64
22	945.28	38854.	912.55	310.39	11644.	886.97
23	990.60	41086.	986.59	340.28	13111.	958.82
24	1058.8	44431.	1099.0	385.60	15342.	1063.5
25	605.00	25743.	661.16	453.75	18688.	1213.3

STAGE	H2	**** X-PROFILE **** CO2	CO	CH4	H2S
1	.13169E-01	.92655	.26744E-01	.33533E-01	.24974E-08
2	.89562E-02	.92132	.26267E-01	.43452E-01	.11018E-07
3	.64966E-02	.91753	.24512E-01	.51465E-01	.42086E-07
4	.51183E-02	.91432	.22449E-01	.58118E-01	.14964E-06
5	.43552E-02	.91124	.20507E-01	.63893E-01	.51282E-06
6	.39319E-02	.90804	.18848E-01	.69178E-01	.17291E-05
7	.36936E-02	.90451	.17506E-01	.74281E-01	.58148E-05
8	.35557E-02	.90049	.16467E-01	.79468E-01	.19708E-04
9	.34718E-02	.89576	.15697E-01	.85008E-01	.67939E-04
10	.34168E-02	.88996	.15167E-01	.91217E-01	.24049E-03
11	.33764E-02	.88236	.14852E-01	.98524E-01	.88390E-03
12	.33418E-02	.87088	.14745E-01	.10761	.34265E-02
13	.23680E-02	.86766	.14689E-01	.11087	.44155E-02
14	.16373E-02	.86675	.14378E-01	.11282	.44064E-02
15	.11220E-02	.86625	.13867E-01	.11436	.43998E-02
16	.76324E-03	.86617	.13187E-01	.11548	.43953E-02
17	.51570E-03	.86662	.12360E-01	.11611	.43929E-02
18	.34605E-03	.86781	.11398E-01	.11605	.43930E-02
19	.23036E-03	.87013	.10311E-01	.11493	.43966E-02
20	.15181E-03	.87415	.91046E-02	.11219	.44056E-02
21	.98681E-04	.88064	.77913E-02	.10704	.44232E-02
22	.62853E-04	.89048	.63934E-02	.98604E-01	.44568E-02
23	.38747E-04	.90436	.49514E-02	.86124E-01	.45235E-02
24	.22531E-04	.92239	.35250E-02	.69401E-01	.46640E-02
25	.11594E-04	.94370	.21843E-02	.49141E-01	.49587E-02

Sour Gas Stripper -- FRACTIONATION UNIT

UNIT OPERATION BLOCK SECTION

FRACTIONATIO (RADFRC): FRACTION (CONTINUED)

		****	Y-PROFILE	****	
STAGE	H2	CO2	CO	CH4	H2S
1	.85514E-01	.71598	.10510	.93411E-01	.16843E-08
2	.51634E-01	.73895	.95290E-01	.11412	.77633E-08
3	.34818E-01	.75040	.84568E-01	.13021	.30366E-07
4	.26274E-01	.75490	.75129E-01	.14370	.10927E-06
5	.21832E-01	.75486	.67442E-01	.15586	.37625E-06
6	.19499E-01	.75153	.61438E-01	.16753	.12683E-05
7	.18289E-01	.74545	.56905E-01	.17935	.42475E-05
8	.17709E-01	.73673	.53621E-01	.19193	.14286E-04
9	.17504E-01	.72516	.51403E-01	.20588	.48697E-04
10	.17549E-01	.71013	.50120E-01	.22203	.16970E-03
11	.17790E-01	.69040	.49703E-01	.24149	.61043E-03
12	.18216E-01	.66332	.50162E-01	.26601	.22938E-02
13	.12632E-01	.66426	.49223E-01	.27091	.29721E-02
14	.85527E-02	.66806	.47510E-01	.27289	.29898E-02
15	.57597E-02	.67163	.45297E-01	.27430	.30062E-02
16	.38574E-02	.67547	.42645E-01	.27501	.30233E-02
17	.25666E-02	.68016	.39586E-01	.27464	.30437E-02
18	.16935E-02	.68652	.36134E-01	.27258	.30710E-02
19	.11046E-02	.69570	.32295E-01	.26779	.31101E-02
20	.70865E-03	.70928	.28077E-01	.25877	.31677E-02
21	.44390E-03	.72927	.23520E-01	.24351	.32534E-02
22	.26843E-03	.75773	.18720E-01	.21990	.33795E-02
23	.15399E-03	.79586	.13877E-01	.18655	.35644E-02
24	.81351E-04	.84264	.92930E-02	.14415	.38406E-02
25	.37114E-04	.89397	.53124E-02	.96413E-01	.42711E-02

Sour Gas Stripper -- FRACTIONATION UNIT

UNIT OPERATION BLOCK SECTION

COLUMN SUMMARY

BLOCK ID	FRACTION
MODEL TYPE	RADFRC
NUMBER OF STAGES	25
CONDENSER DUTY (BTU/HR)	.13024+05
REBOILER DUTY (BTU/HR)	.10848+07
TOP STAGE TEMPERATURE (C)	4.3590
BOT STAGE TEMPERATURE (C)	19.6431
DISTILLATE RATE(LBMOL/HR)	35.0000
BOTTOMS RATE (LBMOL/HR)	605.0000
REFLUX RATIO	21.5913
VAP VFLOW STG1 (CUFT/HR)	117.8967
LIQ VFLOW STG1 (CUFT/HR)	646.3741
LIQ VFLOW STGN (CUFT/HR)	661.1551
LIQ DENS. STG1 (LB/CUFT)	49.2102
LIQ DENS. STGN (LB/CUFT)	38.9369
COLUMN SECTION 1	
NUMBER OF STAGES	25
NUMBER OF FEEDS	2
AT MAX. VAPOR VELOCITY STG	
LIQUID DENSITY (LB/CUFT)	38.9369
VAPOR DENSITY (LB/CUFT)	15.4016
LIQUID FLOW (LB/HR)	.25743+05
VAPOR FLOW (LB/HR)	.18688+05
SURFACE TENSION(DYNE/CM)	1.2881
LIQ VISCOSITY (CP)	0.0631

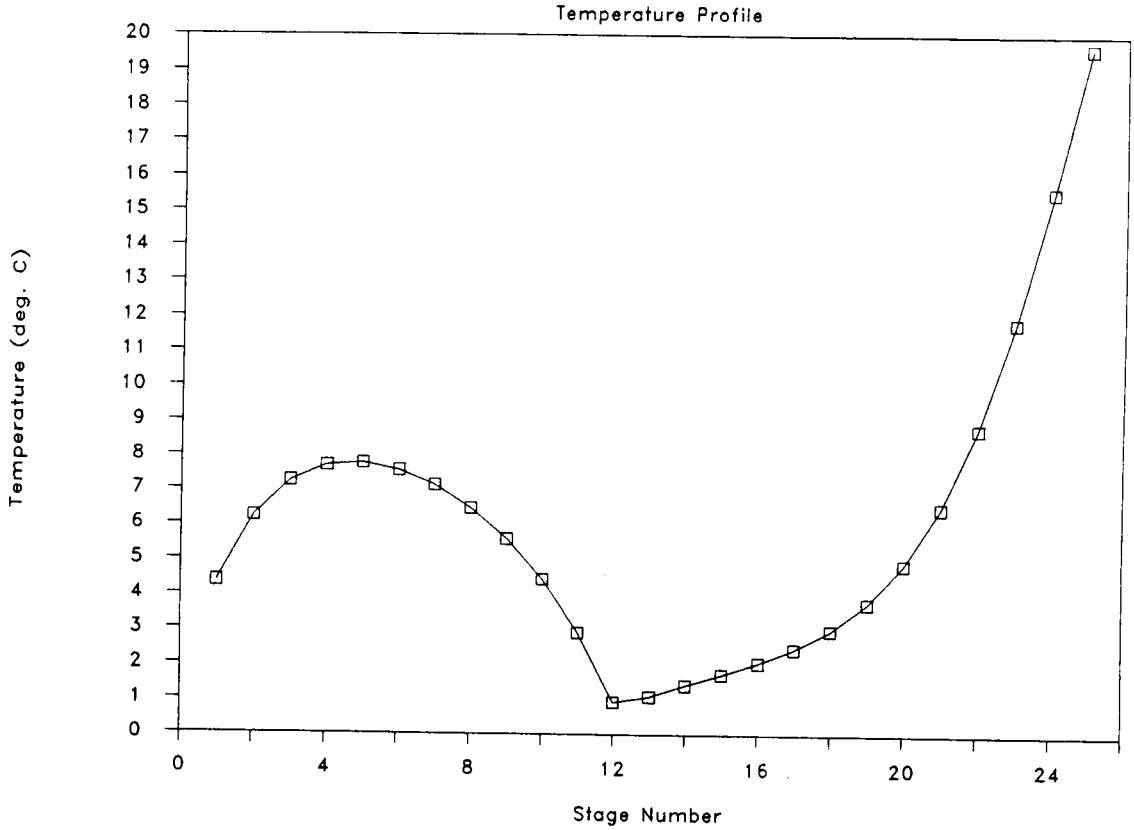
Sour Gas Stripper -- FRACTIONATION UNIT

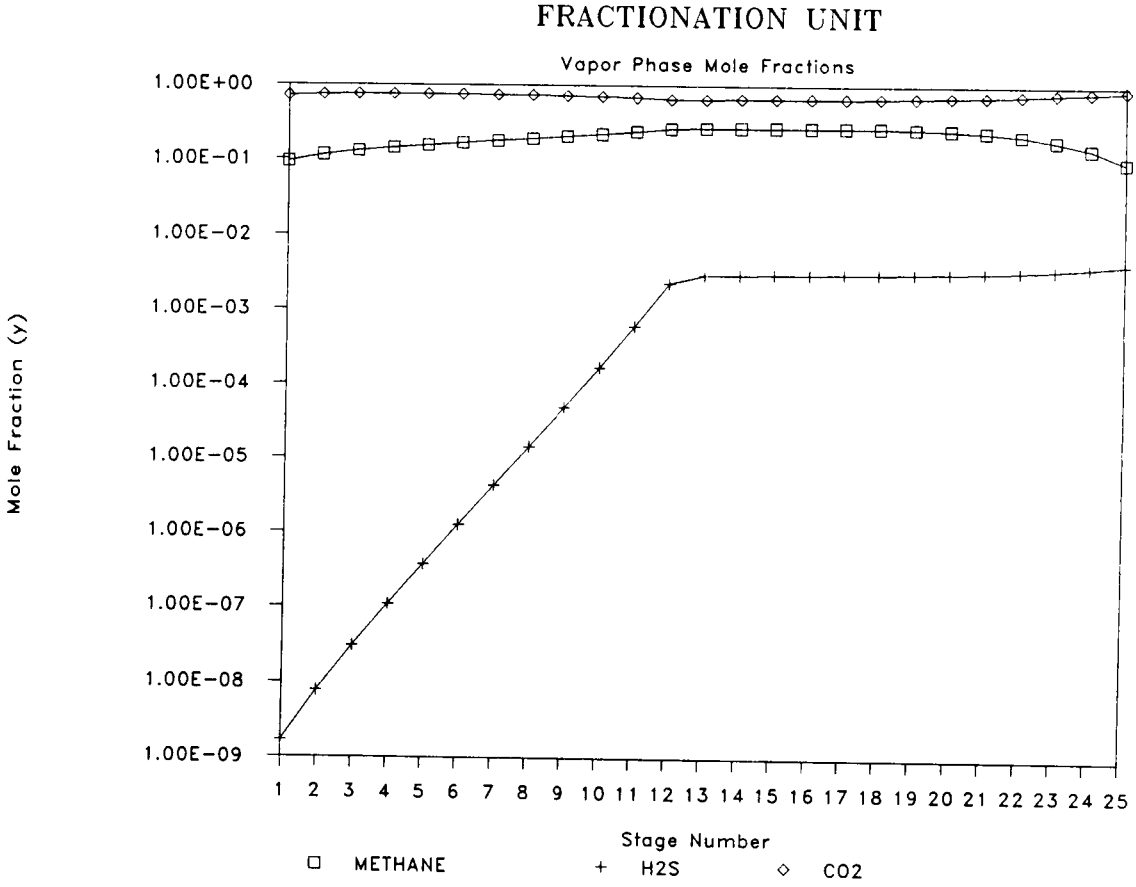
STREAM SECTION

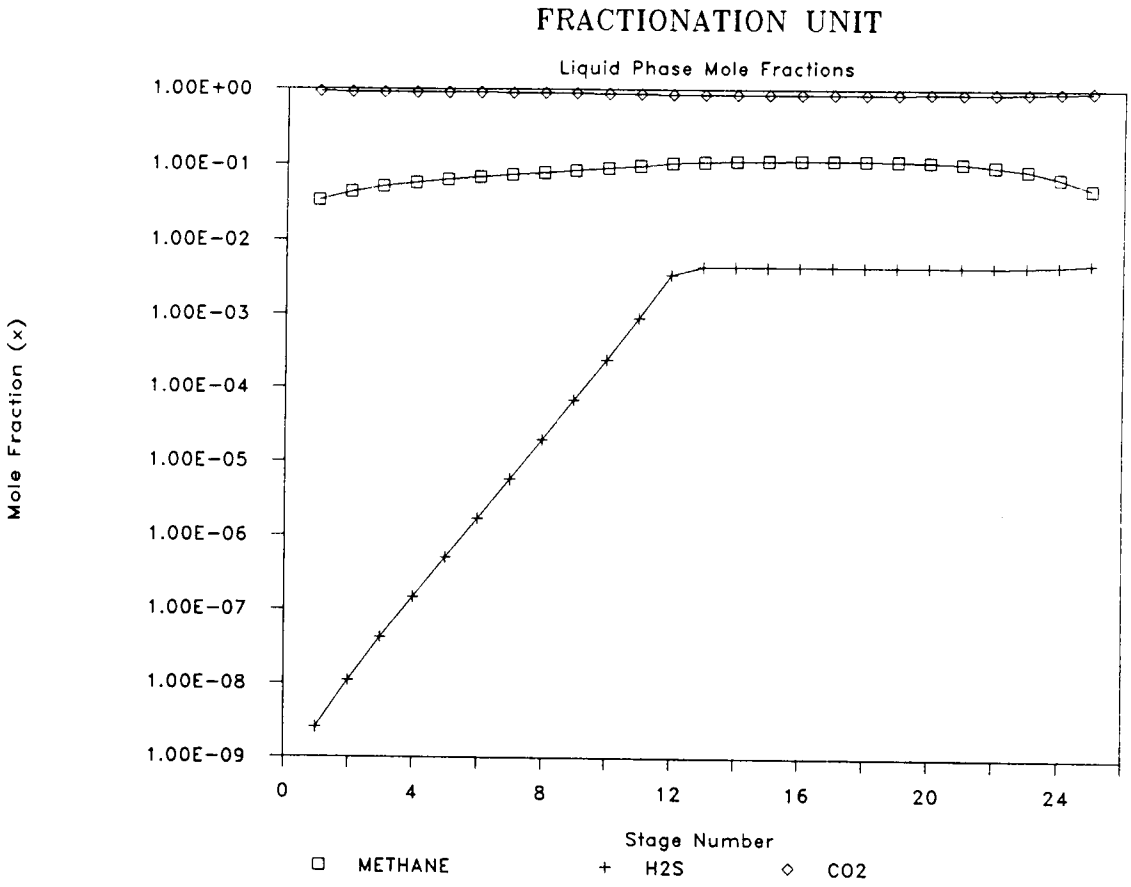
RCY2 BTM5 FD1 SRB8
FLOW DETAILS

	RCY2	BTM5	FD1	SRB8
COMPONENT FLOWS <LBMOL/HR>				
HYDROGEN	2.9929	0.0070	3.0000	0.0
CARBON-DIOXIDE	25.0591	570.9408	56.0000	540.0000
CARBON-MONOXIDE	3.6784	1.3215	5.0000	0.0
METHANE	3.2693	29.7306	33.0000	0.0
HYDROGEN-SULFIDE	.58950-07	2.9999	3.0000	0.0
TOTAL	35.0000	605.0000	100.0000	540.0000
PHASE SPLITS				
VAPOR FRACTION <MOLE BASIS>	1.0000	0.0	0.7000	0.0
LIQUID FRACTION <MOLE BASIS>	0.0	1.0000	0.3000	1.0000
SOLID FRACTION <MOLE BASIS>	0.0	0.0	0.0	0.0
INTENSIVE PROPERTIES				
TEMPERATURE <C>	4.3590	19.6431	0.0	-10.0000
PRESSURE <PSIA>	1000.000	1000.000	1369.6544	1000.000
MOLECULAR WEIGHT	36.1249	42.5509	32.4231	44.0100
ENTHALPY <BTU/LBMOL>	-.13083+06	-.16558+06	-.11049+06	-.17557+06
ENTROPY <BTU/LBMOL-R>	-8.1482	-14.9291	-15.4281	-18.6599
DENSITY <LBMOL/CUFT>	0.2968	0.9150	0.5435	1.4533

FRACTIONATION UNIT




FRACTIONATION UNIT
Vapor Phase Mole Fractions
Mole Fraction (y)
1.00E+00
1.00E-01
1.00E-02
1.00E-03
1.00E-04
1.00E-05
1.00E-06
1.00E-07
1.00E-08
1.00E-09
1 2 3 4 5 6 7 8 9 10 11 12 13 14 15 16 17 18 19 20 21 22 23 24 25
Stage Number
METHANE
H2S
CO2


FRACTIONATION UNIT
Liquid Phase Mole Fractions
1.00E+00
1.00E-01
1.00E-02
1.00E-03
1.00E-04
1.00E-05
1.00E-06
1.00E-07
1.00E-08
1.00E-09
Mole Fraction (x)
0
4
8
12
16
20
24
Stage Number
METHANE
H2S
CO2

```
NEW
;
TITLE 'Sour Gas Stripper -- H2S STRIPPER '
;
DESCRIPTION "A Syn-gas stream is purified by stripping with
  liquid CO2. The absorber requires a fractionation section and a
  stripping section, as well as a third unit which strips H2S.  From a
  computational viewpoint the first two units are computed as a single unit
  with a nonconventional top part in which pure liquid CO2 enters as the
  recycle stream in the style of an absorber. This part is included in the
  first program. The third unit, simulated hereis a conventional
  still which is operated at 1000 psia.  April 1988."
;
HISTORY MSG-LEVEL PROPERTIES=2
;
IN-UNITS TEMP=C
OUT-UNITS TEMP=C
RUN-CONTROL MAX-TIME=60
;
COMPONENTS H2 HYDROGEN/CO2 CARBON-DIOXIDE/CO CARBON-MONOXIDE/CH4 METHANE/
           H2S HYDROGEN-SULFIDE
;
FORMULA CO2 CO2/H2 H2/CO CO/CH4 CH4/H2S H2S
;
PROPERTIES SYSOP4 GLOBAL
;
PROP-DATA
    PROP-LIST PRKIJ
    BPVAL CO CO2 -0.0659 ; From Literature
    BPVAL H2 CO2 -0.0564 ; From Literature
    BPVAL CH4 CO2 0.1001 ; Our Experiments
    BPVAL CO CH4 0.01258 ; Literature Values
    BPVAL CO2 H2S 0.09894 ; Our Experiments
    BPVAL CH4 H2S 0.08672 ; Our Experiments
;
FLOWSHEET
   STRIPPER IN= FEED OUT=PRODUCT BOTTOM
;
STREAM FEED TEMP = 20  PRES = 1000
  MOLE-FLOW H2 .00703/CO2 570.9408/CO 1.3215/CH4 29.7305/H2S 3
;
;
BLOCK STRIPPER RADFRC
  PARAM NS=25 TOLOL=0.02
  FEEDS FEED  12
  PRODUCTS PRODUCT 1 1 /BOTTOM 25 0
  COL-SPECS RDV=1 RR=8. D=33
  P-SPEC 1 1000/25 1000
  T-EST 1 0/25 10
```

Sour Gas Stripper -- H2S STRIPPER
DESCRIPTION

A Syn-gas stream is purified by stripping with liquid CO2. The absorber requires an fractionation section and a stripping section, as well as a third unit which strips H2S. From a computational viewpoint the first two units are computed as a single unit with a nonconventional top part in which pure liquid CO2 enters as the recycle stream in the style of an absorber. This part is included in the first program (SOUR). The third unit, simulated hereis a conventional still which is operated at 1000 psia. April 1988.

RUN CONTROL INFORMATION

TYPE OF RUN: NEW

INPUT FILE NAME: SOR5

INPUT PROBLEM DATA FILE NAME: SOR5 UPDATE NO. 0

MAIN CALLING PROGRAM NAME: SOR5

SIMULATION REQUESTED FOR ENTIRE FLOWSHEET

Sour Gas Stripper -- H2S STRIPPER
TABLE OF CONTENTS

FLOWSHEET SECTION..... 1
FLOWSHEET CONNECTIVITY BY STREAMS..... 1
FLOWSHEET CONNECTIVITY BY BLOCKS..... 1
COMPUTATIONAL SEQUENCE USED..... 1
OVERALL FLOWSHEET BALANCE..... 1

PHYSICAL PROPERTIES SECTION..... 2
COMPONENTS..... 2
OPTION SETS..... 2

UNIT OPERATION BLOCK SECTION..... 3
FRACTIONATIO (RADFRC): STRIPPER..... 3
COLUMN SUMMARY..... 8

STREAM SECTION..... 9
PRODUCT BOTTOM FEED..... 9

Sour Gas Stripper -- H2S STRIPPER
FLOWSHEET SECTION

FLOWSHEET CONNECTIVITY BY STREAMS

STREAM	SOURCE	DESTINATION	STREAM	SOURCE	DESTINATION
PRODUCT	STRIPPER	----	BOTTOM	STRIPPER	----
FEED	----	STRIPPER			

FLOWSHEET CONNECTIVITY BY BLOCKS

BLOCK	INLETS	OUTLETS
STRIPPER	FEED	PRODUCT BOTTOM

COMPUTATIONAL SEQUENCE USED

*STRIPPER

OVERALL FLOWSHEET BALANCE

*** MASS AND ENERGY BALANCE ***

	IN	OUT	RELATIVE DIFF.
CONVENTIONAL COMPONENTS (LBMOL/HR)			
H2	.703000E-02	.703000E-02	-.807316E-07
CO2	570.941	570.941	.203390E-08
CO	1.32150	1.32150	-.542535E-07
CH4	29.7305	29.7305	-.371865E-07
H2S	3.00000	3.00000	.553450E-08
TOTAL BALANCE			
MOLE(LBMOL/HR)	605.000	605.000	.000000E+00
MASS(LB/HR)	25743.3	25743.3	.124015E-08
ENTHALPY(BTU/HR)	-.100119E+09	-.100082E+09	-.371084E-03

CONVENTIONAL MASS BALANCE SATISFACTORY

Sour Gas Stripper -- H2S STRIPPER
PHYSICAL PROPERTIES SECTION

COMPONENTS

ID	TYPE	FORMULA	DATABANK REFERENCE	ALIAS
H2	C	H2	HYDROGEN	H2
CO2	C	CO2	CARBON-DIOXIDE	CO2
CO	C	CO	CARBON-MONOXIDE	CO
CH4	C	CH4	METHANE	CH4
H2S	C	H2S	HYDROGEN-SULFIDE	H2S

OPTION SETS

SYSOP0

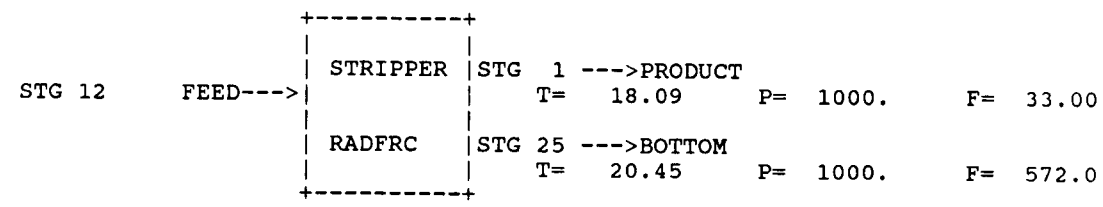
MAJOR PROPERTY ROUTE ID						
	PHILMX	HVMX	HLMX	GVMX	GLMX	SVMX
	PHILMX00	HVMX00	HLMX00	GVMX00	GLMX00	SVMX00
	SLMX	VVMX	VLMX	MUVMX	MULMX	KVMX
	SLMX00	VVMX00	VLMX01	MUVMX01	MULMX01	KVMX01
	KLMX	DVMX	DLMX	SIGLMX	PHIV	PHIL
	KLMX01	DVMX01	DLMX01	SIGLMX01	PHIV01	PHIL00
	HV	HL	GV	GL	SV	SL
	HV00	HL00	GV00	GL00	SV00	SL00
	VV	VL	KS	VS	PHISMX	HSMX
	VV00	VL01	KS01	VS01	PHISMX02	HSMX02
	GSMX	SSMX	VSMX	KSMX	PHIS	HS
	GSMX02	SSMX01	VSMX02	KSMX01	PHIS02	HS02
	GS	SS				
	GS02	SS02				

SYSOP4

MAJOR PROPERTY ROUTE ID						
	PHIVMX	PHILMX	HVMX	HLMX	GVMX	GLMX
	PHIVMX04	PHILMX04	HVMX04	HLMX04	GVMX04	GLMX04
	SVMX	SLMX	VVMX	VLMX	MUVMX	MULMX
	SVMX04	SLMX04	VVMX04	VLMX04	MUVMX02	MULMX02
	KVMX	KLMX	DVMX	DLMX	SIGLMX	VV
	KVMX02	KLMX01	DVMX02	DLMX01	SIGLMX01	VV04
	VL	PHIV	PHIL	HV	HL	SV
	VL04	PHIV04P	PHIL04P	HV04	HL04	SV04
	SL	GV	GL			
	SL04	GV04	GL04			

Sour Gas Stripper -- H2S STRIPPER
UNIT OPERATION BLOCK SECTION

FRACTIONATIO (RADFRC): STRIPPER



PROPERTY OPTION SET: SYSOP4

****
*
* ERROR IN BLOCK CALCULATIONS *
* COLUMN NOT CONVERGED *
*
****

Sour Gas Stripper -- H2S STRIPPER
UNIT OPERATION BLOCK SECTION

FRACTIONATIO (RADFRC): STRIPPER (CONTINUED)

*** INPUT DATA ***

**** INPUT PARAMETERS ****

NUMBER OF THEORETICAL STAGES	25
* ALGORITHM OPTIONS *	
MAXIMUM OUTSIDE LOOPS	25
MAXIMUM INSIDE LOOPS PER OUTSIDE LOOP	10
MAXIMUM ITERATIONS FOR FEED FLASH	30
NONIDEAL OPTION	OFF
NUMBER OF INTERNAL DESIGN SPECS	0
BOUNDED WEGSTEIN MODULUS ON OUTSIDE LOOP NUMBER	1
ENTHALPY BALANCE OPTION CODE	MOLAR
INSIDE LOOP ITERATION METHOD	BROYDEN
KB UPDATING OPTION CODE	1
KB WEIGHTING OPTION CODE	Y/(1+K)
LIQUID PHASE STABILITY CHECKING	OFF
* CONVERGENCE METHOD VARIABLES *	
FEED FLASH CONVERGENCE TOLERANCE	0.100000-05
OUTSIDE LOOP CONVERGENCE TOLERANCE	0.020000
MINIMUM INSIDE LOOP CONV TOLERANCE	0.300000-05
INITIAL INSIDE LOOP CONV TOLERANCE	0.010000
INSIDE LOOP CONV TOL REDUCTION FACTOR	0.30000
INSIDE LOOP RMS ERR FOR JACOBIAN UPDATE	0.100000-05
COMPONENT MASS BALANCE CONV TOLERANCE	0.100000-06
SIMPLE MODEL SLOPE PARAMETER UPDATE TOLERANCE	0.050000
QMIN FOR BOUNDED WEGSTEIN IN OUTSIDE LOOP	0.0
QMAX FOR BOUNDED WEGSTEIN IN OUTSIDE LOOP	0.50000
BOUNDED WEGSTEIN SLOPE TOLERANCE	0.050000
QMIN FOR BOUNDED WEGSTEIN IN INSIDE LOOP	0.0
QMAX FOR BOUNDED WEGSTEIN IN INSIDE LOOP	0.50000

**** COL-SPECS ****

VAPOR DISTILLATE / TOTAL DISTILLATE (RDV)		1.00000
REFLUX RATIO		8.00000
DISTILLATE RATE	LBMOL/HR	33.0000

**** PROFILES ****

TEMP-EST	STAGE	1	TEMP, C	0.0
		25		10.0000

Sour Gas Stripper -- H2S STRIPPER
UNIT OPERATION BLOCK SECTION

FRACTIONATIO (RADFRC): STRIPPER (CONTINUED)

P-SPEC	STAGE	1	PRES, PSIA	1,000.000
		25		1,000.000

*** RESULTS ***

TOP TRAY TEMPERATURE	C	18.0911
BOTTOM TRAY TEMPERATURE	C	20.4534
TOP TRAY LIQUID FLOW	LBMOL/HR	264.000
BOTTOM TRAY LIQUID FLOW	LBMOL/HR	572.000
TOP TRAY VAPOR FLOW	LBMOL/HR	33.0000
BOTTOM TRAY VAPOR FLOW	LBMOL/HR	201,950.
CONDENSER DUTY	BTU/HR	-0.530597+08
REBOILER DUTY	BTU/HR	0.354052+09

**** PROFILES ****

STG	TEMPERATURE C	PRESSURE PSIA	FEED RATE LBMOL/HR LIQUID	FEED RATE LBMOL/HR VAPOR	PRODUCT RATE LBMOL/HR LIQUID	PRODUCT RATE LBMOL/HR VAPOR
1	18.091	1000.0				33.0000
2	5243.3	1000.0				
3	18.072	1000.0				
4	19.409	1000.0				
5	19.923	1000.0				
6	19.906	1000.0				
7	19.981	1000.0				
8	20.002	1000.0				
9	20.006	1000.0				
10	20.005	1000.0				
11	20.003	1000.0				
12	20.001	1000.0	604.9998			
13	20.004	1000.0				
14	20.006	1000.0				
15	20.008	1000.0				
16	19.996	1000.0				
17	19.996	1000.0				
18	19.997	1000.0				
19	19.822	1000.0				
20	18.258	1000.0				
21	18.097	1000.0				
22	11.793	1000.0				
23	16.015	1000.0				
24	16.209	1000.0				
25	20.453	1000.0			571.9998	

Sour Gas Stripper -- H2S STRIPPER
UNIT OPERATION BLOCK SECTION
FRACTIONATIO (RADFRC): STRIPPER (CONTINUED)

	TOTAL LIQUID FLOW			TOTAL VAPOR FLOW		
STG	LBMOL/HR	LB/HR	CUFT/HR	LBMOL/HR	LB/HR	CUFT/HR
1	264.00	11254.	270.37	33.000	1360.2	80.416
2	.60500	26.611	1.3220	297.00	12614.	31775.
3	.65074	27.741	.66623	33.605	1386.8	80.675
4	1.5496	66.031	1.6608	33.651	1388.0	88.086
5	2.1967	93.596	2.4030	34.550	1426.3	92.111
6	2.2587	96.241	2.4680	35.197	1453.8	93.404
7	2.2710	96.762	2.4901	35.259	1456.5	93.855
8	2.2546	96.063	2.4747	35.271	1457.0	93.970
9	2.2336	95.167	2.4524	35.255	1456.3	93.954
10	2.2153	94.385	2.4325	35.234	1455.4	93.907
11	2.2017	93.803	2.4175	35.215	1454.6	93.860
12	582.08	24800.	639.11	35.202	1454.0	93.823
13	582.04	24798.	639.11	10.082	416.46	26.873
14	582.21	24805.	639.40	10.036	414.53	26.753
15	582.54	24818.	639.89	10.210	421.72	27.223
16	582.23	24806.	639.16	10.536	435.18	28.079
17	582.85	24831.	639.99	10.228	422.44	27.265
18	582.27	24807.	639.26	10.846	447.98	28.906
19	578.87	24666.	630.33	10.274	424.29	27.205
20	572.63	24409.	589.68	6.8665	282.73	17.104
21	576.33	24554.	592.46	.62850	25.691	1.6457
22	804.72	33735.	764.71	4.3325	171.09	10.635
23	663.64	27965.	682.66	232.73	9349.2	621.81
24	.20252E+06	.83821E+07	.24238E+06	91.636	3568.6	278.92
25	572.00	24383.	637.60	.20195E+06	.83577E+07	.54238E+06

	**** X-PROFILE ****				
STAGE	H2	CO2	CO	CH4	H2S
1	.10012E-04	.94660	.20015E-02	.46402E-01	.49857E-02
2	.58438E-12	.99746	.25166E-07	.12223E-05	.25419E-02
3	.10134E-04	.94661	.20137E-02	.46441E-01	.49277E-02
4	.10443E-04	.94592	.20449E-02	.47051E-01	.49768E-02
5	.10584E-04	.94577	.20563E-02	.47184E-01	.49818E-02
6	.10595E-04	.94585	.20537E-02	.47102E-01	.49881E-02
7	.10630E-04	.94577	.20580E-02	.47172E-01	.49880E-02
8	.10643E-04	.94574	.20598E-02	.47204E-01	.49878E-02
9	.10651E-04	.94571	.20611E-02	.47230E-01	.49875E-02
10	.10656E-04	.94569	.20621E-02	.47250E-01	.49872E-02
11	.10659E-04	.94568	.20627E-02	.47264E-01	.49869E-02
12	.10661E-04	.94567	.20632E-02	.47274E-01	.49867E-02
13	.10659E-04	.94567	.20629E-02	.47269E-01	.49868E-02
14	.10665E-04	.94566	.20637E-02	.47281E-01	.49866E-02
15	.10677E-04	.94563	.20652E-02	.47305E-01	.49863E-02
16	.10667E-04	.94566	.20638E-02	.47283E-01	.49866E-02
17	.10689E-04	.94561	.20666E-02	.47327E-01	.49859E-02
18	.10668E-04	.94565	.20642E-02	.47290E-01	.49865E-02
19	.10556E-04	.94587	.20503E-02	.47081E-01	.49901E-02

Sour Gas Stripper -- H2S STRIPPER
UNIT OPERATION BLOCK SECTION

FRACTIONATIO (RADFRC): STRIPPER (CONTINUED)

		****	X-PROFILE	****	
STAGE	H2	CO2	CO	CH4	H2S
20	.10294E-04	.94642	.20165E-02	.46553E-01	.49977E-02
21	.11145E-04	.94560	.20818E-02	.47316E-01	.49894E-02
22	.30381E-04	.92063	.38998E-02	.70729E-01	.47108E-02
23	.22270E-04	.92864	.32713E-02	.63263E-01	.48055E-02
24	.31587E-04	.90145	.47641E-02	.89417E-01	.43408E-02
25	.10254E-04	.94650	.20118E-02	.46481E-01	.49986E-02

		****	Y-PROFILE	****	
STAGE	H2	CO2	CO	CH4	H2S
1	.35294E-04	.89526	.51750E-02	.95259E-01	.42661E-02
2	.12832E-04	.94087	.23556E-02	.51852E-01	.49054E-02
3	.34665E-04	.89708	.50828E-02	.93562E-01	.42354E-02
4	.34791E-04	.89629	.51117E-02	.94282E-01	.42793E-02
5	.34172E-04	.89755	.50336E-02	.93081E-01	.42982E-02
6	.33749E-04	.89842	.49800E-02	.92252E-01	.43108E-02
7	.33710E-04	.89851	.49748E-02	.92170E-01	.43124E-02
8	.33704E-04	.89852	.49740E-02	.92158E-01	.43126E-02
9	.33715E-04	.89850	.49754E-02	.92181E-01	.43123E-02
10	.33729E-04	.89847	.49772E-02	.92208E-01	.43119E-02
11	.33741E-04	.89844	.49788E-02	.92232E-01	.43115E-02
12	.33750E-04	.89842	.49799E-02	.92250E-01	.43113E-02
13	.33739E-04	.89844	.49788E-02	.92236E-01	.43114E-02
14	.33754E-04	.89843	.49800E-02	.92248E-01	.43113E-02
15	.33782E-04	.89840	.49824E-02	.92273E-01	.43110E-02
16	.33781E-04	.89839	.49828E-02	.92287E-01	.43109E-02
17	.33837E-04	.89833	.49876E-02	.92340E-01	.43104E-02
18	.33775E-04	.89839	.49825E-02	.92284E-01	.43110E-02
19	.33839E-04	.89805	.49979E-02	.92606E-01	.43081E-02
20	.35506E-04	.89365	.52387E-02	.96795E-01	.42807E-02
21	.44320E-04	.88271	.60301E-02	.10703	.41812E-02
22	.12468E-03	.83131	.11006E-01	.15376	.38080E-02
23	.80210E-04	.85659	.85741E-02	.13076	.39982E-02
24	.10097E-03	.81166	.11520E-01	.17318	.35409E-02
25	.31648E-04	.90132	.47720E-02	.89541E-01	.43389E-02

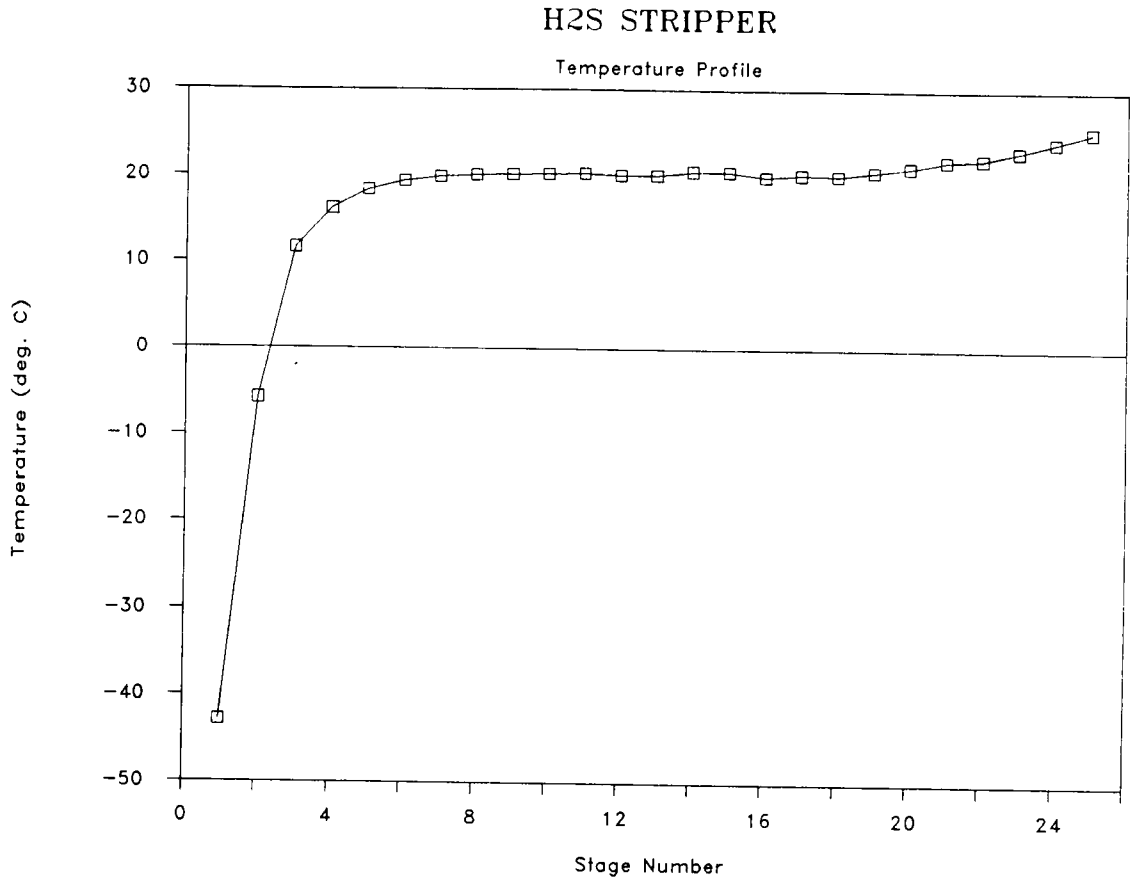
Sour Gas Stripper -- H2S STRIPPER
UNIT OPERATION BLOCK SECTION

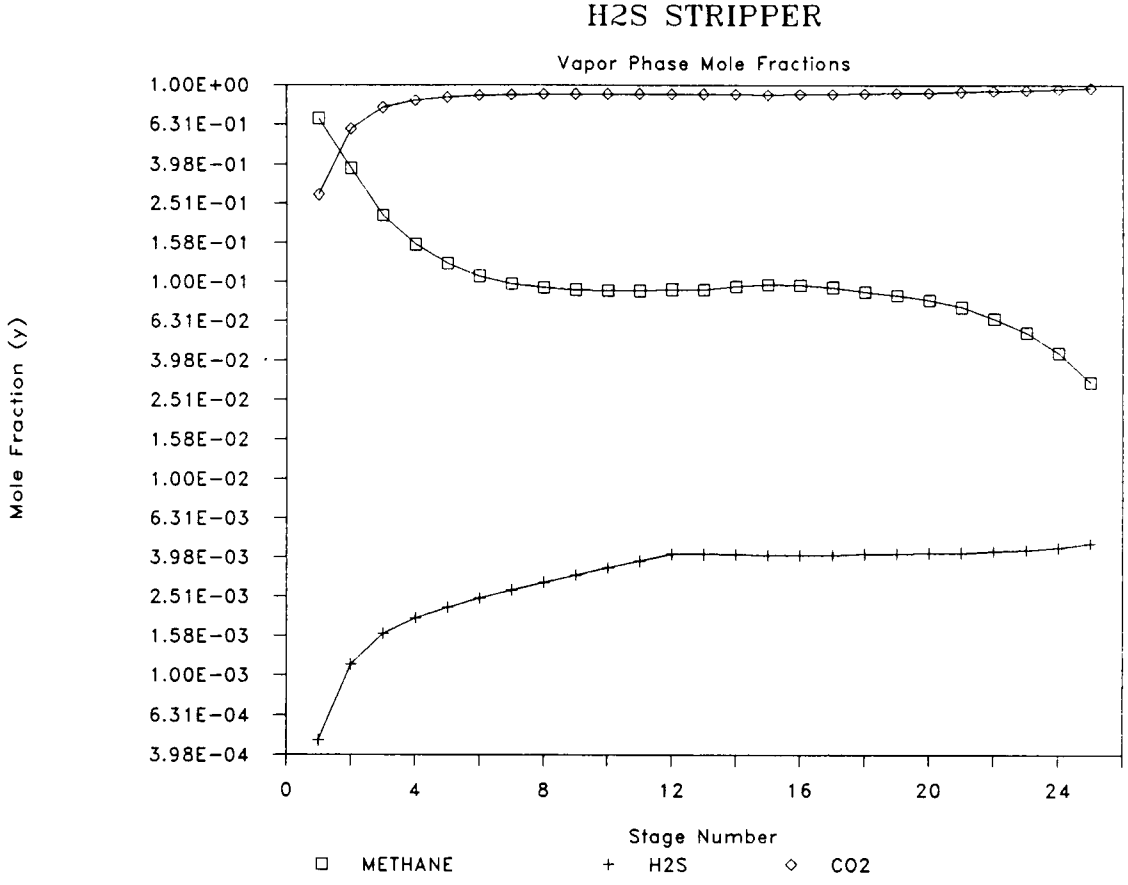
COLUMN SUMMARY

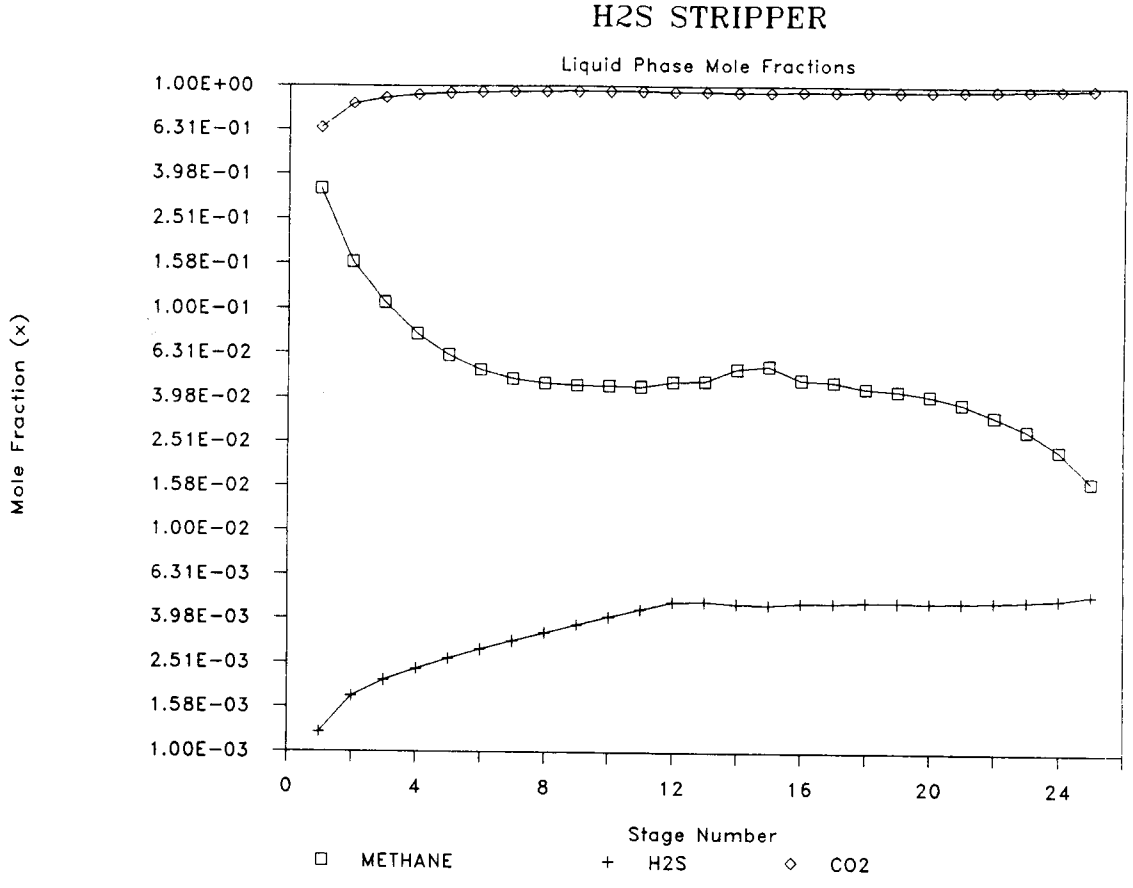
BLOCK ID	STRIPPER
MODEL TYPE	RADFRC
NUMBER OF STAGES	25
CONDENSER DUTY (BTU/HR)	-.53060+08
REBOILER DUTY (BTU/HR)	.35405+09
TOP STAGE TEMPERATURE (C)	18.0910
BOT STAGE TEMPERATURE (C)	20.4534
DISTILLATE RATE(LBMOL/HR)	33.0000
BOTTOMS RATE (LBMOL/HR)	571.9998
REFLUX RATIO	8.0000
VAP VFLOW STG1 (CUFT/HR)	80.4164
LIQ VFLOW STG1 (CUFT/HR)	270.3702
LIQ VFLOW STGN (CUFT/HR)	637.6047
LIQ DENS. STG1 (LB/CUFT)	41.6259
LIQ DENS. STGN (LB/CUFT)	38.2417
COLUMN SECTION 1	
NUMBER OF STAGES	25
NUMBER OF FEEDS	1
AT MAX. VAPOR VELOCITY STG	
LIQUID DENSITY (LB/CUFT)	38.2417
VAPOR DENSITY (LB/CUFT)	15.4093
LIQUID FLOW (LB/HR)	.24383+05
VAPOR FLOW (LB/HR)	.83577+07
SURFACE TENSION(DYNE/CM)	1.1834
LIQ VISCOSITY (CP)	0.0632

Sour Gas Stripper -- H2S STRIPPER
STREAM SECTION

PRODUCT FLOW DETAILS	PRODUCT	BOTTOM	FEED
COMPONENT FLOWS <LBMOL/HR>			
HYDROGEN	0.0011	0.0058	0.0070
CARBON-DIOXIDE	29.5437	541.3970	570.9408
CARBON-MONOXIDE	0.1707	1.1507	1.3215
METHANE	3.1435	26.5869	29.7305
HYDROGEN-SULFIDE	0.1407	2.8592	3.0000
TOTAL	33.0000	571.9998	604.9998
PHASE SPLITS			
VAPOR FRACTION <MOLE BASIS>	1.0000	0.0	0.0406
LIQUID FRACTION <MOLE BASIS>	0.0	1.0000	0.9593
SOLID FRACTION <MOLE BASIS>	0.0	0.0	-.41633-16
INTENSIVE PROPERTIES			
TEMPERATURE <C>	18.0910	20.4534	20.0000
PRESSURE <PSIA>	1000.000	1000.000	1000.000
MOLECULAR WEIGHT	41.2192	42.6278	42.5509
ENTHALPY <BTU/LBMOL>	-.15716+06	-.16590+06	-.16549+06
ENTROPY <BTU/LBMOL-R>	-12.1369	-14.7746	-14.7469
DENSITY <LBMOL/CUFT>	0.4103	0.8971	0.8606


H2S STRIPPER
Temperature Profile
30
20
10
0
-10
-20
-30
-40
-50
Temperature (deg. C)
0
4
8
12
16
20
24
Stage Number


H2S STRIPPER
Vapor Phase Mole Fractions
1.00E+00
6.31E-01
3.98E-01
2.51E-01
1.58E-01
1.00E-01
6.31E-02
3.98E-02
2.51E-02
1.58E-02
1.00E-02
6.31E-03
3.98E-03
2.51E-03
1.58E-03
1.00E-03
6.31E-04
3.98E-04
Mole Fraction (y)
0
4
8
12
16
20
24
Stage Number
METHANE
H2S
CO2


H2S STRIPPER
Liquid Phase Mole Fractions
Mole Fraction (x)
1.00E+00
6.31E-01
3.98E-01
2.51E-01
1.58E-01
1.00E-01
6.31E-02
3.98E-02
2.51E-02
1.58E-02
1.00E-02
6.31E-03
3.98E-03
2.51E-03
1.58E-03
1.00E-03
0
4
8
12
16
20
24
Stage Number
METHANE
H2S
CO2

VITA

James S. Morris was born in Sweetwater, Tennessee on December 21, 1959. He graduated from Sweetwater High School and entered Tennessee Technological University in Cookeville, Tennessee in 1977. He received a Bachelor of Science in Chemical Engineering in 1982 after participating in cooperative education programs with Olin Corporation in Charleston, Tennessee and the Union Carbide Corporation Oak Ridge Gaseous Diffusion Plant in Oak Ridge, Tennessee.

After graduation, he was employed by the Union Carbide Corporation Y-12 Plant as a process engineer in the lithium production facilities. He is now a General Supervisor at the Y-12 Plant, now operated by Martin Marietta Energy Systems, Inc., in the depleted uranium production facilities. James began study toward his Master's degree in the fall of 1983 at the University of Tennessee, and received his degree in the spring of 1988.